TECHNICAL REPORT

THEORETICAL PREDICTION OF THE FLOW IN THE WAKE OF A HELICOPTER ROTOR

PART 1 - DEVELOPMENT OF THEORY AND RESULTS OF COMPUTATIONS

By: Peter Crimi

CAL No. BB-1994-S-1

Prepared for:

U.S. Army
Ballistic Research Laboratories
Aberdeen Proving Ground, Maryland 21005

Final Report - Part 1
Contract No. DA30-069-AMC-645(R)
September 1965

Code 1

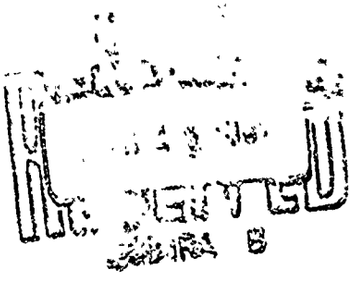

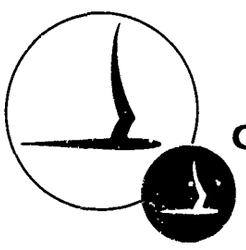

CORNELL AERONAUTICAL LABORATORY, INC.
OF CORNELL UNIVERSITY, BUFFALO, N. Y. 14221

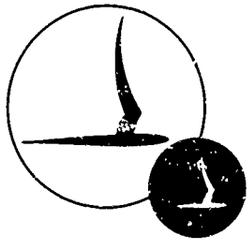

CORNELL AERONAUTICAL LABORATORY, INC.
BUFFALO, NEW YORK 14221

THEORETICAL PREDICTION OF THE FLOW IN THE WAKE OF A HELICOPTER ROTOR

PART I
DEVELOPMENT OF THEORY
AND RESULTS OF COMPUTATIONS

By:
PETER CRIMI

CAL NO. BB-1994-S-1

FINAL REPORT - PART I
CONTRACT NO. DA30-069-AMC-645 (R)

SEPTEMBER 1965

Prepared for:
U.S. ARMY
BALLISTIC RESEARCH LABORATORIES
ABERDEEN PROVING GROUND, MARYLAND 21005

SUMMARY

A study was performed with the objective of predicting the time-varying flow in the vicinity of a helicopter in hovering or forward flight. An analytical model was formulated which represents the rotor, its wake and the fuselage of the aircraft. The model for the wake has been simplified in a manner consistent with flow visualization studies by representing the wake as tip vortices emanating from each blade. The wake vortices are assumed to be free to convect under the influence of the blades, the fuselage and the wake itself. The fuselage has been replaced by a surface distribution of sources, the strength per unit area being determined by assuming that the fuselage is subjected to a uniform, steady free stream.

A digital computer program was written which implements the model developed. Flow calculations were performed which agree well with measurements of the time average of the flow in the wake of a two-bladed rotor. Extensive calculations were then carried out which define the flow in the vicinity of a UH-1B helicopter for a range of flight conditions from hover to high-speed cruise.

Upon analysis of the results, it was concluded that the model developed provides a valid representation of the unsteady flow in the vicinity of a helicopter. It was pointed out that the formulation is somewhat restrictive, in that the flow in the rotor plane and immediately adjacent to the fuselage cannot be accurately predicted. However, with suitable refinements incorporated, these regions could be investigated as well.

FOREWORD

The work reported herein, performed between September 1964 and September 1965, was accomplished by the Cornell Aeronautical Laboratory, Inc. (CAL), Buffalo, New York for the Director of Ballistic Research Laboratories, (BRL) Aberdeen Proving Ground, Maryland. The research effort was performed under Contract DA 30-069-AMC-645(R) and was monitored for BRL by Mr. Thomas Coyle as Technical Supervisor. Dr. Peter Crimi of CAL conducted the study and received assistance from Mr. Alexander Sowydra during the development of the mathematical model and Mr. Harvey Selib for the digital computer programming.

This document is Part 1 of the final report under the contract. It describes the development of the theory, discusses the results of the computation, and provides a comprehensive discussion of the work performed under the contract. Part 2 of the final report describes the formulation and application of the rotor wake-flow computer program and is of use primarily to those who plan to use the digital computing program.

CAL Report Numbers have been assigned as follows:

BB-1994-S-1, THEORETICAL PREDICTION OF THE FLOW IN THE WAKE OF A HELICOPTER ROTOR, Part 1 - Development of Theory and Results of Computations

BB-1994-S-2, THEORETICAL PREDICTION OF THE FLOW IN THE WAKE OF A HELICOPTER ROTOR, Part 2 - Formulation and Application of the Rotor Wake Flow Computer Programs

CONTENTS

ILLUSTRATIONS

SYMBOLS

a	vortex core radius
N_B	number of rotor blades
P_i	designation for i^{th} wake reference point
R	rotor radius
$\underline{r}$	position vector of a point in the flow
(V_x, V_y, V_z)	components of fluid velocity in the directions of x, y and z respectively, nondimensionalized by $\lambda \Omega R$
$(\overline{V}_x, \overline{V}_y, \overline{V}_z)$	time averages of V_x, V_y and V_z respectively
$(V_{x_i}, V_{y_i}, V_{z_i})$	wake and blade induced contributions to V_x, V_y and V_z respectively
$\underline{V}_f$	free-stream velocity
v	induced downwash
$\overline{v}$	time average of v
v_o	momentum value for the time average of v
W	aircraft weight
(x, y, z)	rectilinear coordinates with origin in the tip-path plane, nondimensionalized by R
α_T	inclination of the free stream to the tip-path plane
Γ	circulation
λ	blade loading parameter; $\lambda = 4W/(\pi^2 N_B \rho \Omega^2 R^4)$
μ	advance ratio; $\mu = V_f/(\Omega R)$
ρ	air density
σ	source strength per unit area
ψ	rotor azimuth angle
Ω	rotor angular speed

GLOSSARY OF TERMS

Circulation:	The line integral about a closed curve of the component of fluid velocity tangent to the curve.
Convection:	The process of transport of fluid particles.
Roll-up of the Wake:	The concentration of wake vorticity into isolated vortices.
Self-induced Velocity:	The contribution to the velocity of convection of a vortex from the vortex itself.
Vortex:	A concentration of rotational fluid (i. e., having nonzero vorticity), resulting in a swirling flow; bound - constrained to move in a prescribed manner; free - allowed to convect; root - vortex emanating from the blade root; sheet - a distribution of concentrated vortices in the form of a surface; tip - vortex emanating from the blade tip.
Vorticity:	The curl of the fluid velocity; a measure of rotationality.
Wake of a Blade:	The vortex elements created by the passage of the blade through the fluid.

1. INTRODUCTION

A method for accurately predicting the time-varying flow in the vicinity of a translating or hovering helicopter would be of considerable value as both an engineering tool and an aid to research and development. Possible areas of application are the determination of harmonic airloads on the blades, fuselage or auxiliary lifting surfaces, investigation of rotor transient response and flutter, vibration and fatigue analyses, and study of downwash impingement and debris entrainment in ground effect. The method of flow prediction which is reported here is presently limited to application in only certain of these areas, but it appears that, with further development, the scope of its applicability might be considerably broadened.

Direct analysis of the flow in the wake of a rotor for arbitrary flight conditions is a formidable task, particularly if fuselage effects are important in the region of interest. The dependent variables are nonlinear functions of three space variables, time and each other, with no means available for linearization. Some results have been obtained previously by retaining the complex structure of the flow but specifying the wake geometry. For example, good agreement with experimental measurements of blade loading were obtained by calculating the flow at the rotor plane in this way (Reference 1). The time average of the induced downwash in certain limited regions was fairly well approximated using a similar assumption as to wake geometry (Reference 2).

The objective of the study reported here is to predict the time-varying flow at an arbitrary point in the wake of a helicopter rotor. If the wake geometry were assumed known, unacceptably large errors would result. Instead, the wake structure has been simplified in a manner consistent with the findings of flow visualization studies (see Chapter 2). The wake can then be allowed to convect under the influence of the blades, the fuselage and self-induced effects by constructing a numerical analogue with the aid of a digital computer.

In developing the theory, consideration has been limited to aircraft having a single rotor. No restriction has been placed on the number of blades which the rotor may have, however. The aircraft has been assumed to be in steady level flight or hover, out of ground effect, and the forward speed, rotor rotational speed and loading have been assumed to be within the limits of presently operational single-rotor helicopters. Also, in representing the fuselage, the flow has been assumed to be attached and noncirculatory and the fuselage geometry has been somewhat idealized by omitting appendages such as landing skids.

The results of the study are reported in two parts. The development of the theory, the basic formulation, the major assumptions for numerical analysis and the results of computations are presented here. The second part, contained in a separate document, concerns the detailed information related to the coding and operation of the digital computer programs which implement the theory.

2. DISCUSSION OF THE PHYSICAL FLOW

It is desired to analytically define the flow in the vicinity of a helicopter in translational or hovering flight out of ground effect. In order that a rational framework for the analytical model may be constructed the essential features of the physical flow should first be outlined.

Generally, there are three primary contributions to the flow at a given point relative to the aircraft. Specifically, the rotor blades, their wake and the fuselage all affect the fluid velocity. These three effects are, of course, interrelated in an extremely complicated and nonlinear manner, but for the purposes of this discussion they can be considered separately.

The rotor blades may be regarded as wings of very high aspect ratio in a harmonically varying stream. While the wake and fuselage do alter the loading on the blades, the total lift at a given azimuth position of the rotor must still be approximately equal to the weight of the aircraft. This implies that the circulation about a given blade must vary approximately sinusoidally with azimuth. The spanwise variation of circulation about a blade is also a function of wake and fuselage effects, and depends on blade twist and planform as well. Results of theoretical computations of harmonic airloads (Reference 1), which agree well with experimentally obtained data, indicate, though, that the spanwise variation of circulation generally does not differ a great deal from an elliptic distribution.

The wake of each blade is generated as a thin sheet of vortical fluid. The vorticity in this sheet has components in the spanwise direction (shed vortices) and in the chordwise direction (trailing vortices). It has been observed from flow visualization studies that this sheet rolls up within a few chord lengths to form a single concentrated vortex trailing from near the tip of the blade (see, for example, Reference 3). While, at least in theory, a vortex should also trail from the vicinity of the root, it appears from the smoke pictures as well as from the results of an analytical treatment of the wake of a hovering rotor (Reference 4) that self-induced effects rapidly carry the root vortices up through the center of the rotor plane where they are dissipated. The tip

vortices are quite stable, however, and experience little or no diffusion due to viscous effects for several rotor revolutions.

From the point of view of the fuselage, the flow appears as the superposition of a steady free stream caused by the translation of the aircraft and the periodic flow induced by the rotor and its wake. The contribution of the fuselage to the flow at any point, then, is essentially that due to a body of complicated geometry in unsteady potential flow.

3. FORMULATION OF THE ANALYTICAL MODEL

If the fluid is assumed to be inviscid and incompressible, the flow described in Chapter 2 has an exact analytical counterpart. The rotor blades could be replaced by doublet sheets, the wake by vortex sheets and the fuselage by a surface distribution of sources. The strengths of these potential singularities would be functions of time and spacial coordinates. The requirement of flow tangency at the blades and the fuselage would provide a pair of nonlinear integral equations for the determination of the strength distributions. The problems involved in the formulation and solution of these equations preclude such an approach. Therefore, three major simplifying assumptions have been utilized in the formulation of the model.

First, the rotor blades have been replaced by line vortices of constant strength spanwise and harmonically varying strength azimuthally. Except in the immediate vicinity of the blades, blade-induced effects should be reasonably well reproduced by such a model. That is, more than one or two chord lengths from a given blade, higher harmonic variations in circulation cannot have an appreciable effect on the flow, at least in comparison with fuselage or wake effects. For present purposes, then, blade loading can be regarded as a known quantity.

Second, the wake is represented by individual free vortices, one trailing from the tip of each blade vortex; the strength of each tip vortex varies along its length in accordance with the (known) azimuthal variation of the blade vortex from which it trails. The wake vortices are assigned finite circular cores of rotational fluid (as physical vortices must have), so that the velocity which a vortex induces on itself may be correctly computed. The requirement of constancy of circulation as specified by Kelvin's theorem has not been met. However, as noted in Chapter 2, the vortex elements needed to fulfill that requirement - shed vortices and trailing root vortices - do not contribute significantly to the flow. For the same reason, the detailed structure of the wake near the blades, where roll-up occurs, and the vortices in the far wake (more then two or three rotor radii downstream of the rotor) have also been omitted.

Lastly, the fuselage is assumed to experience a uniform free stream of constant magnitude and direction. This stream is made up of two components, one being the negative of the velocity of translation of the aircraft, and the other consisting of a time and spacial average of the downwash which would be induced by the rotor and its wake in the absence of the fuselage. At high forward speed, the time and spacial variations of the stream in which the fuselage is immersed are comparatively small and so may be neglected without causing large errors. At low forward speed, the downwash may vary substantially over the fuselage, but the total effect of the fuselage on the flow is generally small compared to rotor and wake effects, so that the error is, presumably, again not appreciable. It is also assumed that the flow about the fuselage is not separated, so consideration must be limited to regions where separation effects are unimportant.

The model for the flow as so simplified can be formulated in a straightforward manner. A coordinate system fixed in the tip-path plane, as shown in Figure 1 for a two-bladed rotor, is utilized. The vector $\underline{V}_f$ in the figure is the free stream velocity (the negative of the translational velocity of the aircraft), inclined at an angle α_T to the x-axis and parallel to the x-z plane. The angle ψ denotes the azimuth position of the rotor, and $\underline{r}$ is the vector positioning a given point with respect to the origin.

The fluid velocity $\underline{V}$ at a given point located by the vector $\underline{r}_p$ may be expressed in the form

$$\underline{V}(\underline{r}_p) = \frac{-1}{4\pi}\int_{C_V} \frac{\Gamma(\underline{r})\underline{r}_1 \times d\underline{r}}{r_1^3} + \frac{1}{4\pi}\int_{A_f} \sigma(\underline{r})\underline{r}_1 \, dA_f + \underline{V}_f \qquad (1)$$

where $\underline{r}_1 = \underline{r}_p - \underline{r}$, Γ is the local circulation about a vortex, and σ is the source strength per unit area on the surface replacing the fuselage. The first integral is a line integral taken over all vortices in the flow, which curves are collectively denoted by C_V, and the second is an integral over the surface A_f replacing the fuselage.

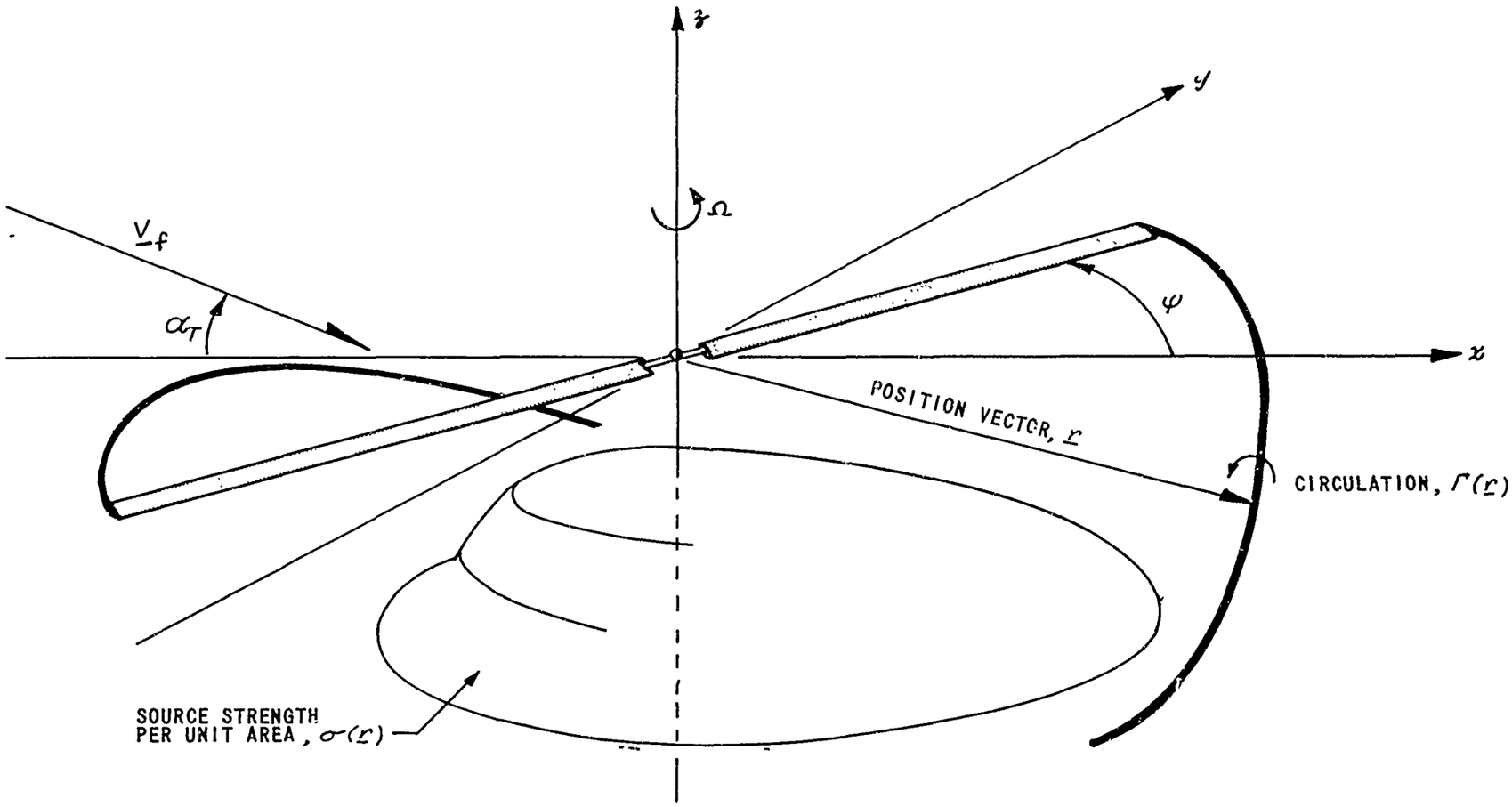

Figure 1 THE COORDINATE SYSTEM

The circulation Γ about the blade vortices is known directly in terms of flight parameters. The circulation about a wake vortex at a given point is simply that value assigned to the blade vortex when it was generating that segment of wake. The source strength σ may also be regarded as known insofar as the wake flow calculations are concerned. That distribution is assumed to be such as to produce the flow about a body of known geometry in a uniform free stream, so $\sigma(\underline{r})$ may be determined from a separate calculation.

The only information lacking for the complete specification of the flow at a given instant, then, is the location of the wake vortices at that instant. The position of a given point on a wake vortex located by the vector $\underline{r}$ is the time integral of the velocity experienced by that fluid particle:

$$\underline{r}(t) = \underline{r}(t_o) + \int_{t_o}^{t} \underline{V}(\underline{r}(\tau))\, d\tau . \qquad (2)$$

Thus, even after simplifying, the flow can only be obtained as the solution of the nonlinear integral equation formed by the substitution of Equation (1) into Equation (2). A direct analytical solution is not feasible, but the problem is amenable to solution by numerical methods using a high-speed digital computer. The manner in which the formulations of Equations (1) and (2) were implemented for digital computation is discussed in Chapter 4.

4. IMPLEMENTATION OF THE MODEL

WAKE POSITIONING AND DISPLACEMENT

For purposes of numerical analysis, a series of points $P_1, P_2, \cdots, P_{N_W}$ is marked off on each wake vortex, as shown schematically in Figure 2.

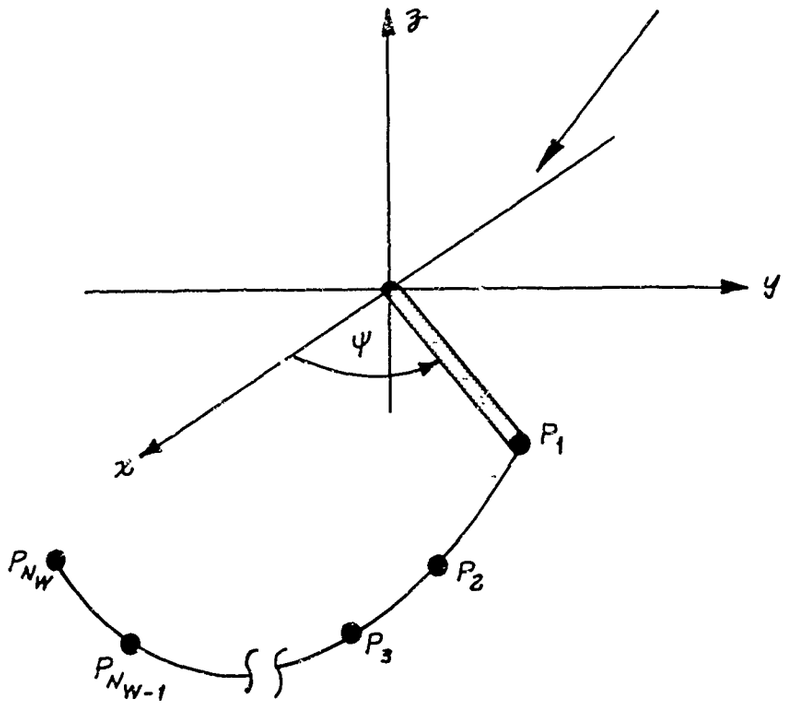

Figure 2 WAKE REFERENCE POINT IDENTIFICATION

The points are placed sufficiently close together so that for purposes of computation of wake-induced velocities, the segment (i) of wake between points P_i and P_{i+1} may be considered as a rectilinear vortex having constant circulation along its length. The wake configuration at any instant is then defined by the locations of these points.

Computations are initiated by specifying that each of the wake vortices lies on a prescribed curve. Generally, the curve is chosen to be a skewed helix with pitch and skew selected from simple momentum considerations. The numerical analogues to Equations (1) and (2) are then performed by first summing the velocity contributions of all vortex and source elements in the flow at each reference point (Equation (1)), and then convecting each point at the computed velocity for a time interval Δt (Equation (2)). The time interval Δt is chosen to correspond to a small finite change $\Delta\psi$ in the azimuth position of the blades:

$$\Delta t = \frac{\Delta\psi}{\Omega} \tag{3}$$

where Ω is rotor angular speed. Once the new coordinates of each reference point are computed, the azimuth of the blade vortices is increased by $\Delta\psi$ and the velocity computation is performed again. As the blade vortices are repositioned, a wake vortex element is added to the flow at the tip of each blade vortex, the added vortex having a length of approximately $R\Delta\psi$, where R is rotor radius. A corresponding element is dropped from the computations at the downstream end of each wake vortex, so the program is not encumbered by a wake of ever increasing size. The computations may be continued indefinitely in this manner, but it has been found that a periodic wake is eventually established in most cases, after which there is, of course, no need to perform further calculations.

The total number of wake vortices taken into account and the magnitude of $\Delta\psi$ determine the accuracy of the flow representation at a given point. It has been found that, for a two-bladed rotor, a value for $\Delta\psi$ of thirty degrees is sufficiently small to define the time variations of the flow. The number of wake elements considered depends on the region of interest and the forward speed. If the flow beneath the rotor plane is desired, then the wake generated by only a few revolutions of the rotor is needed. It has been found, for example, that with an advance ratio, $\mu = \frac{V_f}{\Omega R}$, of about .25, just two revolutions of wake sufficiently define the flow under the rotor plane. At lower advance ratios, the free stream does not clear the wake from under

the rotor as rapidly, so more wake must be retained. With $\mu = .15$, four revolutions of wake are needed, and for hovering, seven or eight revolutions must be retained to compute the flow within about $0.5R$ of the rotor plane.

COMPUTATION OF VELOCITY INDUCED BY WAKE AND BLADES

The velocity induced at an arbitrary point P by the vortices representing the wake and blades is simply the sum of the effects of an array of rectilinear vortex segments. If V_{w_i} denotes the velocity induced at P by the element between points P_i and P_{i+1}, it is found from Equation (1) that

$$V_{w_i} = \frac{\Gamma_i}{4\pi h} (\cos\theta_1 - \cos\theta_2) \qquad (4)$$

where Γ_i is the strength of the element and θ_1, θ_2 and h are defined in Figure 3. The velocity is directed normal to the plane containing P_i, P_{i+1} and P.

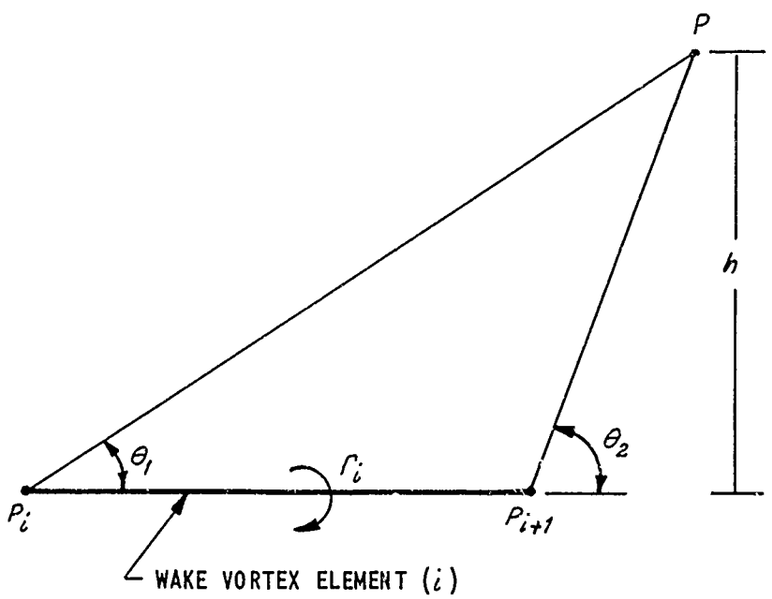

Figure 3 GEOMETRIC RELATIONSHIPS DEFINING THE FLOW INDUCED BY A RECTILINEAR VORTEX ELEMENT

The necessity for specifying that the wake vortices have a finite core size is evident from Equation (4). If P is coincident with either P_i or P_{i+1}, the formula for V_{w_i} is indeterminate. When computing wake-induced flow at a given wake reference point, the effect of the two wake elements adjacent to that point must, therefore, be computed by taking core size into account (if a point lies outside the core substance of a vortex, the formula for induced velocity is the same as for a vortex with infinitesimal core size, i. e., Equation (4)). Locally induced velocities depend directly on the curvature of (the centerline of) the vortex at the point in question. An approximation to the actual curvature is obtained by assuming that the two elements whose effects at point P_i are to be computed lie on the circular arc which passes through points P_{i-1}, P_i and P_{i+1}, as shown in Figure 4. Then it is assumed that the two vortex segments have circular cores of rotational fluid of radii a_{i-1} and a_i, respectively, and that the vorticity within the core is tangent to the arc and of a magnitude which varies linearly with distance from the center of the arc. The assumption of linear variation of vorticity would seem plausible, since this is the case for a vortex ring. The self-induced velocity V_{s_i} at point P_i - i. e., the contributions of the elements adjacent to P_i - may then be written in integral form by summing the effects of circular-arc vortex filaments of differential cross-section. If it is then assumed that the core radii are much less than the radius of curvature $\mathcal{R}$, the integrand may be simplified and the integral evaluated. It is then found that

$$V_{s_i} = \frac{1}{8\pi\mathcal{R}} \left\{ \Gamma_{i-1} \left[\ln\left(\frac{8\mathcal{R}}{a_{i-1}} \tan\frac{\phi_{i-1}}{4}\right) + \frac{1}{4} \right] + \Gamma_i \left[\ln\left(\frac{8\mathcal{R}}{a_i} \tan\frac{\phi_i}{4}\right) + \frac{1}{4} \right] \right\} \tag{5}$$

where ϕ_{i-1} and ϕ_i are defined in Figure 4. The self-induced velocity is directed normal to the plane of the arc. The core radius of a given element may be assigned on a rational basis using energy considerations, as discussed later.

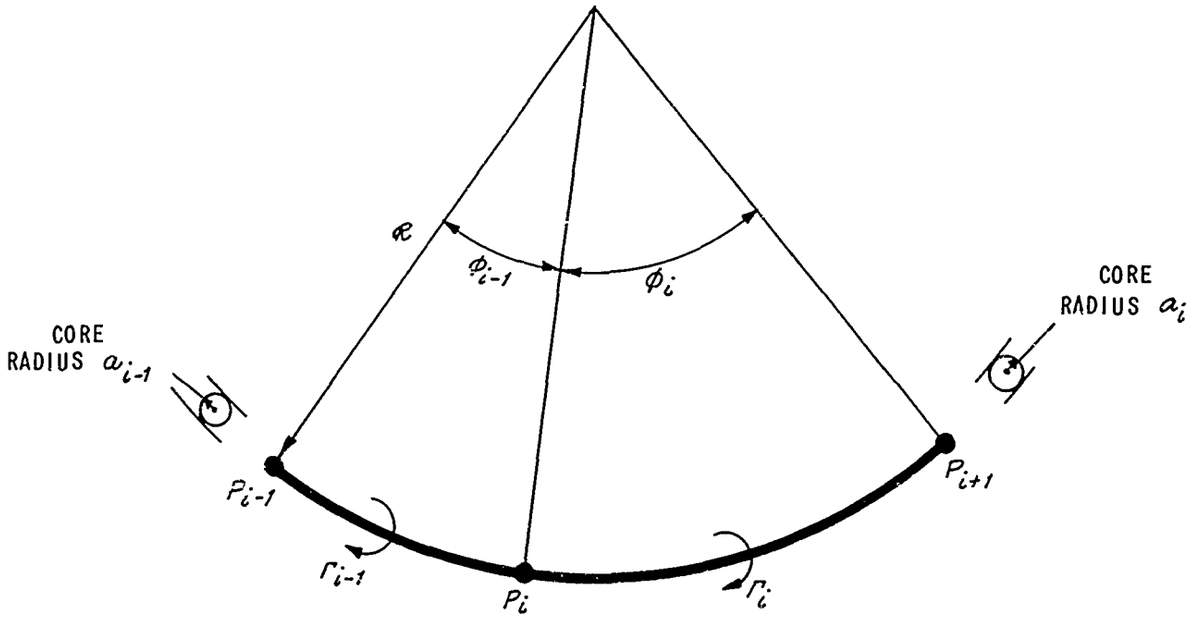

Figure 4 GEOMETRIC RELATIONSHIPS DEFINING THE SELF-INDUCED VELOCITY AT WAKE POINT P_i

THE FUSELAGE REPRESENTATION

As noted previously, the source-strength distribution is determined for a fuselage in a uniform, steady free stream. Once this distribution is obtained, the effect of the fuselage is taken into account in a straightforward manner according to the second integral in Equation (1).

The computation of the source-strength distribution may be treated as a separate problem, since the source strength per unit area σ at a given point $\underline{r}$ may be normalized. That is, σ may be written in the form

$$\sigma(\underline{r}) = V_{x_\infty}\,\sigma_x(\underline{r}) + V_{y_\infty}\,\sigma_y(\underline{r}) + V_{z_\infty}\,\sigma_z(\underline{r}) \qquad (6)$$

where V_{x_∞}, V_{y_∞} and V_{z_∞} are the components of the free stream experienced by the fuselage, and the normalized strengths σ_x, σ_y and σ_z are functions only of fuselage geometry. The values for the free stream velocity components may be obtained by simply computing the flow in the absence of the fuselage and taking appropriate averages.

The normalized source strengths are computed according to the method reported in Reference 5. The fuselage surface is approximated by an array of quadrilateral elements. The source strength per unit area on a given quadrilateral is taken to be constant. Thus, if there are N_f of these elements replacing the fuselage, there are $3N_f$ strengths to be determined. The requirement of flow tangency at N_f points (one on each of the quadrilaterals) then produces $3N_f$ linear algebraic equations for determining the $3N_f$ unknown strengths.* A digital computer program was coded for determining the source strengths in this manner.

The method as developed in Reference 5 was used to obtain surface pressure distributions, so no assessment was made there as to the number of quadrilateral source elements needed to adequately reproduce the flow an arbitrary distance from the fuselage. Calculations were therefore performed for an ellipsoid of revolution having a ratio of minor to major axis of 0.4 so that the numerical approximation to the flow could be compared with an analytically prescribable flow. Representation by 56, 136, and 184 surface elements were considered. The flows produced in these three cases were then compared with the exact potential solution. The results are shown plotted in Figures 5 and 6. Figure 5 compares the surface-element and exact solutions for the free stream parallel to the axis of revolution, and Figure 6 presents th-

---

* In applying the method to the flow about the fuselage, V_{y_∞} was assumed zero and the fuselage assumed to have one plane of symmetry, which reduces the number of unknowns to N_f.

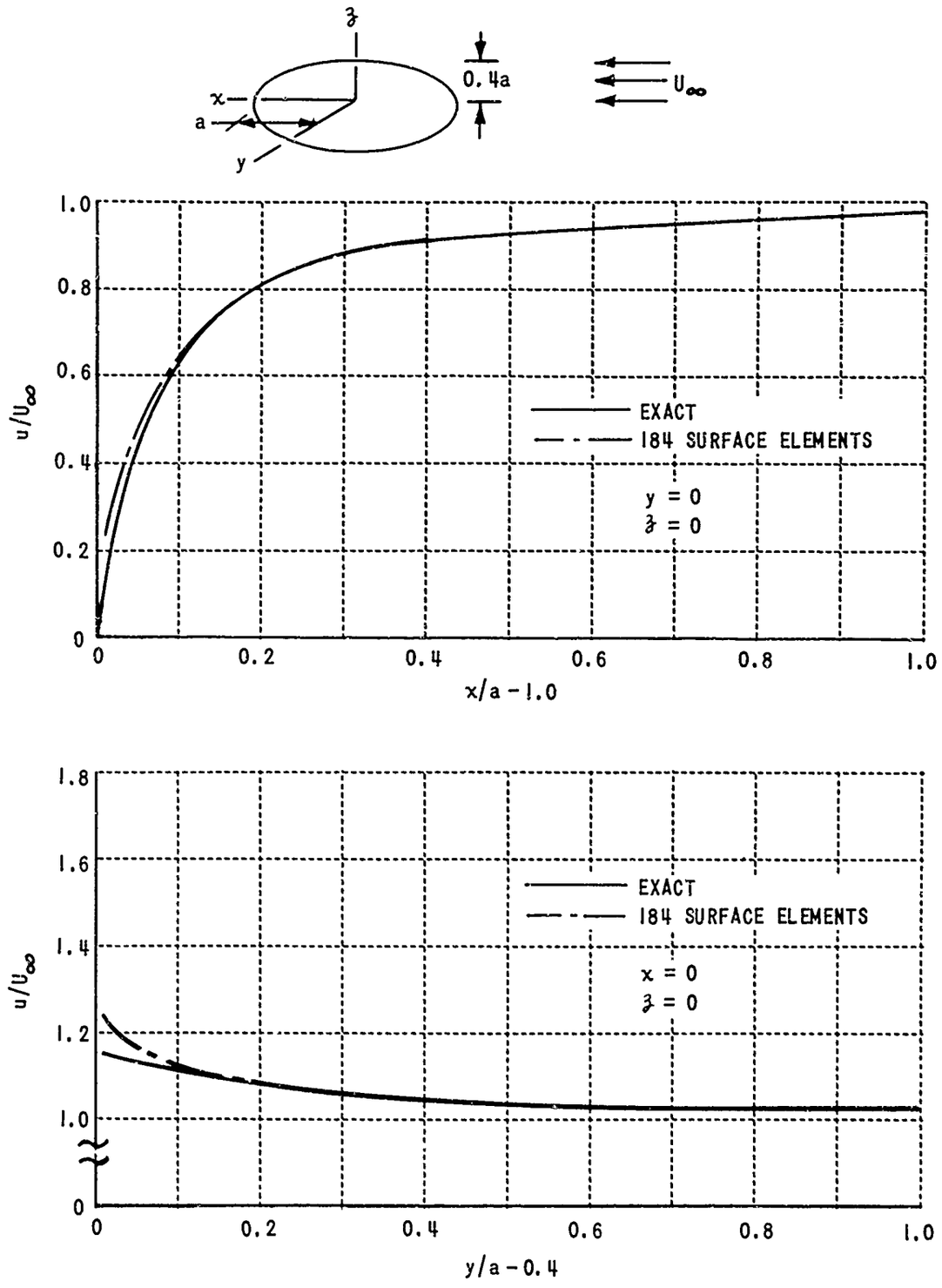

Figure 5 COMPARISON OF THE EXACT POTENTIAL SOLUTION FOR THE FLOW ABOUT AN ELLIPSOID WITH APPROXIMATIONS BY A FINITE NUMBER OF SOURCE SHEETS - AXIAL FLOW CASE

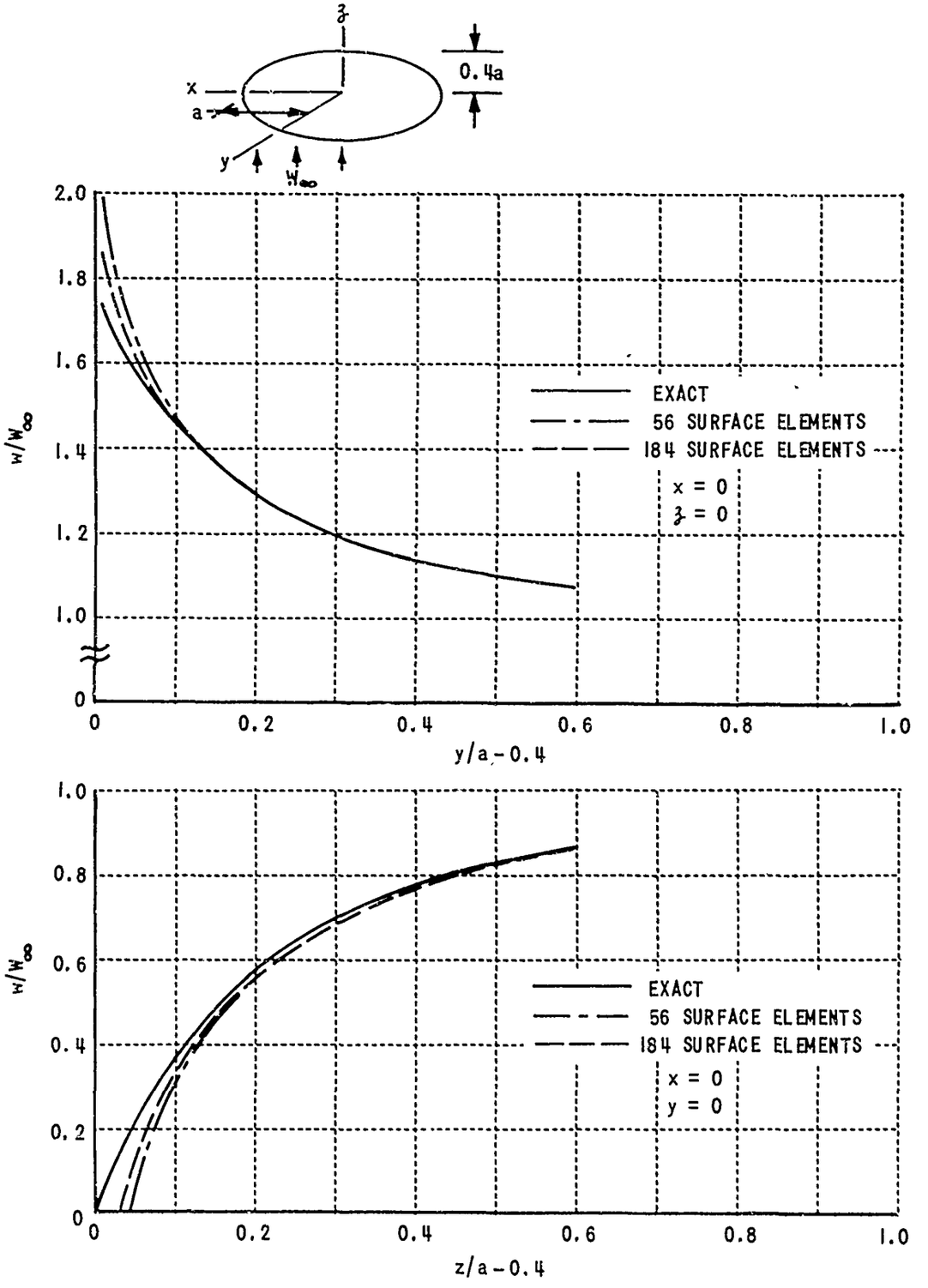

Figure 6 COMPARISON OF THE EXACT POTENTIAL SOLUTION FOR THE FLOW ABOUT AN ELLIPSOID WITH APPROXIMATIONS BY A FINITE NUMBER OF SOURCE SHEETS - CROSS-FLOW CASE

results for a cross-flow. The quantities u and w plotted are the fluid velocity components in the x and z directions, respectively, for the coordinate system sketched on the figures.

In the case of axial flow, the differences among the results for 56, 136, and 184 elements were too small to be seen on the plot, so only the 184-element case is shown in Figure 5. It may be noted from this figure that the approximate solutions only differ from the exact solution very near the body, and the differences which do occur are very small.

Somewhat larger differences are apparent in the case of cross-flow, Figure 6, with noticeable improvements resulting by increasing the number of surface elements. The largest differences are seen to occur along the z-axis. These are caused by the singular nature of the flow very near the juncture of two surface elements.

These results would indicate that a fuselage with approximately the proportions of the ellipsoid considered would be adequately represented by 136 surface elements. A more accurate representation would not be justified in the light of the errors introduced by assuming uniform steady flow. It should be noted, though, that areas having large curvature must be represented by elements smaller in size than are adequate elsewhere, thereby increasing the number of elements required. Thus, even if the fuselage has approximately the proportions of the ellipsoid treated, considerably more than 136 elements may be needed for an accurate representation if the surface is at all irregular.

DETERMINATION OF SYSTEM PARAMETERS

The formulations of the model were nondimensionalized for purposes of coding, with lengths made dimensionless by rotor radius R and velocities by rotor tip speed ΩR. The flight conditions of the aircraft being represented relate to the computer program through the following dimensionless parameters: advance ratio $\mu = \frac{V_f}{\Omega R}$, nondimensionalized blade vortex circulation $\frac{\Gamma_B}{\Omega R^2}$, tip-path plane angle α_T and the ratio of wake-vortex core radius to rotor radius, $\frac{a}{R}$. The quantities which determine μ are, of course, generally

available. Specification of the other parameters is accomplished in the manner discussed below.

Blade Vortex Strength, $\Gamma_B(\psi)$

The circulation about a rotor blade at a given azimuth position ψ is actually varying in the radial direction (more or less elliptically). It was felt, though, that a sufficient approximation to blade-induced effects would be obtained by making the circulation constant spanwise and of a magnitude equal to the maximum attained on the actual blade. It might be supposed that blade-induced effects would then be somewhat exaggerated, but comparisons of computed and measured flows indicate that the error so introduced is not large enough to be discernable (see Chapter 5).

If the circulation is assumed to vary elliptically in the spanwise direction, the maximum circulation Γ_m about a blade is given by (neglecting root effects and making small-angle approximations where appropriate),

$$\Gamma_m = \frac{8L_B(\psi)}{\pi\rho\Omega R^2(1+\mu\sin\psi)^2}$$

$$\approx \frac{8L_B(\psi)(1-2\mu\sin\psi)}{\pi\rho\Omega R^2}$$

where L_B is the total lift acting on the blade and ρ is the air density. Then, assuming that the total lift acting on the rotor is constant and equal to the gross weight W of the aircraft, it follows that

$$\frac{\Gamma_m}{\Omega R^2} = 2\pi\lambda(1-2\mu\sin\psi) \tag{7}$$

where λ is a blade loading parameter, defined by

$$\lambda = \frac{4W}{\pi^2 N_B \rho \Omega^2 R^4}$$

with N_B denoting the number of blades on the rotor.

Inclination of the Tip-Path-Plane, α_T

The tip-path-plane angle is a complicated function of flight conditions, rotor dynamics and blade cyclic and collective pitch settings. Various methods are available for computing this angle (see, for example, Reference 6), but their use requires iterative or graphical procedures and the values of parameters which are generally not well defined.

Reasonable values for α_T have been obtained without resorting to elaborate methods by using the formula

$$\alpha_T = \frac{2C_{D_f}}{\pi N_B} \frac{\mu^2}{\lambda} \tag{8}$$

where C_{D_f} is the fuselage drag coefficient, defined as the ratio of fuselage drag to $\frac{\pi}{2}\rho V_f^2 R^2$. Equation (8) was obtained by neglecting rotor in-plane drag and fuselage lift. The angle α_T, if assumed small, must then be simply the ratio of fuselage drag to rotor thrust (aircraft weight). Values for α_T obtained from Equation (8) were found to be within 20 to 30 percent of measured values for a UH-1A helicopter (from Reference 7) using a value for C_{D_f} of .014 (Reference 8).

Wake-Vortex Core Radius, a

The nondimensionalized core radius of each vortex element must be specified as it is generated by a blade vortex. This core size should correspond to that of the tip vortex formed in the physical flow when the wake rolls up.

In order to obtain an estimate of the core size, three major simplifying assumptions have been made. First, all vorticity in the flow except that contained in the wake under analysis has been neglected. This may be rigorously justified as an adjunct to the development which follows, but the calculations are somewhat lengthy and so have been omitted. The justification uses the fact that some distance from the wake the flow before and after roll-up is effectively the same. Second, it is assumed that the wake may be considered as though it were generated by a wing of the same

geometry as the blade in steady translational flight. That is, the tip and root vortices of a rotor blade are assumed to have the same core size as the tip vortices generated by a wing of the same aspect ratio in steady translational flight, and having the same loading as the blade had when it generated the segment of wake being analyzed. Third, it is assumed that the roll-up of the wake of a wing in steady translational flight can be treated as an unsteady two-dimensional problem rather than a steady three-dimensional one. The only justification (other than intuitive argument) for the latter two assumptions is that they do yield results which appear to be realistic.

Consider, then, a wing of large aspect ratio in steady translational flight, as shown in Figure 7. If Γ denotes the circulation about the wing, then at some position x in the wake upstream of the point where roll-up begins (View A-A, Figure 7), the circulation per unit length $\gamma(y)$ is given by

$$\gamma(y) = -\frac{d\Gamma}{dy} = \omega h \tag{9}$$

where $\omega(y)$ is the magnitude of the vorticity in the wake and $h(y)$ is the thickness of the wake sheet (see Figure 7). Given the loading on the wing - i.e., on the rotor blade at some azimuth - $\gamma(y)$ may then be specified through Equation (9). Note that $\gamma = 0$ at some point, say y_o, where Γ is a maximum. Also, since $\Gamma(-b) = \Gamma(b) = 0$, $-b$ corresponding to blade root and b to blade tip, it follows that

$$-\int_{-b}^{y_o} \gamma(y)\,dy = \int_{y_o}^{b} \gamma(y)\,dy = \Gamma_m$$

where Γ_m denotes the maximum value of $\Gamma(y)$. Replacing variation in x in the wake by variation in time in a plane parallel to the y-z plane and fixed in the wake, the sheet of vorticity would be observed to roll up into a pair of vortices whose cores consist of the rotational fluid which was contained in the sheet.

This process will be assumed, in what follows, to be two-dimensional. That is, the flow in the wake-fixed plane is taken to be the same as though the wake were extended to positive and negative infinity in the x-direction, and

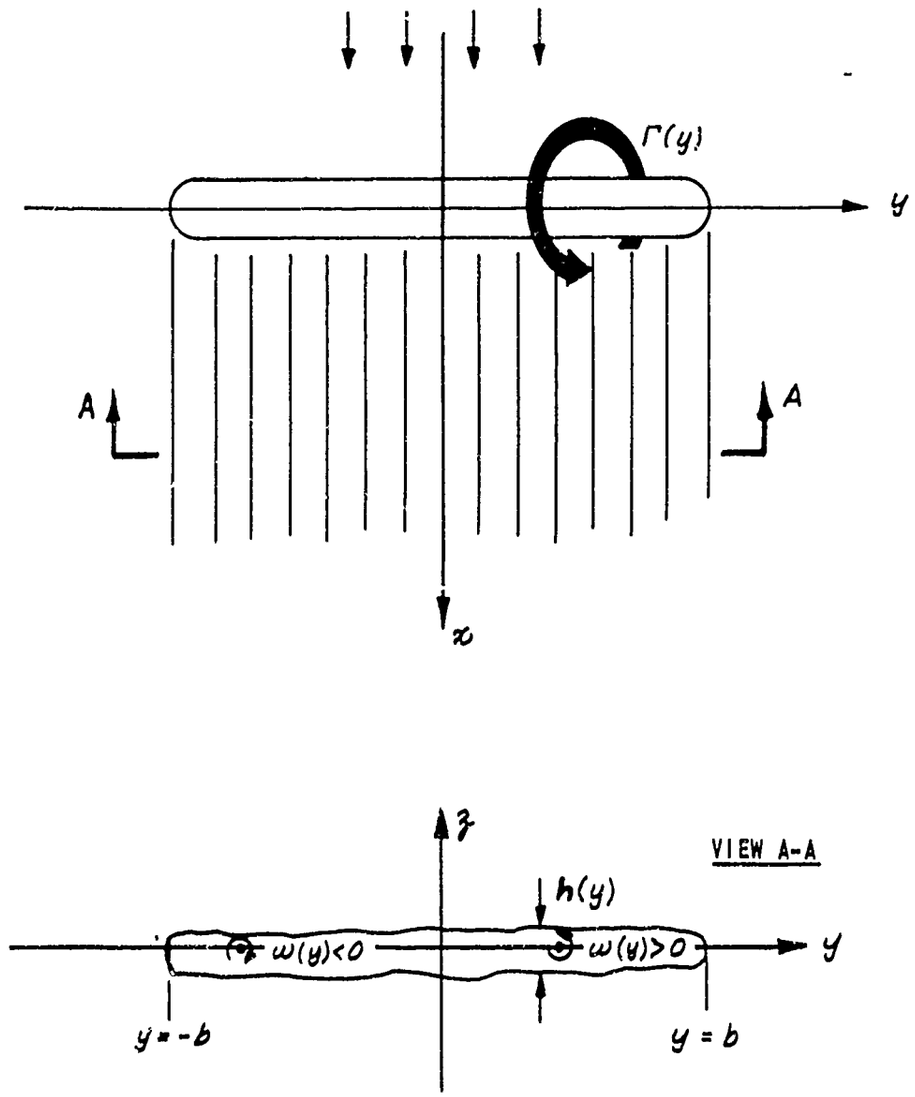

Figure 7 REPRESENTATION OF THE WAKE BEFORE ROLL-UP

that in each plane parallel to that plane the flows are identical; or taken still another way, it is assumed that derivatives with respect to x are small in comparison to changes in y or z insofar as roll-up is concerned.

If the cores of the vortices formed by the roll-up are assumed to be of circular section and of approximately uniform vorticity, and if it is further assumed that ω is constant in the sheet before roll-up (except at y_o, where it changes sign), it follows that the core radii of the two vortices will be equal. Further, because the moment of impulse of the flow is conserved, the vortices locate on the y-axis with their respective positions $y = y_L$ and $y = y_R$ given by

$$y_L = \frac{1}{(-\Gamma_m)} \int_{-b}^{y_o} y\,\gamma(y)\,dy$$

$$y_R = \frac{1}{\Gamma_m} \int_{y_o}^{b} y\,\gamma(y)\,dy\,. \tag{10}$$

The situation after roll-up is as shown in Figure 8.

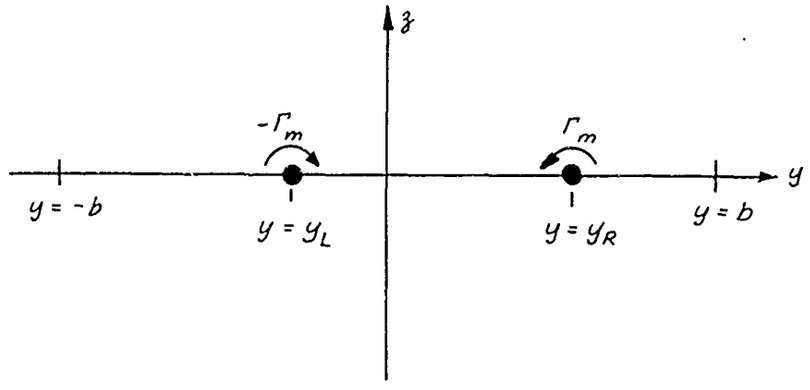

Figure 8 REPRESENTATION OF THE WAKE AFTER ROLL-UP

If viscous effects are neglected, the kinetic energy of the flow per unit depth, T, must be conserved. By deriving expressions for T for before and after roll-up and equating them, a relationship for core radius a may be obtained.

From Reference 9, T is given, in general, by

$$T = -\frac{\rho}{2}\iint \omega \Psi \, dy \, dz \tag{11}$$

where

$$\Psi(y,z) = \frac{1}{2\pi}\iint \omega \ln\left[\frac{(y-\eta)^2+(z-\zeta)^2}{b^2}\right]^{1/2} d\eta \, d\zeta .$$

The integrals are taken over the entire area where ω is not zero. If $\frac{\gamma}{h}$ is substituted for ω in Equation (11) and h is assumed to be much less than b, the integrands may be simplified and the integrals evaluated. It is then found that, in the limit of vanishing sheet thickness, T before roll-up is given by

$$T = -\frac{\rho}{4\pi}\int_{-b}^{b}\int_{-b}^{b} \gamma(y)\,\gamma(\eta) \ln\left|\frac{y-\eta}{b}\right| dy \, d\eta . \tag{12}$$

Similarly, it is found that after roll-up,

$$T = \frac{\rho \Gamma_m^2}{2\pi}\left[\ln\left(\frac{y_R - y_L}{a}\right) + \frac{1}{4}\right] \tag{13}$$

so that the core radius a is determined from

$$\ln\left(\frac{y_R - y_L}{a}\right) = -\frac{1}{2}\int_{-b}^{b}\int_{-b}^{b} \frac{\gamma(y)\gamma(\eta)}{\Gamma_m^2} \ln\left|\frac{y-\eta}{b}\right| dy \, d\eta - \frac{1}{8} . \tag{14}$$

The result of Equation (14) may be put in a form more directly related to blade circulation as follows. Let Γ be expanded in a Fourier series, according to

$$\frac{\Gamma(\theta)}{\Gamma_m} = \frac{2}{\pi}\sum_{k=1}^{\infty} a_k \sin k\theta \qquad (15)$$

where $\cos\theta = \frac{y}{b}$. Then

$$\gamma(\theta) = \frac{1}{b\sin\theta}\frac{d\Gamma}{d\theta}$$

$$= \frac{2\Gamma_m}{\pi b\sin\theta}\sum_{k=1}^{\infty} k a_k \cos k\theta$$

Also, it is found from Equations (10) and (15) that

$$\frac{y_R - y_L}{b} = \frac{1}{b\Gamma_m}\int_{-b}^{b} y\gamma(y)dy$$

$$= a_1$$

If γ and $y_R - y_L$ are then substituted in Equation (14) and the integrations performed, it is found that

$$\frac{a}{R} = \frac{a_1}{2}\left(1 - \frac{r_o}{R}\right) e^{-\left[\sum_{k=1}^{\infty} k a_k^2 - \frac{1}{4}\right]} \qquad (16)$$

where r_o is the radial distance from the axis of revolution to the blade root.

An indication of the order of magnitude of core radius predicted by Equation (16) can be obtained by considering the case of an elliptic distribution for Γ (i.e., minimum induced drag, and hence maximum core radius). Supposing r_o to be zero, and substituting $a_1 = \frac{\pi}{2}$, $a_2 = a_3 = \cdots = 0$, find a value for $\frac{a}{R}$ of .0862.

Some numerical computations were performed, utilizing Equation (16), to determine the order of magnitude of core size predicted by this method and to provide an indication of the amount by which the core size varies with azimuth and forward speed. Data for the computations were generated by a

blade-loads program that CAL developed for the U. S. Army Aviation Materiel Laboratories (these results are generally in good agreement with experimentally obtained loadings). Three flight conditions were considered: (1) a UH-1A rotor at 105 kt. forward speed, (2) a UH-1A rotor at 30 kt. forward speed, and (3) a 5-foot-diameter experimental rotor in hovering flight. The ratio of rotor radius to vortex core radius was calculated for four azimuth positions of the blades in each case, using a 12-point harmonic analysis of circulation distribution. The results of the computations are tabulated below.

	Ratio of Rotor Radius to Core Radius			
Flight Condition	$\psi = 0$	$\psi = 90^{\circ}$	$\psi = 180^{\circ}$	$\psi = 270^{\circ}$
105 kt. - UH-1A	24.0	13.3	17.5	21.0
30 kt. - UH-1A	18.7	15.0	14.4	24.1
Hover - 5 Ft. Rotor	21.9	21.9	21.9	21.9

This method of predicting vortex core radius appears to provide a reasonable order of magnitude for that quantity - from about 4.0 to 7.5 percent of rotor radius. Most notable is the lack of any substantial variation in core radius either with forward speed or azimuth position. The variations obtained may be considered small since a change of 20 or 30 percent in core radius produces a much smaller change in self-induced velocity, with the latter varying as the logarithm of the former.

It was, therefore, possible to incorporate a major simplification in the digital computer program, by assigning a representative value of .05 to the ratio of core radius to rotor radius, independent of azimuth position or flight conditions. It was verified that this simplification does not cause an appreciable error.

5. RESULTS OF COMPUTATIONS

GENERAL REMARKS

Wake flow calculations were carried out in two phases. The program was first operated with the fuselage representation omitted. The sensitivity of the wake model to various parameters and the general character of the solutions were investigated, and a comparison of computed flow with experimental measurements was made. Once it was determined that the model was both operationally practical and consituted a valid representation of the flow, extensive calculations were performed which incorporated the fuselage representation. The latter results correspond to a UH-1B helicopter at five different forward speeds ranging from hover to high-speed cruise. Before discussing the details of the results obtained, though, the following remarks concerning the qualitative nature of the flows computed should be made.

There was some concern during the formulation as to the numerical and/or physical stability of the model; i.e., it was questioned whether the approximations made in integration or possibly the nature of vortical flows themselves would allow a periodic flow to be established. It was found, however, that the model generally does produce a periodic flow, even though the initial, or starting, wake configuration may differ greatly from the periodically varying wake geometry. There was some evidence of nonperiodic behavior at very low advance ratios, however, which appears to be attributable to an inherent instability in free-vortex flows. At an advance ratio below about .07, wake-induced effects are comparable with the magnitude of the free stream, so the individual vortices then interact to a great extent. It results that, for very low advance ratios, an increasingly nonperiodic flow is evident in proceeding down the wake, starting from about two to three revolutions of wake below the rotor. The wake geometry and the flow is periodic above this point (which is about half a rotor radius below the rotor plane, for moderate loading). Halving the interval of integration or adding wake elements does not noticeably alter this situation.

The general character of the wake geometries obtained is illustrated in Figure 9. The tip vortices for a two-bladed rotor are shown drawn in perspective projection for the case of $\mu = .14$, $\lambda = .00236$, $\alpha_T = 2.3$ degrees and $\Delta\psi = 15$ degrees. A periodic flow was obtained for this case. The individual wake elements were projected as straight lines between the wake reference points. Both the initial wake configuration and the configuration at $\psi = 0$ after periodicity was established are shown so that the extent of the wake-induced distortion may be seen. The large vertical displacements two to three rotor radii downstream (which are somewhat exaggerated by the perspective) might in part be attributable to the size of the integration increment taken, and so are not necessarily representative of the flow in the far wake. The concentration of vortices at the lateral extremes of the wake, giving the appearance of the wake behind a conventional wing, is clearly evident in the figure.

COMPARISONS WITH EXPERIMENTAL MEASUREMENTS

In order to properly assess the model of the rotor, it was decided to compare computed and measured flows. Satisfactory quantitative data pertaining to instantaneous fluid velocities could not be located. A rather extensive wind tunnel program was carried out by NACA, however, to measure average velocities in the wake of a two-bladed teetering rotor at moderate to high advance ratios. The results of the program are presented in Reference 10. The data are presented in Reference 10 as plots of $\frac{\bar{v}}{v_o}$ as a function of the three spacial coordinates, where $\bar{v}$ is the time average of the induced downwash (i.e., with the free stream component subtracted off) normal to the tip-path-plane, and v_o is the value for that quantity as predicted by simple momentum theory. For moderate to high advance ratio, $v_o = \Omega R C_T/(2\mu)$ where C_T is rotor thrust coefficient. It was estimated by the authors of that report that the error accumulated in measuring $\bar{v}/v_o$ was less than about $\pm$ 0.1 at the moderate advance ratios.

A comparison was made of the average of computed velocities with these measurements for one of the test flight conditions. For the case chosen,

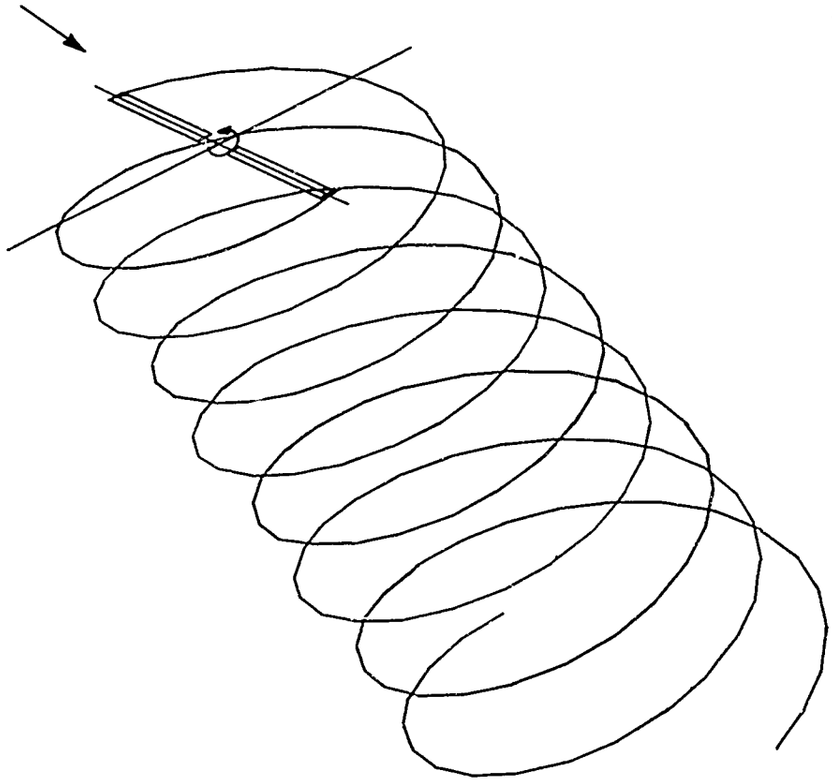

SKEW-HELICAL WAKE CONFIGURATION

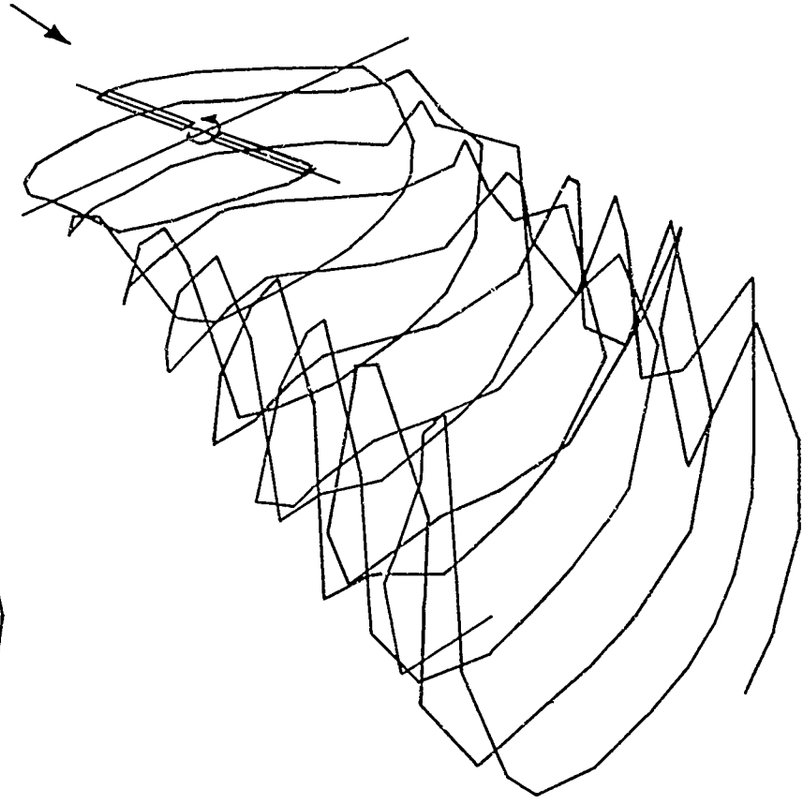

DISTORTED WAKE

Figure 9 COMPARISON OF INITIAL WAKE GEOMETRY WITH THE CONFIGURATION AFTER PERIODICITY IS ESTABLISHED FOR μ = 0.14, λ = 0.00236, AND α_T = 2.3 DEGREES

the advance ratio μ was 0.14, the thrust coefficient C_T was .00371, where C_T is defined as the ratio of rotor thrust to $\pi\rho\Omega^2R^4$, and the inclination of the tip-path plane α_T was 2.3 degrees. The comparison of computed and measured results is shown plotted in Figure 10 through 14. The data is plotted for the coordinate system of Figure 1, with the coordinates non-dimensionalized by rotor radius.

Figures 10 through 12 show the variation of $\bar{v}/v_0$ with y for values of x of -0.5, 0 and 0.5 respectively, with each figure showing the variation at both z = -0.07 and z = -0.2. The computed and measured values are seen to agree quite well for all three values of x. It should be noted that this agreement is obtained even though the instantaneous computed values of the downwash vary a great deal from the mean. The extent of the variation is illustrated in Figure 13. In this figure, the ratio of the induced downwash v to v_0 is plotted against blade azimuth ψ for x = 0.5, and y = 0.5 for both z = -0.07 and z = -0.2. The computed and measured mean values are also indicated on the plots.

Rather poor agreement was obtained downstream of the rotor in the x-z plane. This may be seen in Figure 14, where the variation of $\bar{v}/v_0$ with z is plotted for x = 1.07 and x = 2.07, with y = 0. The lack of agreement may be due in part to the effects of the structure supporting the test rotor. These effects were not discussed by the experimenters in their report. Note that at x = 0.5 (Figure 12), the agreement was poor near y = 0, while this is not the case at x = -0.5 (Figure 10), where the rotor support could have little effect on the flow.

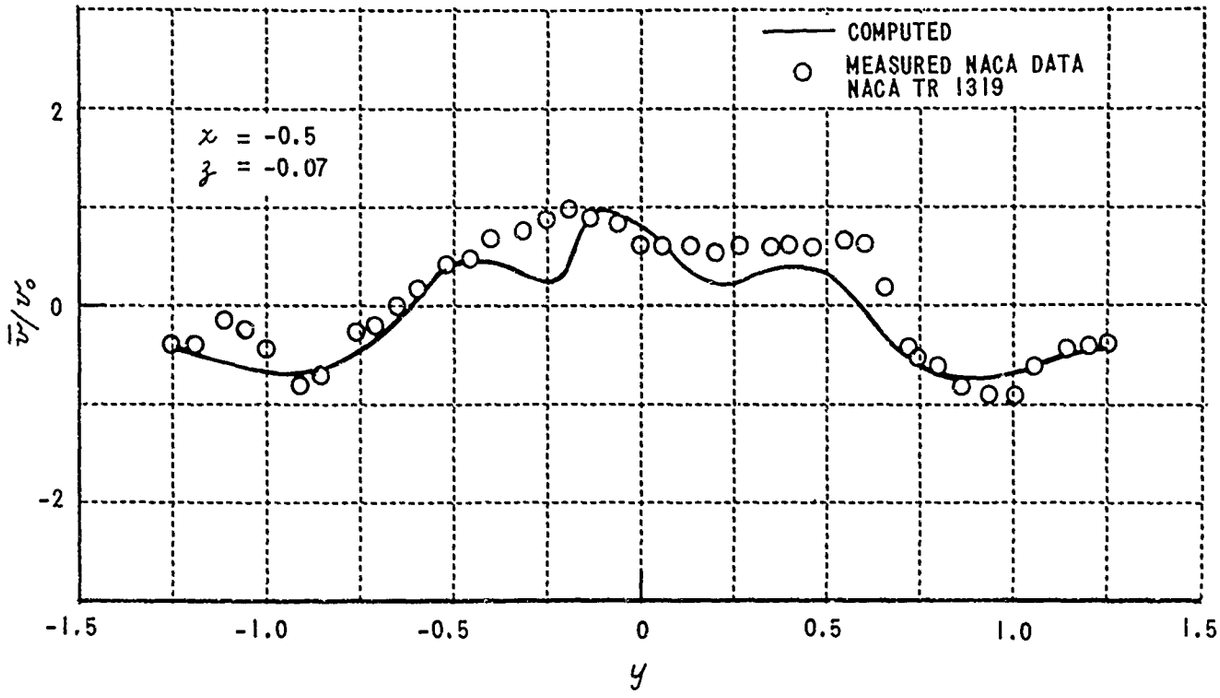

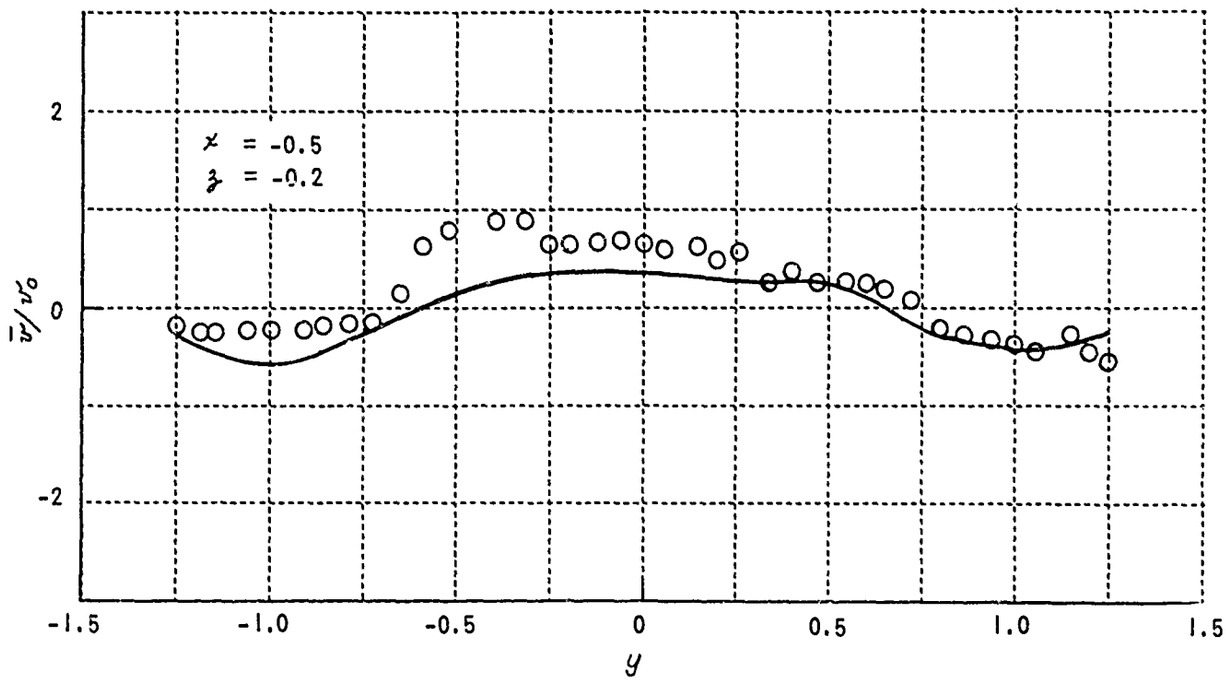

Figure 10 COMPARISON OF COMPUTED AND MEASURED INDUCED DOWNWASH BELOW THE ROTOR PLANE, $\mu = 0.14$, $C_T = 0.00371$, $x = -0.5$

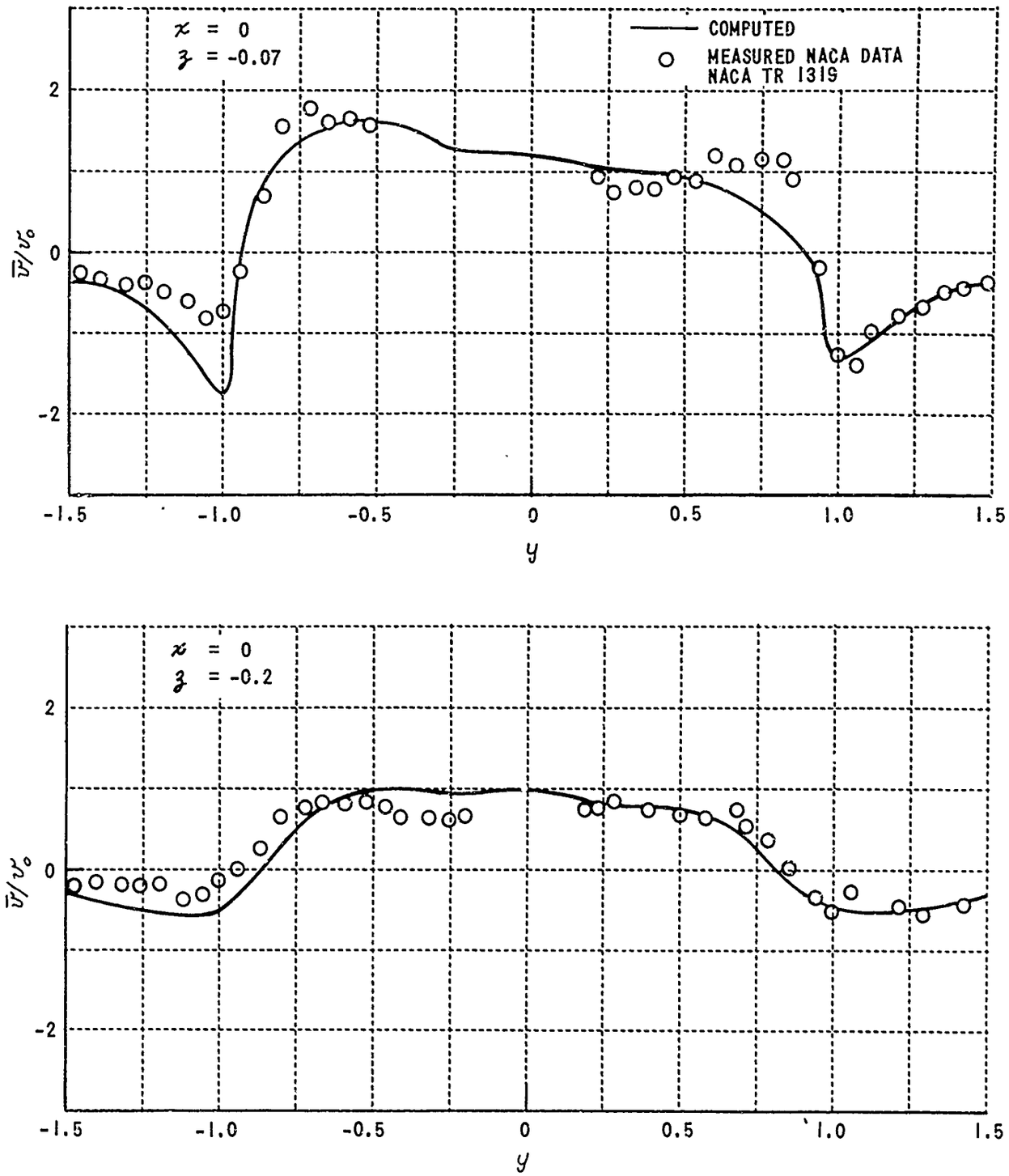

Figure 11 COMPARISON OF COMPUTED AND MEASURED INDUCED DOWNWASH BELOW THE ROTOR PLANE, $\mu = 0.14$, $C_T = 0.00371$, $\chi = 0$

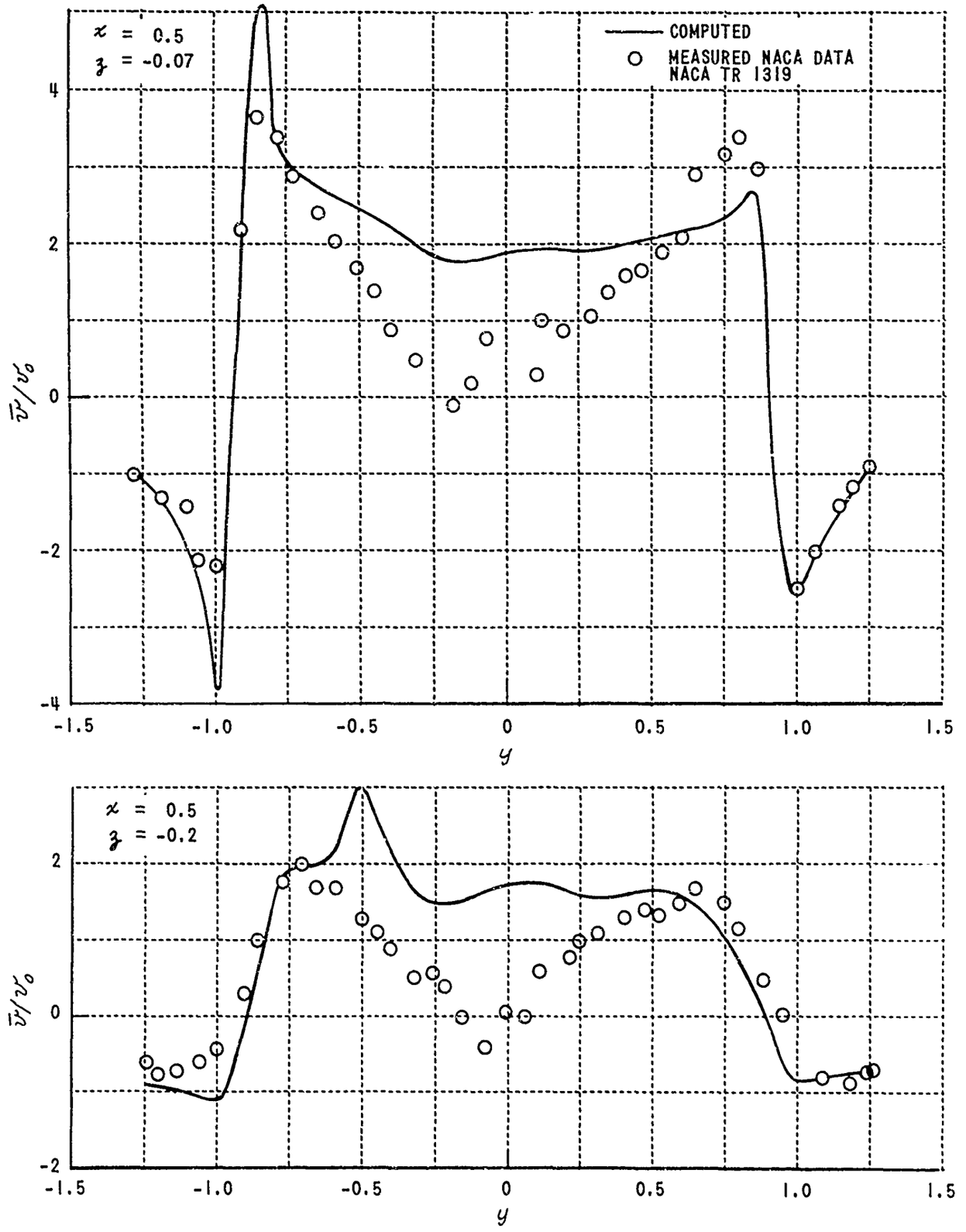

Figure 12 COMPARISON OF COMPUTED AND MEASURED INDUCED DOWNWASH BELOW THE ROTOR PLANE, $\mu = 0.14$, $C_T = 0.00371$, $\chi = 0.5$

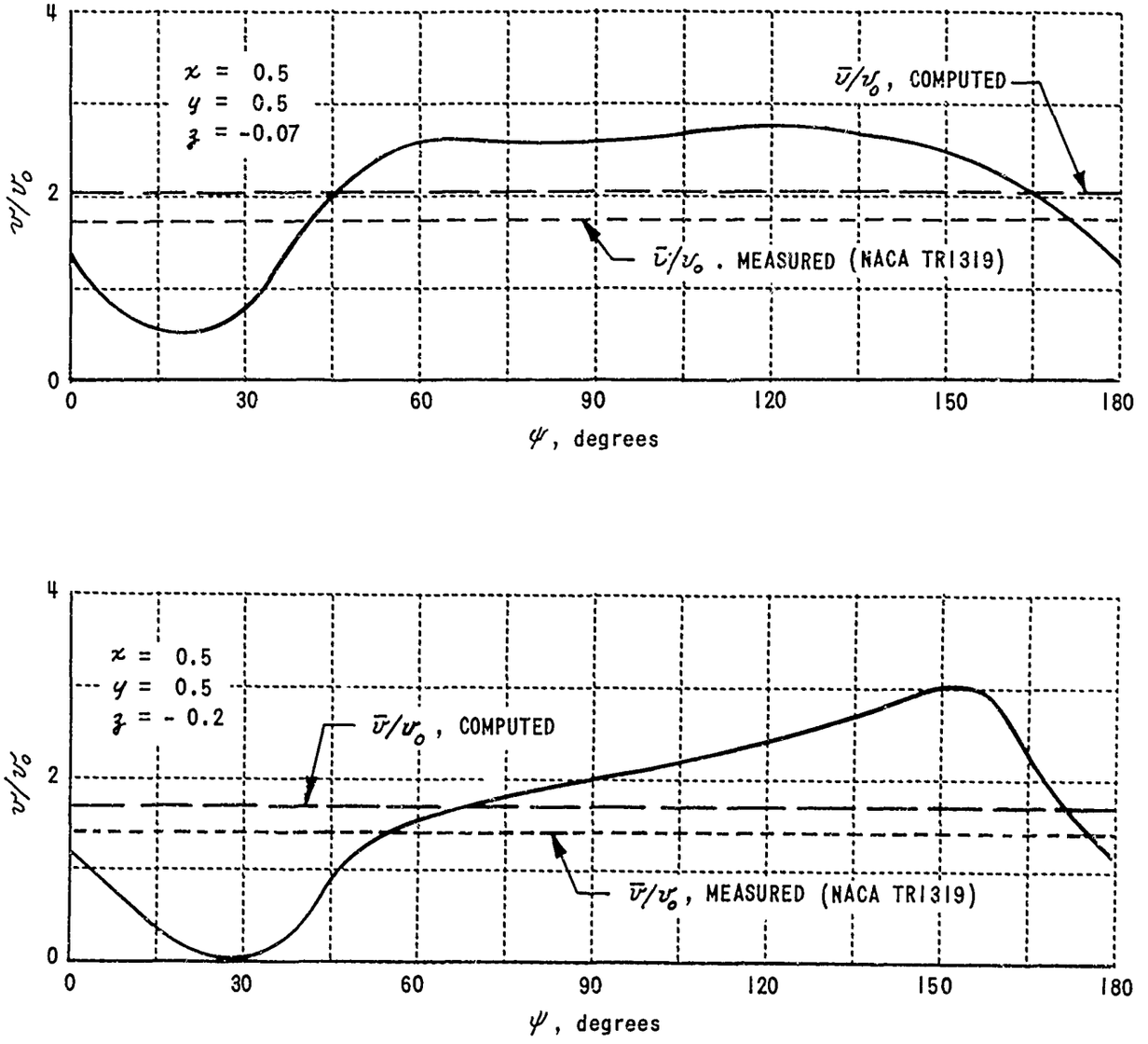

Figure 13 COMPUTED VARIATION OVER ONE PERIOD OF THE INDUCED DOWNWASH AT TWO POINTS BELOW THE ROTOR PLANE

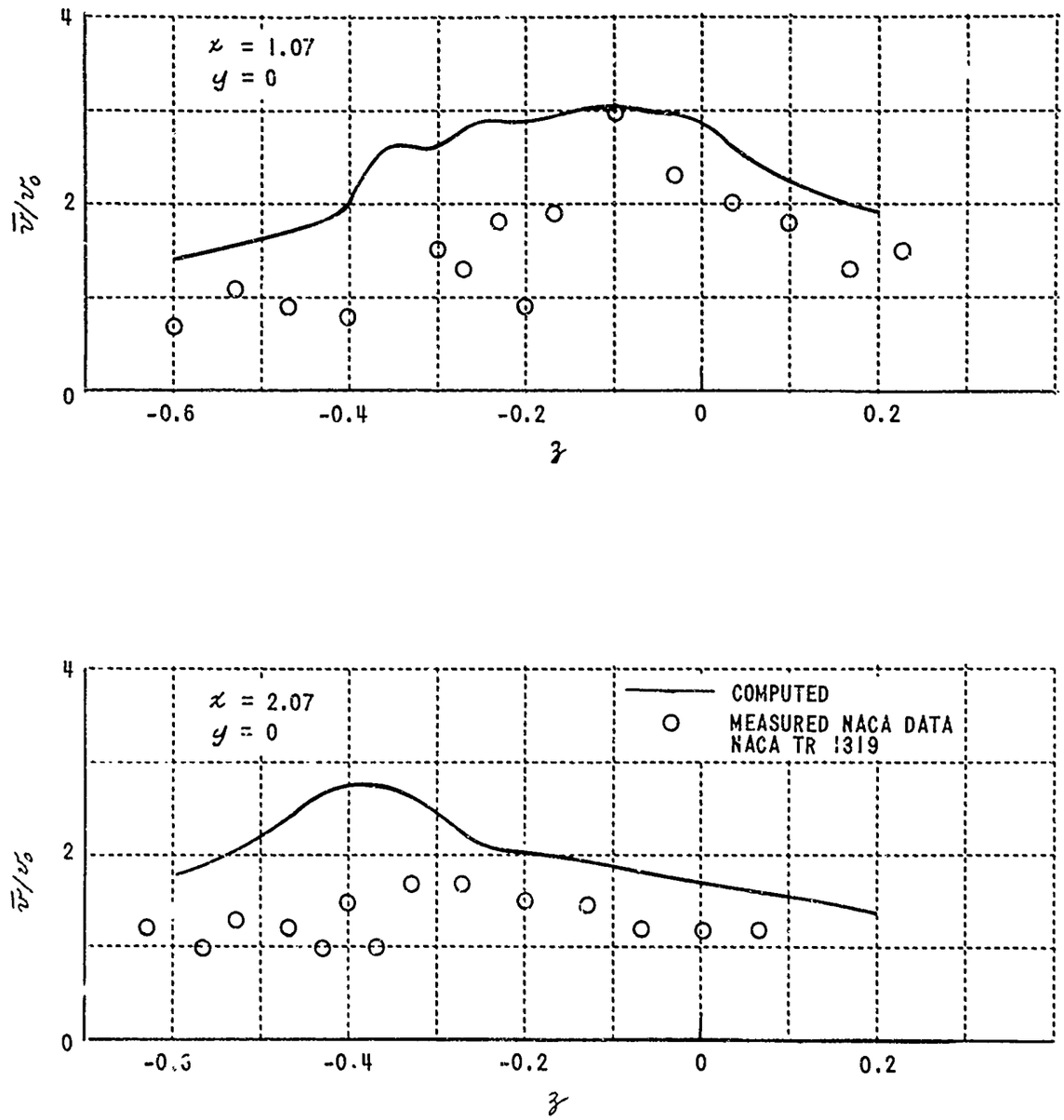

Figure 14 COMPARISON OF COMPUTED AND MEASURED AVERAGE INDUCED DOWNWASH IN THE x-z PLANE, $\mu = 0.14$, $C_T = 0.00371$

FLOW CALCULATIONS FOR A UH-1B HELICOPTER

Extensive calculations were performed to determine the flow in the vicinity of a UH-1B helicopter. The aircraft was assumed to have a gross weight of 5675 pounds (about two thirds of maximum gross weight) and a rotor speed of 31.4 radians per second, giving a value for the blade loading parameter, λ, of .00209. A total of five cases were treated, corresponding to forward speeds from 0 to 110 knots. The values of the important parameters for these cases are tabulated below.

Advance Ratio μ	Tip-Path-Plane Angle α_T, degrees	Number of Revolutions of Wake per Blade
0	0	7
.0732	.655	5
.1465	2.62	4
.220	5.91	3
.269	8.84	2

In subsequent discussions, the above cases will be identified by the appropriate value of advance ratio. In all cases, $\Delta\psi$ = 30 degrees, and of course, N_B = 2. The fuselage was represented by a total of 192 source-sheet elements. The somewhat simplified geometry used for the surface replacing the fuselage is depicted in plan and elevation in Figure 15. The coordinate system in Figure 15, and the one used for the plots of flows following Figure 15, is that of Figure 1, nondimensionalized by rotor radius.

Flow calculations were performed within the volume external to the fuselage and having the limits

$$-1.1 \leq x \leq -0.1$$

$$-0.45 \leq y \leq +0.45$$

$$-0.45 \leq z \leq -0.15$$

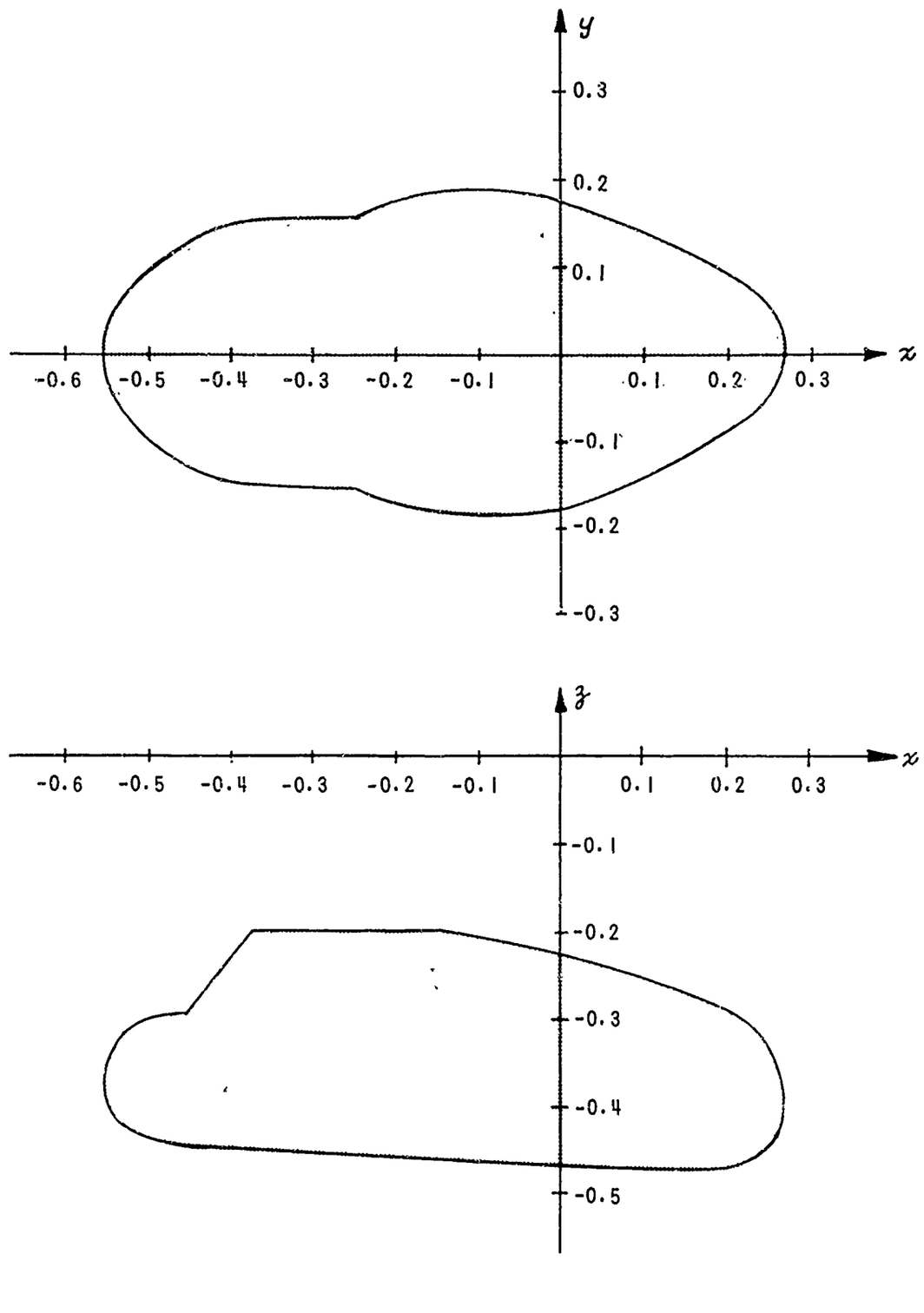

Figure 15 FUSELAGE REPRESENTATION USED IN FLOW CALCULATIONS FOR A UH-1B HELICOPTER

In all five cases, a periodic flow was established within this volume.

The data are presented in Figures 16 though 55, at the end of the Chapter, as plots of the dimensionless velocity components V_x , V_y and V_z, which relate to their dimensional counterparts by a factor $\lambda \Omega R$. The time averages over one period of V_x, V_y and V_z are also plotted; these averages being denoted by $\bar{V}_x$, $\bar{V}_y$ and $\bar{V}_z$, respectively.

Caution should be exercised in comparing plots for different advance ratios. Scales and, in some instances, the quantities plotted, were adjusted for each advance ratio to suit the data.

THE FLOW AT HIGH ADVANCE RATIOS

The flows at advance ratios of .1465, .220, and .269 are characterized by a lack of unsteadiness over most of the region investigated. Figures 16, 17 and 18 show the variation of the flow with x at $y = 0$ and $z = -.45$ for these three advance ratios. The variations for rotor azimuths of 0 and 90 degrees and the time averages for one period are shown on each figure. The variations with x at other azimuth positions are not significantly different from the ones plotted. The flow is nearly constant with azimuth because the fuselage and free-stream contributions dominate at high advance ratios. This may be seen from Figure 19, which compares the total flow with the contributions V_{y_i} and V_{z_i} of the wake and blades to V_y and V_z, for $\mu = .220$ and $\psi = 0$. Wake and blade contributions to V_x were too small to be seen on the scale used.

The dominance of the fuselage and free stream is further illustrated by Figures 20 through 36, on which are plotted flow variations with x and y in selected regions at the three highest advance ratios. In those regions where there were discernable flow variations with azimuth, plots are shown for six azimuth positions. Otherwise, only the plots for $\psi = 0$ and $\psi = 90$ degrees are given. As might be expected, somewhat more effect of the blades is felt closer to the rotor plane (Figures 26, 31, and 36, for example). Spacial variations are still attributable primarily to the fuselage, however.

The assumption that the free stream experienced by the fuselage is constant in time is clearly justified, since time variations of the flow in the region occupied by the fuselage ($z \leq -.2$) are negligible. It should be noted, though, that a similar statement cannot be made regarding the assumption that this free stream is also uniform. Figure 37 shows the spacial variation of the downwash at $\psi = 0$ in the region where the fuselage is located, with the flow due to the fuselage omitted (i.e., with all source strengths zero), for $\mu = .1465$. The downwash can be seen to vary by as much as a factor of two in this region. While undoubtedly the flow is well reproduced some distance from the fuselage by simply averaging these variations in computing source strengths (the fuselage was found to cause only minor distortions of the wake at all five advance ratios) this may very well not be the case within, say, $0.1R$ of the fuselage. The error introduced by taking an average for the downwash in computing fuselage source strengths can be properly determined only by actually computing the source strengths needed to satisfy the flow tangency condition for the spacially varying stream depicted in Figure 37, and then comparing the flow obtained using these strengths with that obtained from strengths computed assuming the stream to be uniform. These calculations were not performed because of time limitations.

THE FLOW FOR HOVER AND LOW ADVANCE RATIO

There is no large free stream component of velocity to convect the wake from beneath the rotor plane in the cases of $\mu = 0$ and $\mu = .0732$, so the opportunity for interactions among the wake elements is much greater than at high advance ratio. As a result, the flow is correspondingly altered.

First, consider the flow for $\mu = .0732$. The computational results for this advance ratio are plotted in Figures 38 through 45. The general character of the curves is seen to be similar to that found at the higher advance ratios. The fluctuations with azimuth are larger, however. Close to the rotor plane ($z = -.25$ and $z = -.15$), a net upwash is obtained in some regions, and the shapes of the curves are considerably altered with changes in azimuth.

The amount contributed to the flow by the blades and wake at $\mu = .0732$ is indicated by the plots of Figure 46. While the fuselage and free stream still dominate the x-component at this advance ratio, the flow normal to the tip-path-plane is largely due to the wake.

The flow at $\mu = 0$ differs greatly from that for nonzero advance ratio both in the spacial variations and in the magnitudes of the velocity components. The results for hovering are plotted in Figures 47 through 53. The flow components in the x and y directions are seen to be comparatively small - on the order of 5 or 10 - over the whole region investigated, while V_z varies from small positive values to negative values of from 30 to 50. Those areas where large downwash occurs can be readily identified as lying within the envelope of the wake. The large azimuthal fluctuations in the flow are caused by the periodic passage of the wake vortices about this envelope.

It will be noted that the downwash within the wake is from three to five times greater in hover than it is when μ is not zero, even though the rotor loading is the same for all cases. An explanation for this may be obtained from simple momentum considerations. The rotor thrust must be derived from a given net flux of momentum in the negative z-direction, regardless of the advance ratio. In hovering flight, this entire flux must be carried by the downwash component of velocity. If the aircraft is in forward flight, however, the z-component of fluid momentum may be convected from a given control volume in both the x and z directions. Thus, the required flux is obtained at nonzero advance ratio without a large downwash component, the wake flow then being somewhat more comparable to that of a wing than a propeller.

The contribution of the fuselage to the total flow may be seen from Figure 54, where the total flow and that due to the wake and blades are compared. Variations with x are shown for $y = .3$, $z = -.45$ and $\psi = 0$. The fuselage may be seen to alter the downwash $(-V_z)$ by only about ten percent.

In further regard to the fuselage, it was found that the use of a uniform, steady downwash in computing the source strengths was well justified for the case of $\mu = 0$. Figure 55 shows the downwash variation in the x-z plane, at $z = -.25$ and $z = -.45$ for $\psi = 0$, which results when the fuselage representation is omitted. The downwash at other azimuths and over the remainder of the volume occupied by the fuselage was found to be approximately the same as shown in Figure 55, i.e., between 30 and 40. Thus, in hover, the fuselage lies well within the wake envelope and is indeed subjected to a nearly constant and uniform free stream.

Also shown in Figure 55 is the downwash in the location of the fuselage for $\mu = .0732$. In this case, large variations can be seen to occur spacially as wake vortices are swept directly over this region. These variations are much larger than those which occurred at the higher advance ratios (Figure 37). It would appear, then, that the approximations used in representing the fuselage are most open to question at the intermediate advance ratios, from about .05 to .10. In this range, the fuselage contributes substantially to the flow while experiencing large flow variations itself.

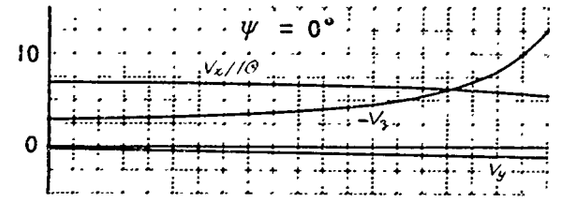

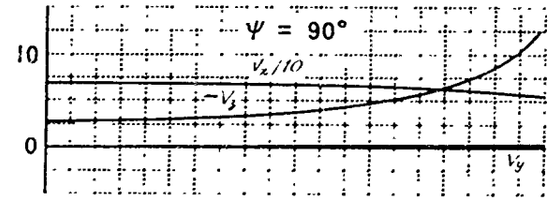

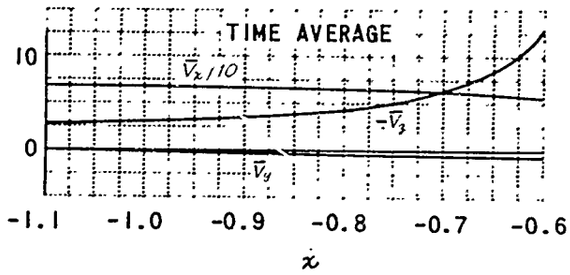

Figure 16 VARIATION OF VELOCITY COMPONENTS WITH x FOR $y = 0$, $z = -0.45$ AND $\mu = 0.1465$

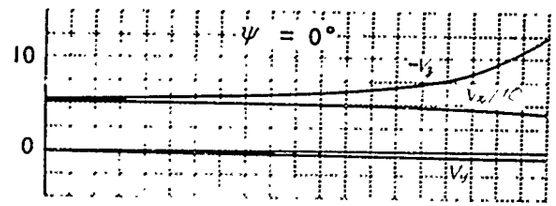

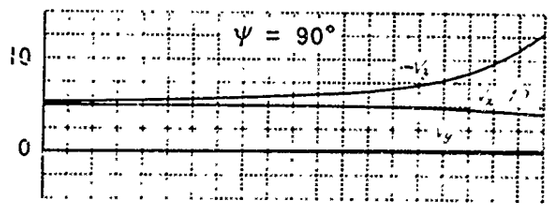

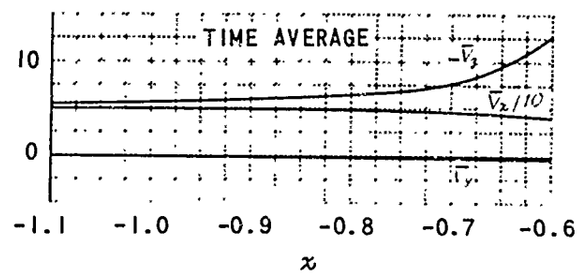

Figure 17 VARIATION OF VELOCITY COMPONENTS WITH x FOR $y = 0$, $z = -0.45$ AND $\mu = 0.220$

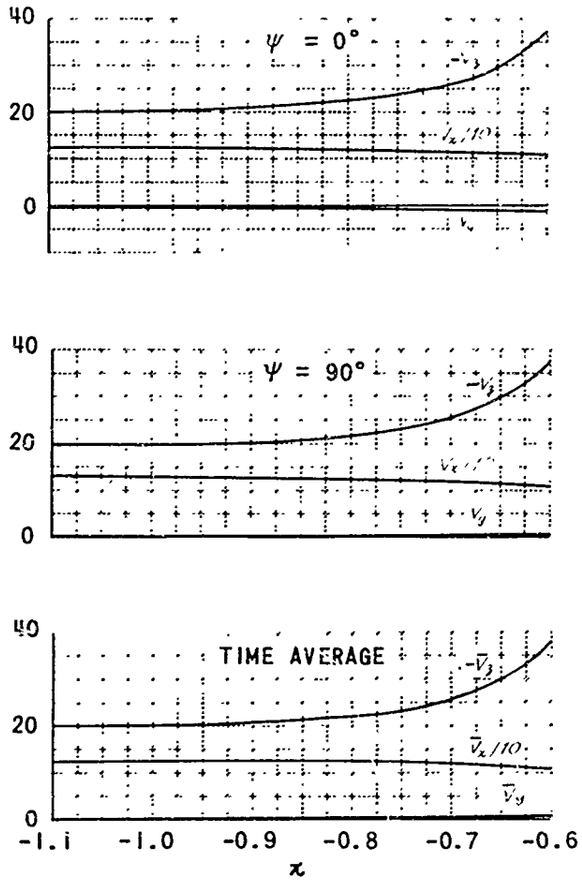

Figure 18 VARIATION OF VELOCITY COMPONENTS WITH x FOR $y = 0$, $z = -0.45$ AND $\mu = 0.269$

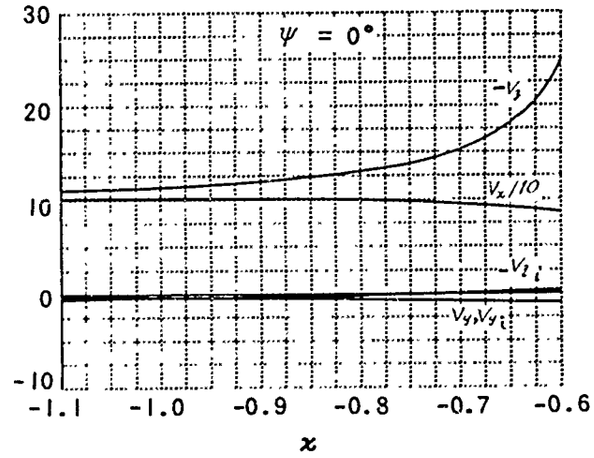

Figure 19 COMPARISON OF TOTAL FLOW WITH WAKE- AND BLADE-INDUCED FLOW FOR $y = 0$, $z = -0.45$ AND $\mu = 0.220$

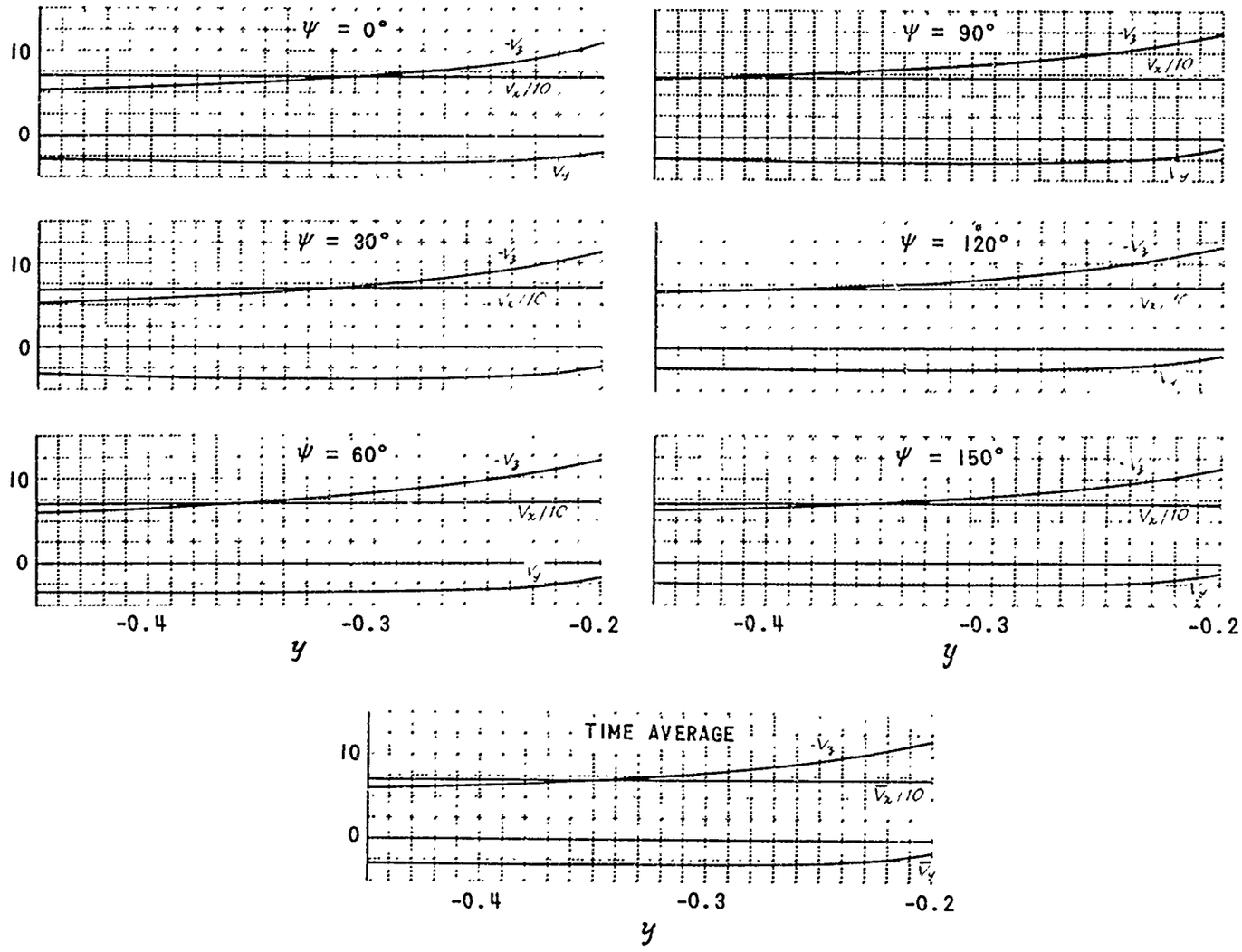

Figure 20 VARIATION OF VELOCITY COMPONENTS WITH y FOR $x = -0.25$, $z = -0.45$, $\mu = 0.1465$ AND $y < 0$

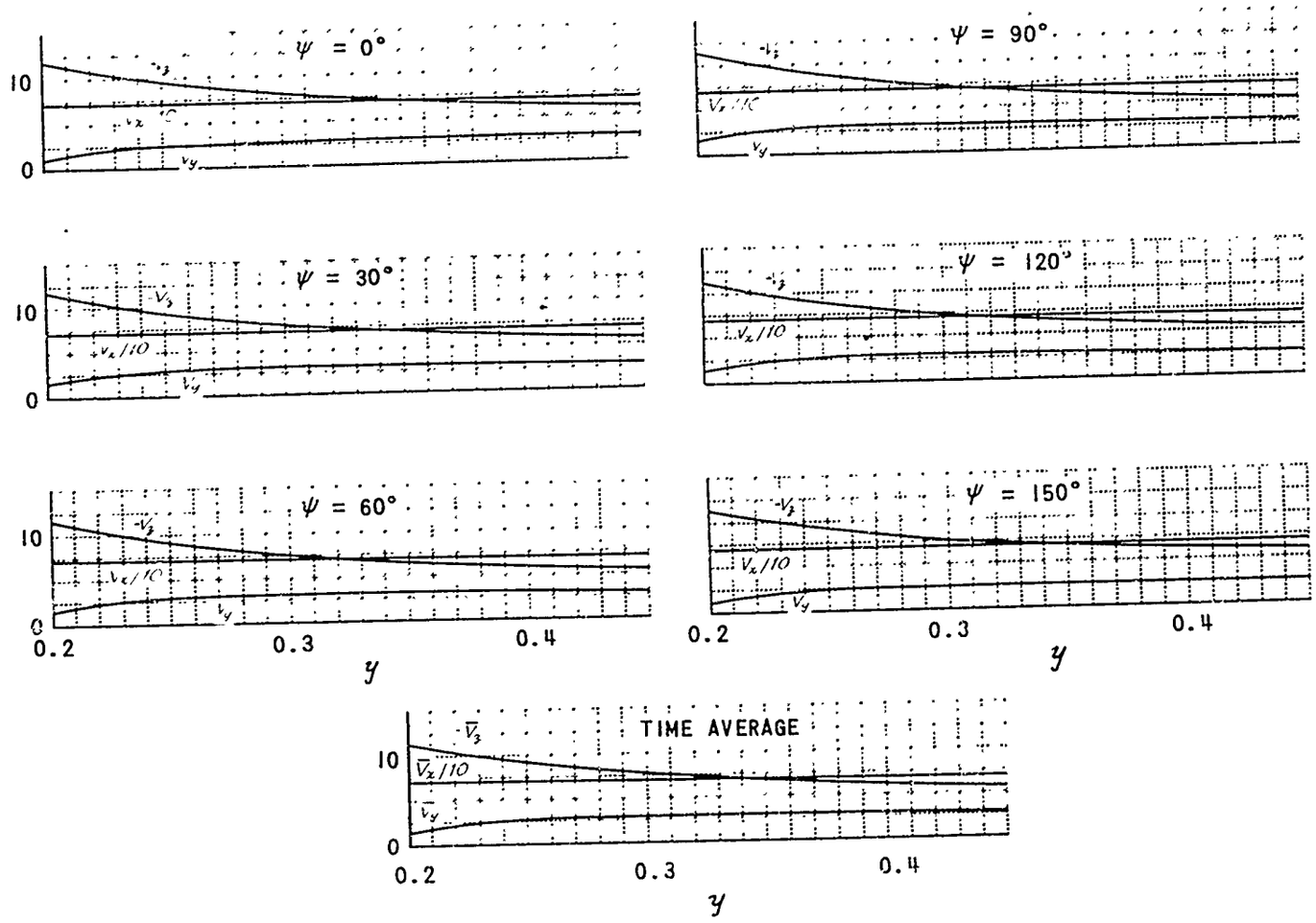

Figure 21 VARIATION OF VELOCITY COMPONENTS WITH y FOR $x = -0.25$, $z = -0.45$, $\mu = 0.1465$ AND $y > 0$

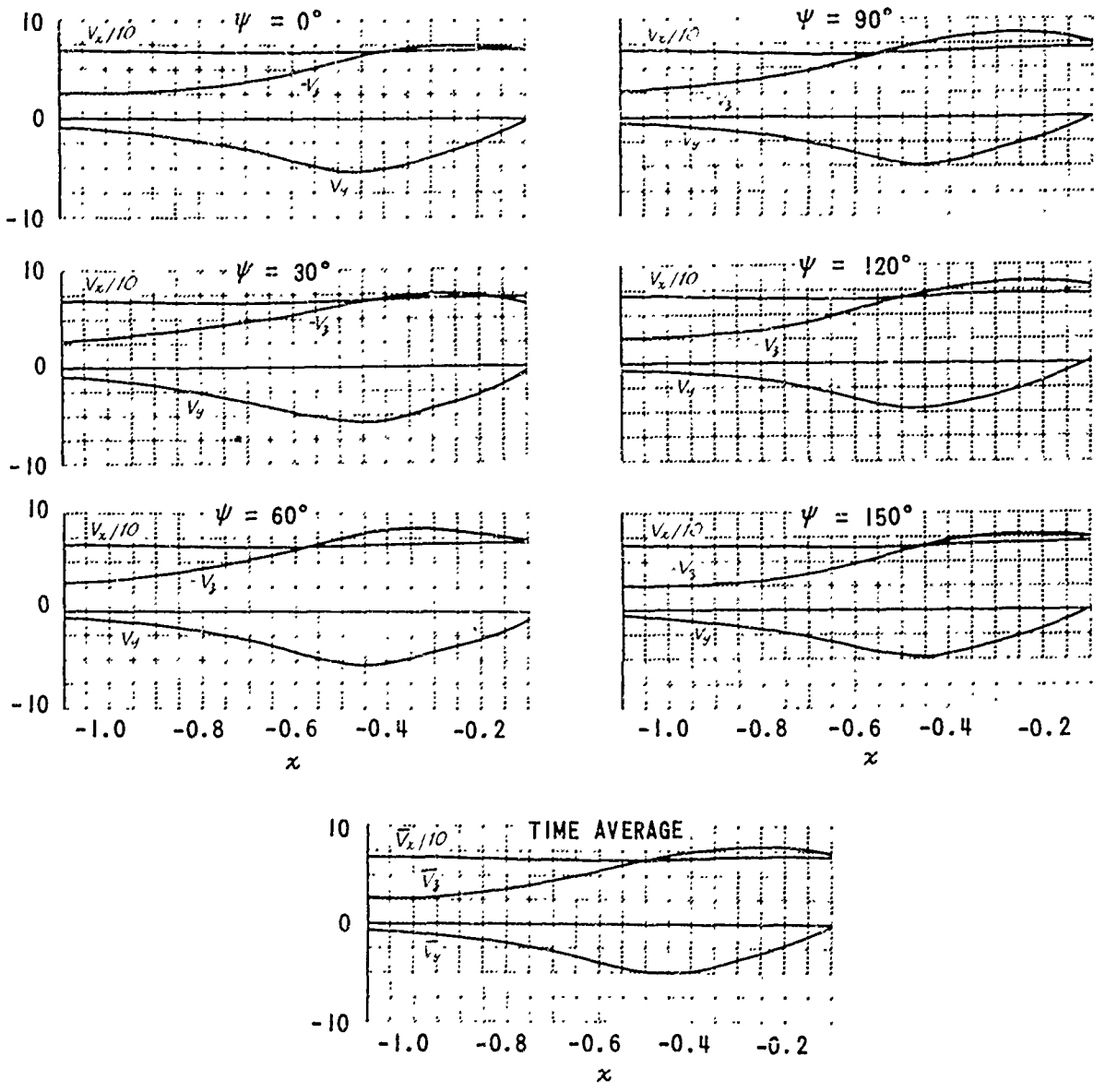

Figure 22 VARIATION OF VELOCITY COMPONENTS WITH x FOR y = -0.3, z = -0.45 AND μ = 0.1465

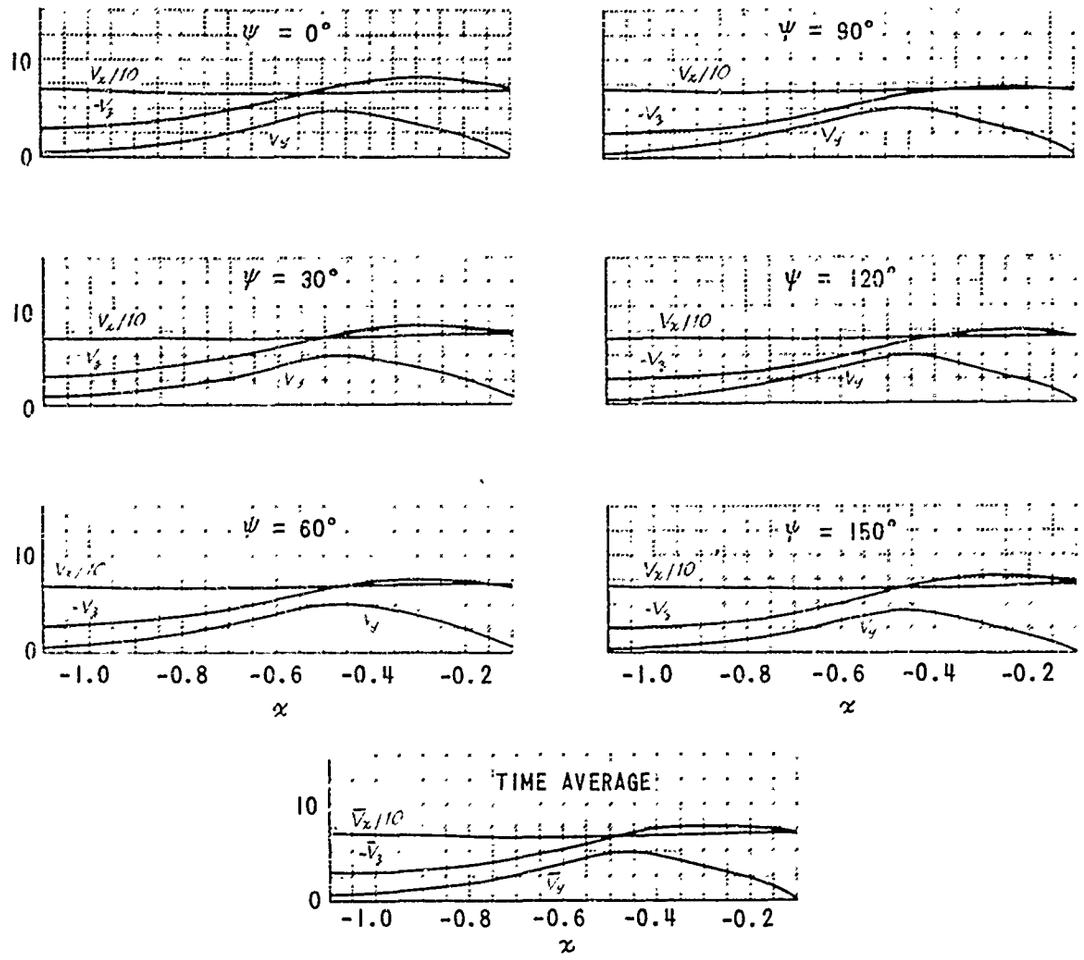

Figure 23 VARIATION OF VELOCITY COMPONENTS WITH x FOR $y = 0.3$, $z = -0.45$ AND $\mu = 0.1465$

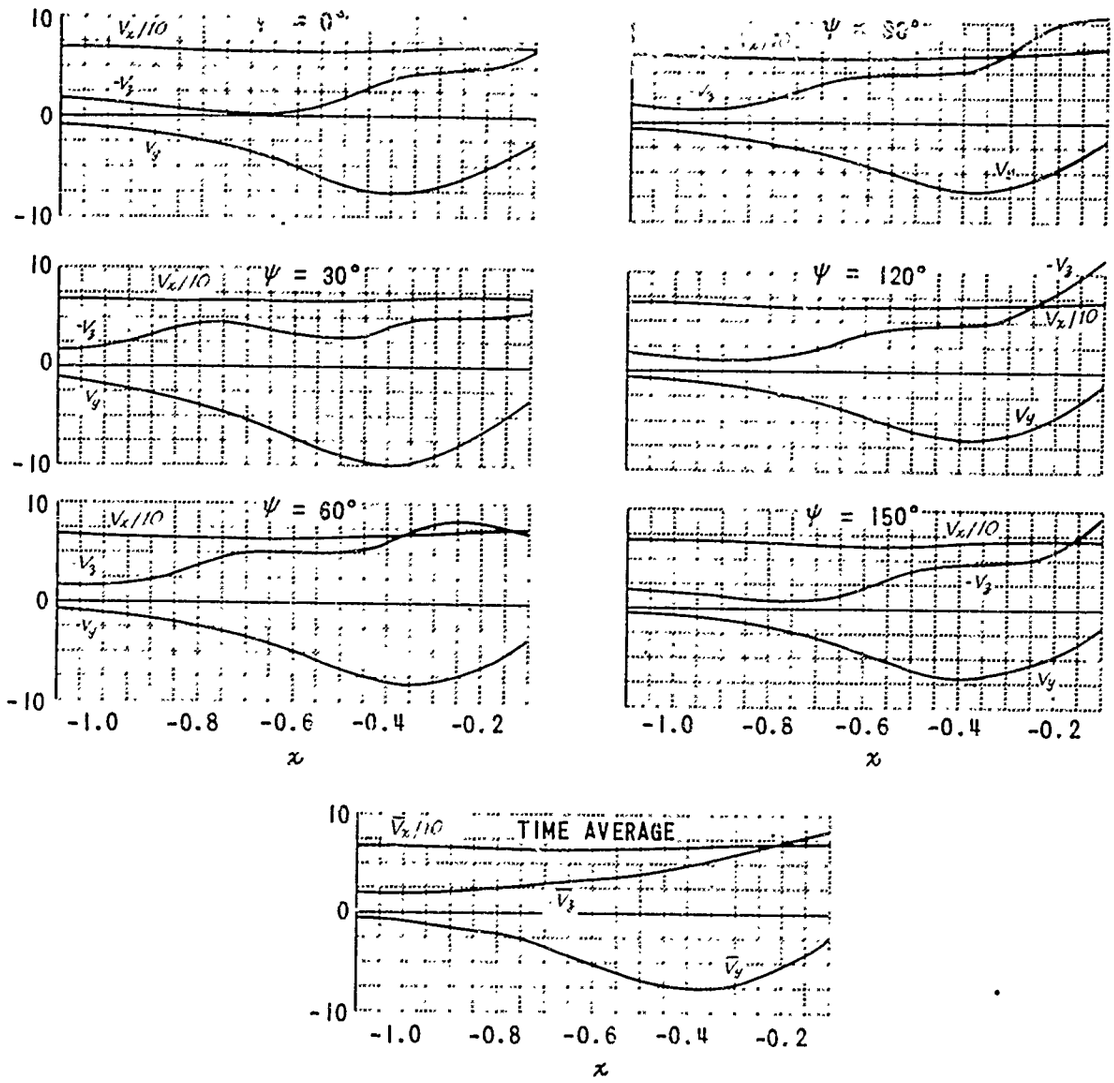

Figure 24 VARIATION OF VELOCITY COMPONENTS WITH x FOR y = -0.3, z = -0.25 AND μ = 0.1465

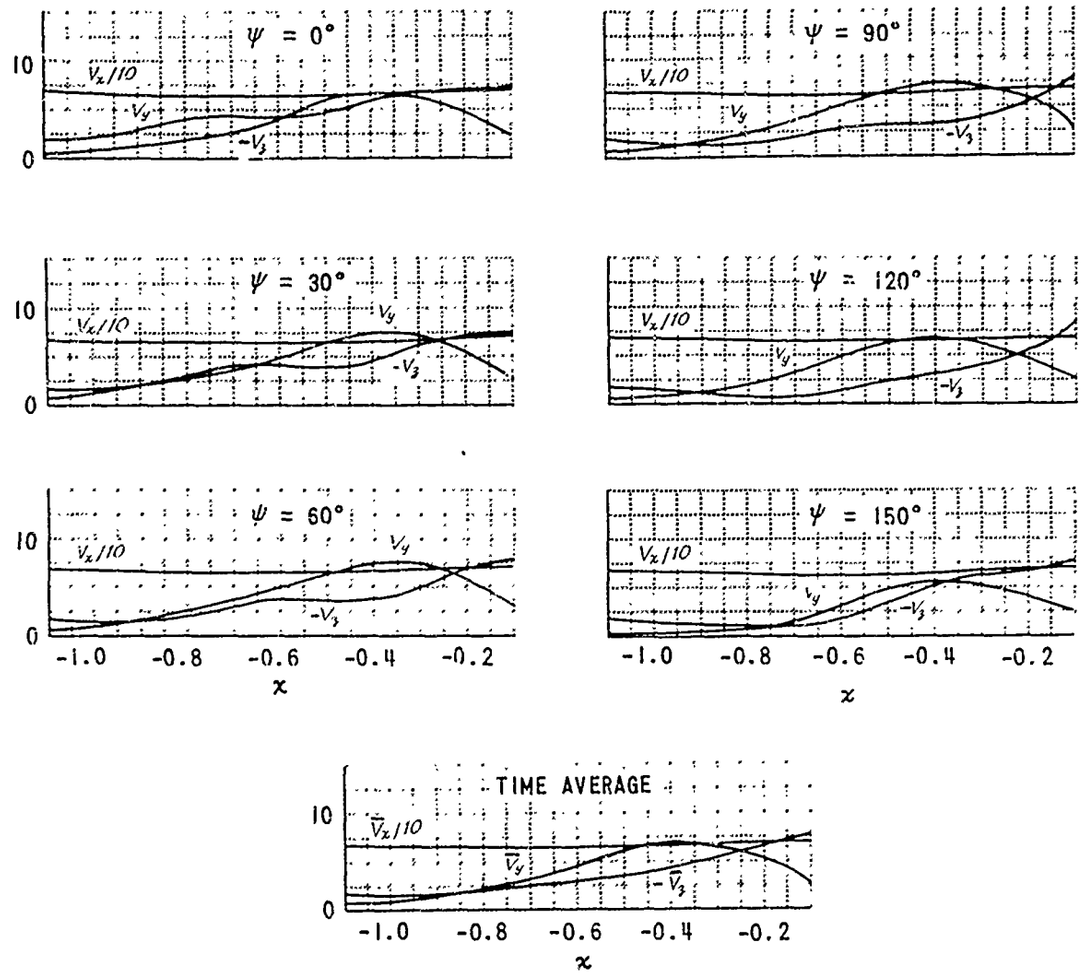

Figure 25 VARIATION OF VELOCITY COMPONENTS WITH x FOR $y = 0.3$, $z = -0.25$ AND $\mu = 0.1465$

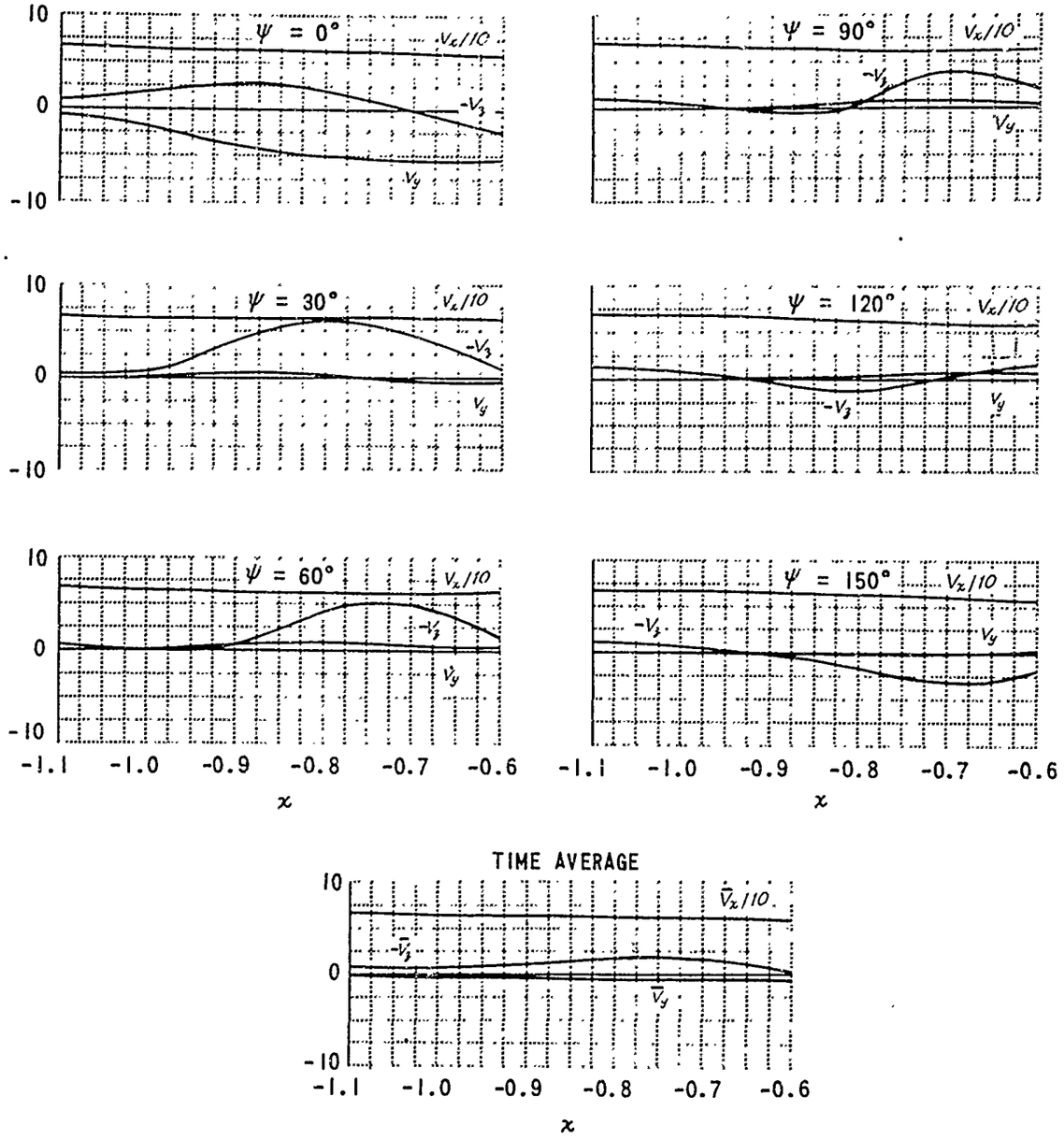

Figure 26 VARIATION OF VELOCITY COMPONENTS WITH x FOR $y = 0$, $z = -0.15$ AND $\mu = 0.1465$

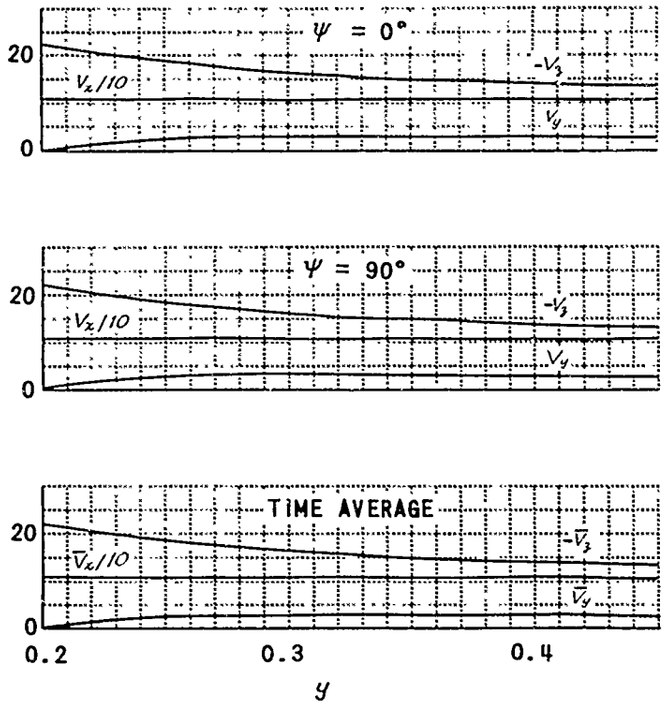

Figure 27 VARIATION OF VELOCITY COMPONENTS WITH y FOR x = -0.25, z = -0.45 AND μ = 0.220

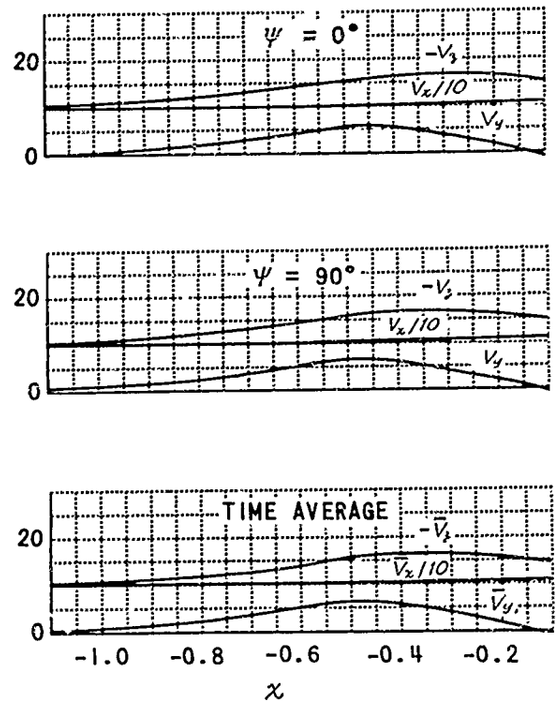

Figure 28 VARIATION OF VELOCITY COMPONENTS WITH x FOR y = 0.3, z = -0.45 AND μ = 0.220

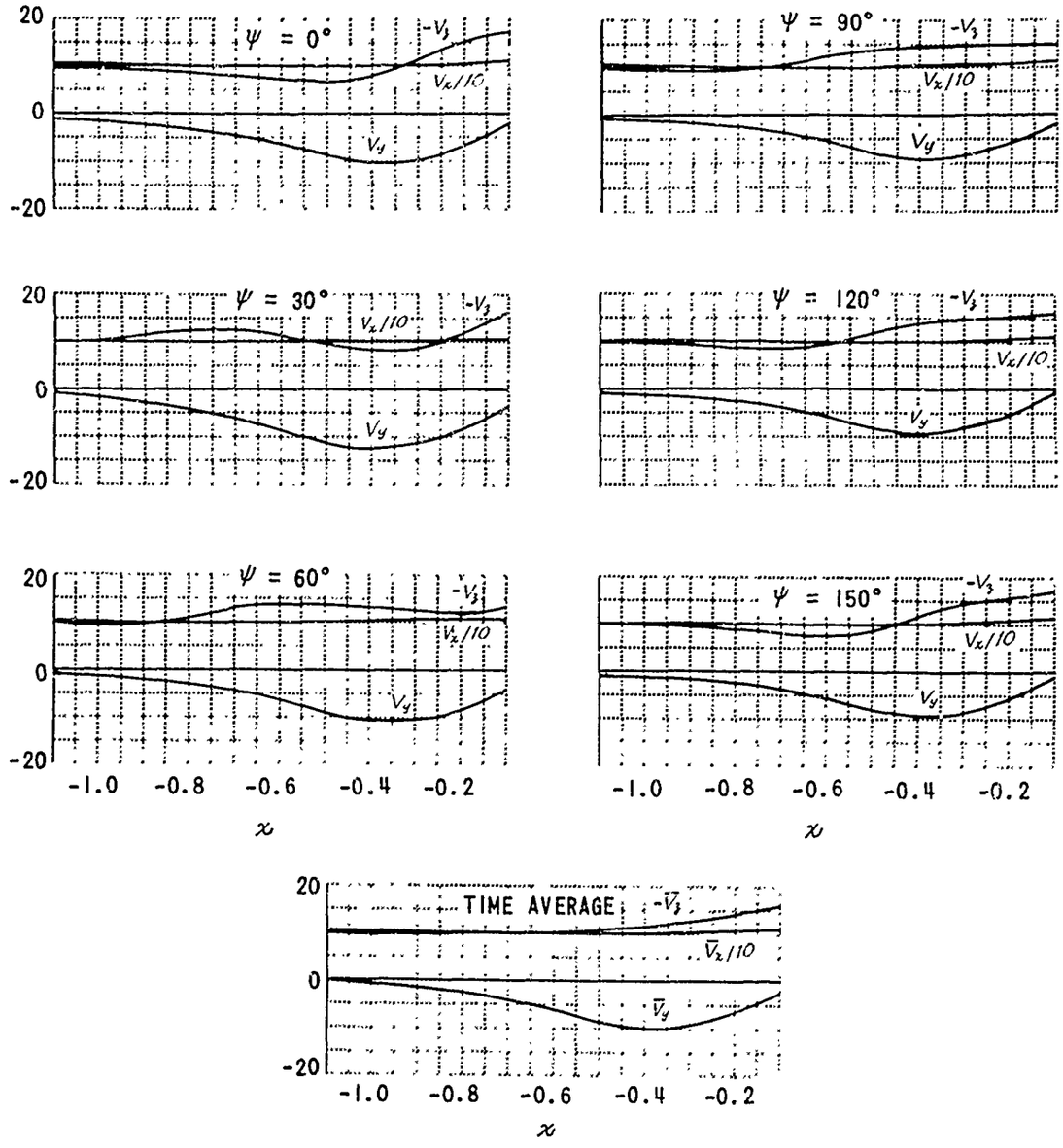

Figure 29 VARIATION OF VELOCITY COMPONENTS WITH x FOR y = -0.3, z = -0.25 AND μ = 0.220

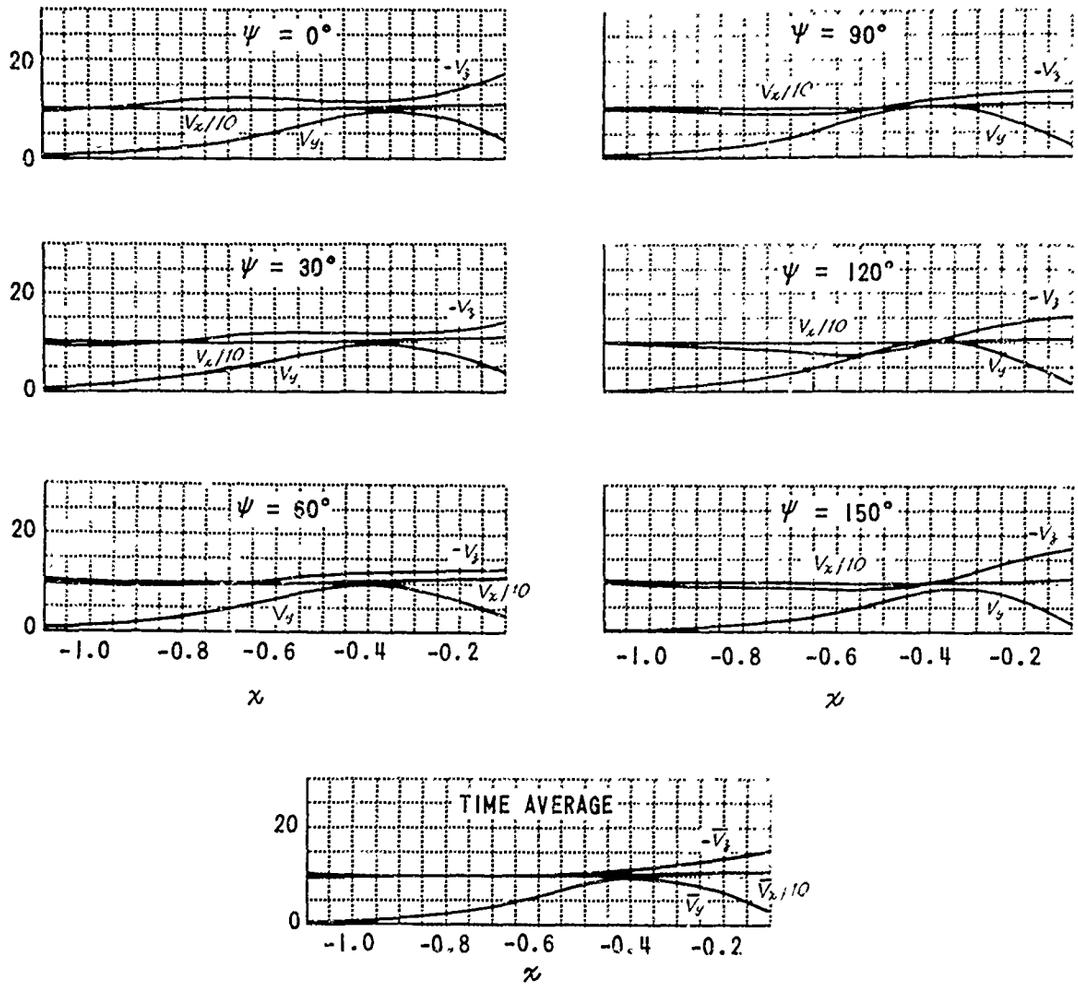

Figure 30 VARIATION OF VELOCITY COMPONENTS WITH x FOR $y = 0.3$, $z = -0.25$ AND $\mu = 0.220$

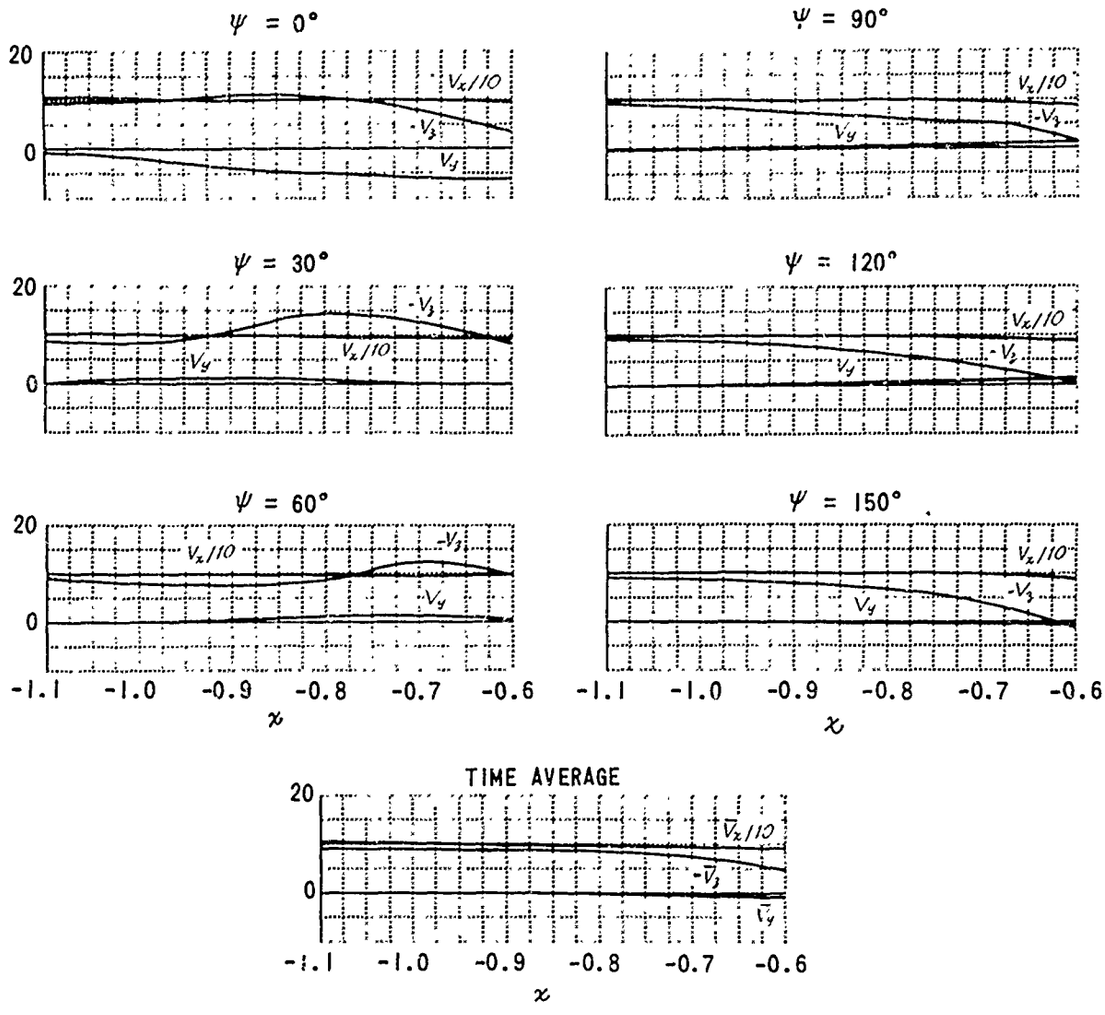

Figure 31 VARIATION OF VELOCITY COMPONENTS WITH x
For $y = 0$, $z = -0.15$ AND $\mu = 0.220$

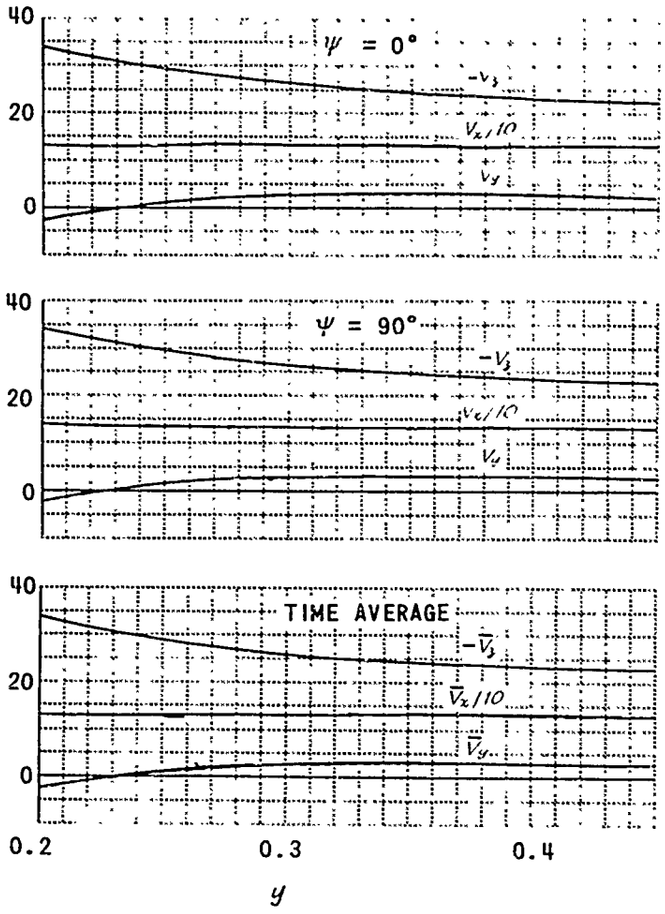

Figure 32 VARIATION OF VELOCITY COMPONENTS WITH y FOR x = -0.25, z = -0.45 AND μ = 0.269

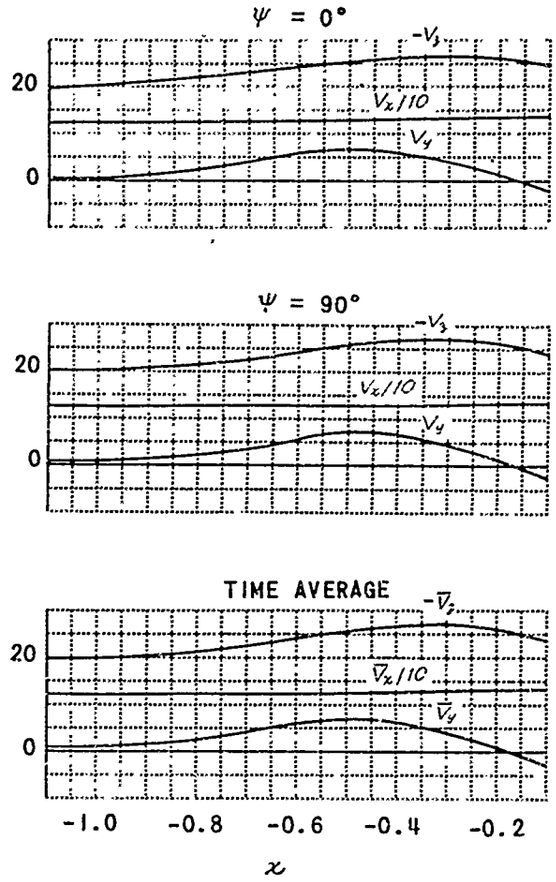

Figure 33 VARIATION OF VELOCITY COMPONENTS WITH x FOR y = 0.3, z = -0.45 AND μ = 0.269

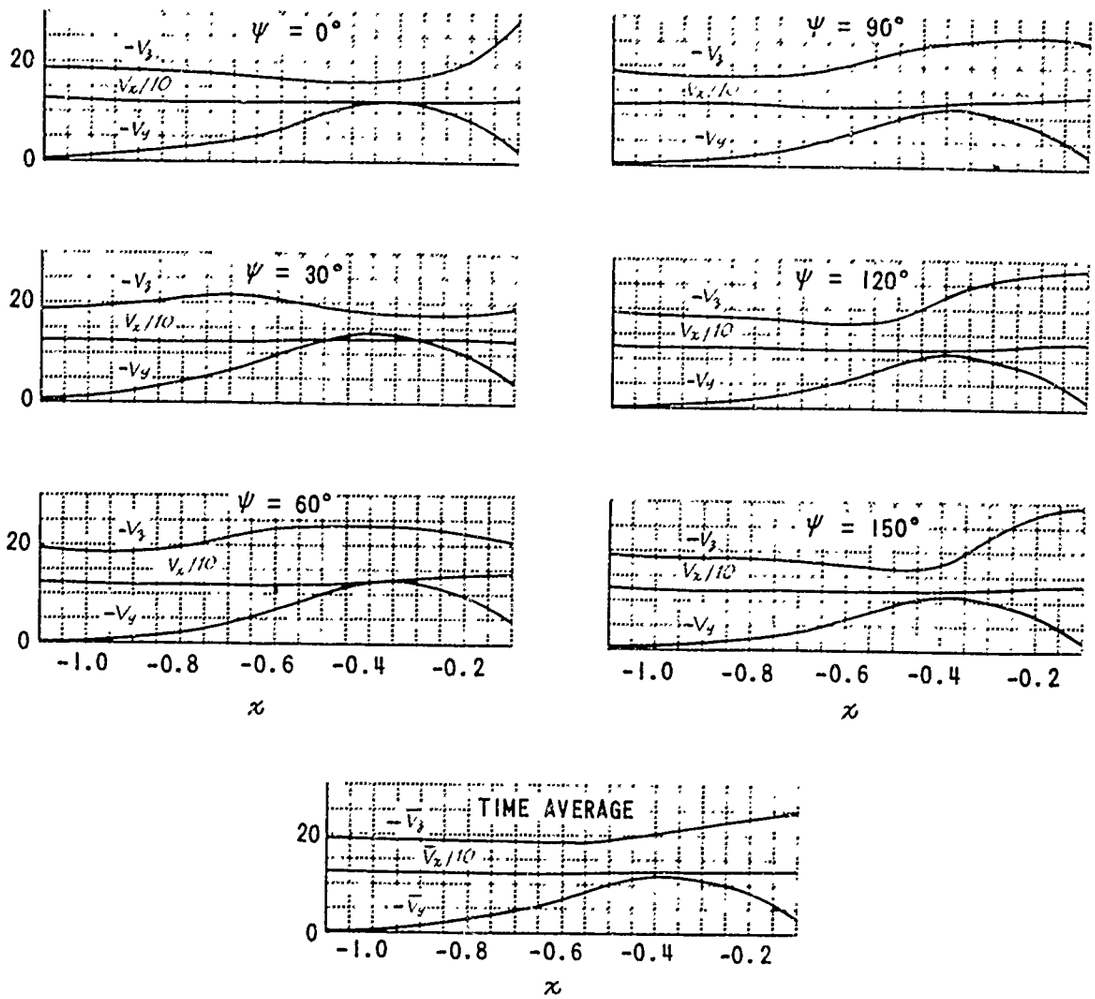

Figure 34 VARIATION OF VELOCITY COMPONENTS WITH x FOR y = -0.3, z = -0.25 AND μ = 0.269

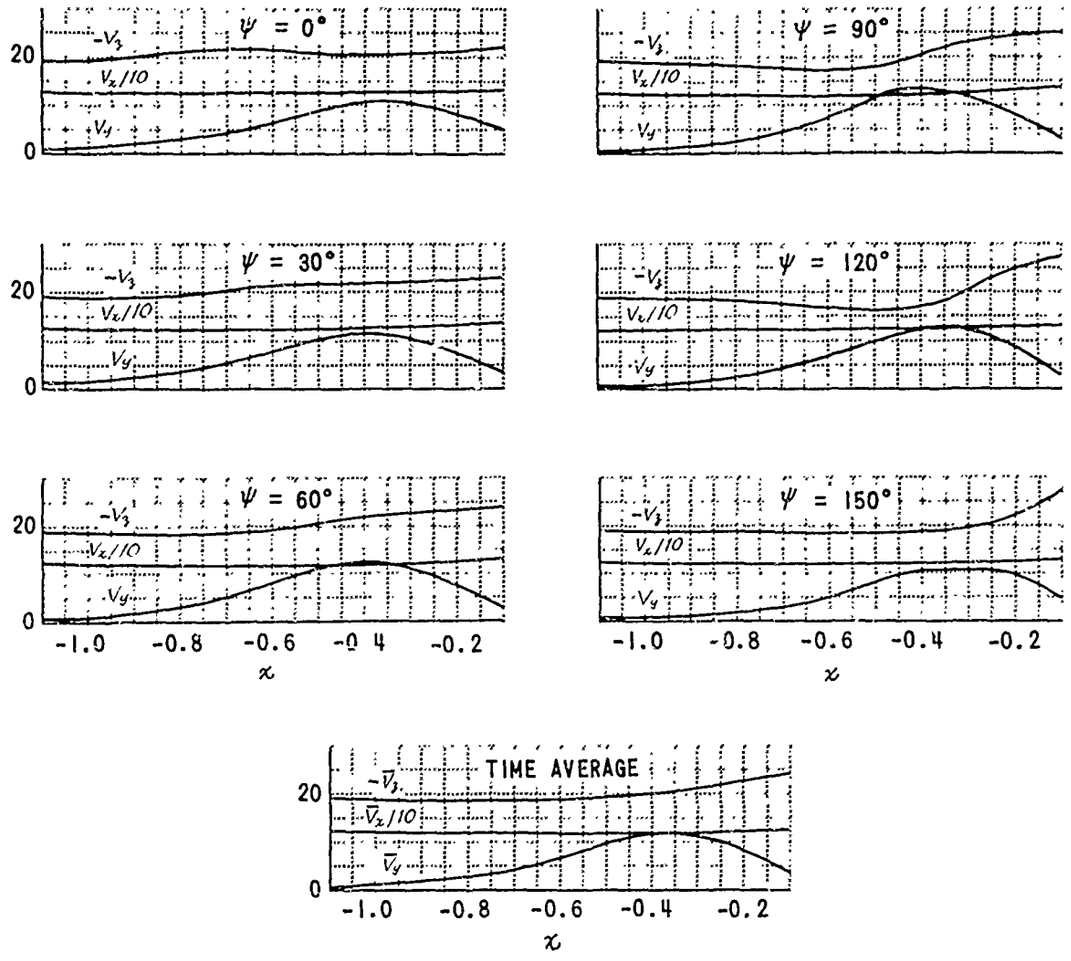

Figure 35 VARIATION OF VELOCITY COMPONENTS WITH x FOR y = 0.3, z = -0.25 AND μ = 0.269

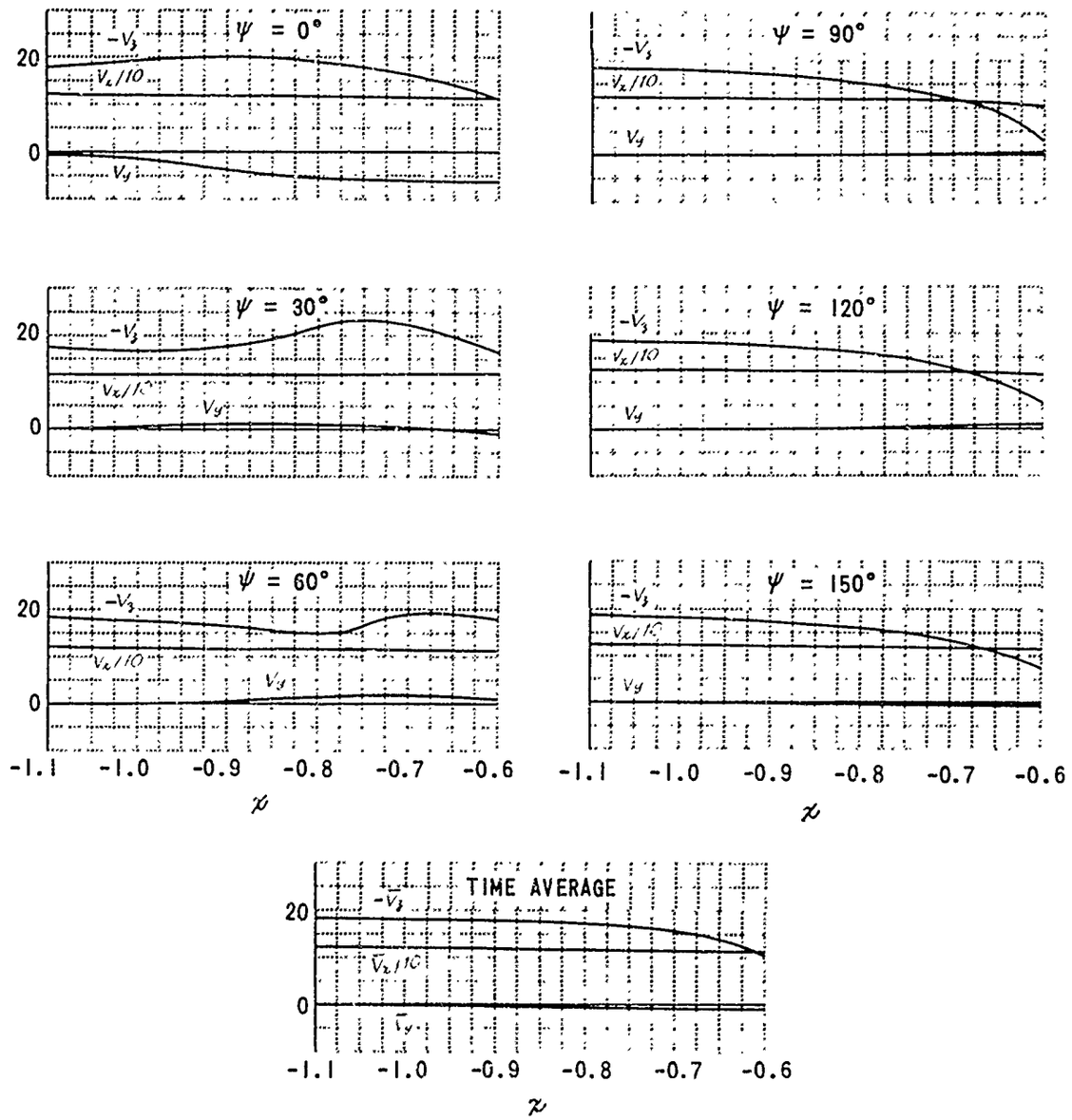

Figure 36 VARIATION OF VELOCITY COMPONENTS WITH x FOR $y = 0$, $z = -0.15$ AND $\mu = 0.269$

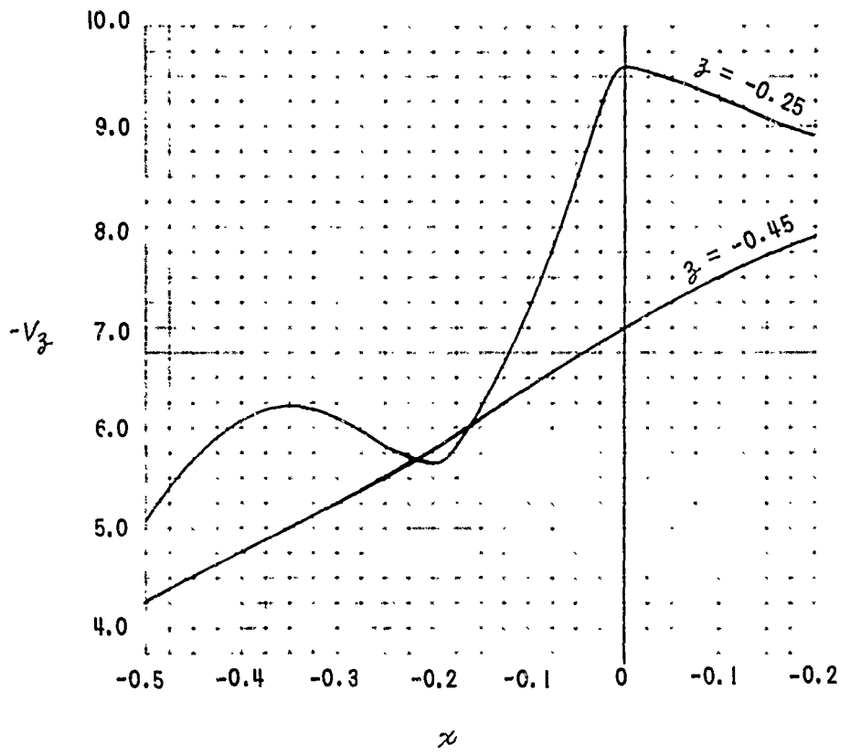

Figure 37 SPACIAL VARIATION OF DOWNWASH IN THE ABSENCE OF A FUSELAGE FOR $y = 0, \mu = 0.1465$ AND $\psi = 0$

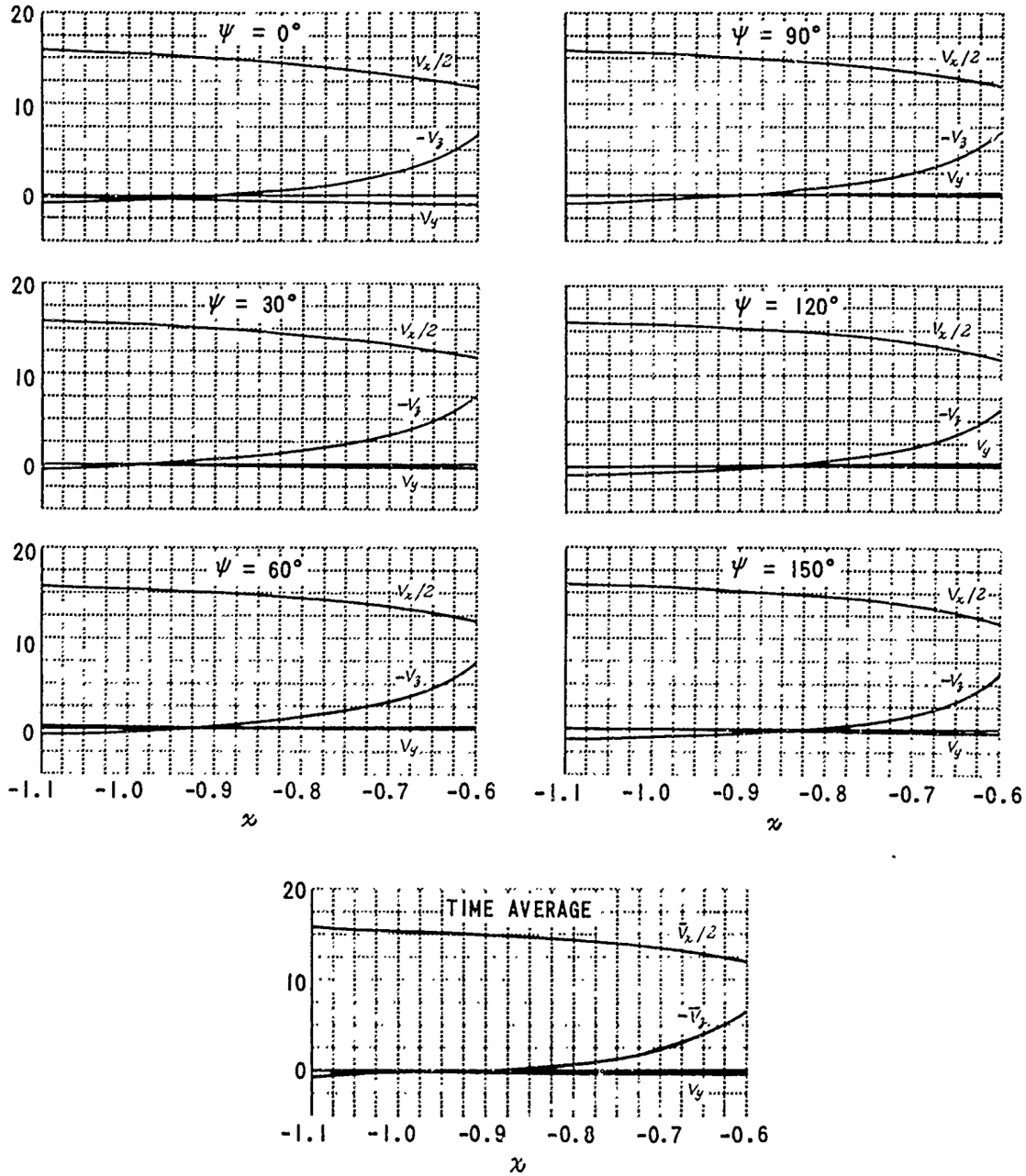

Figure 38 VARIATION OF VELOCITY COMPONENTS WITH x FOR $y = 0$, $z = -0.45$ AND $\mu = 0.0732$

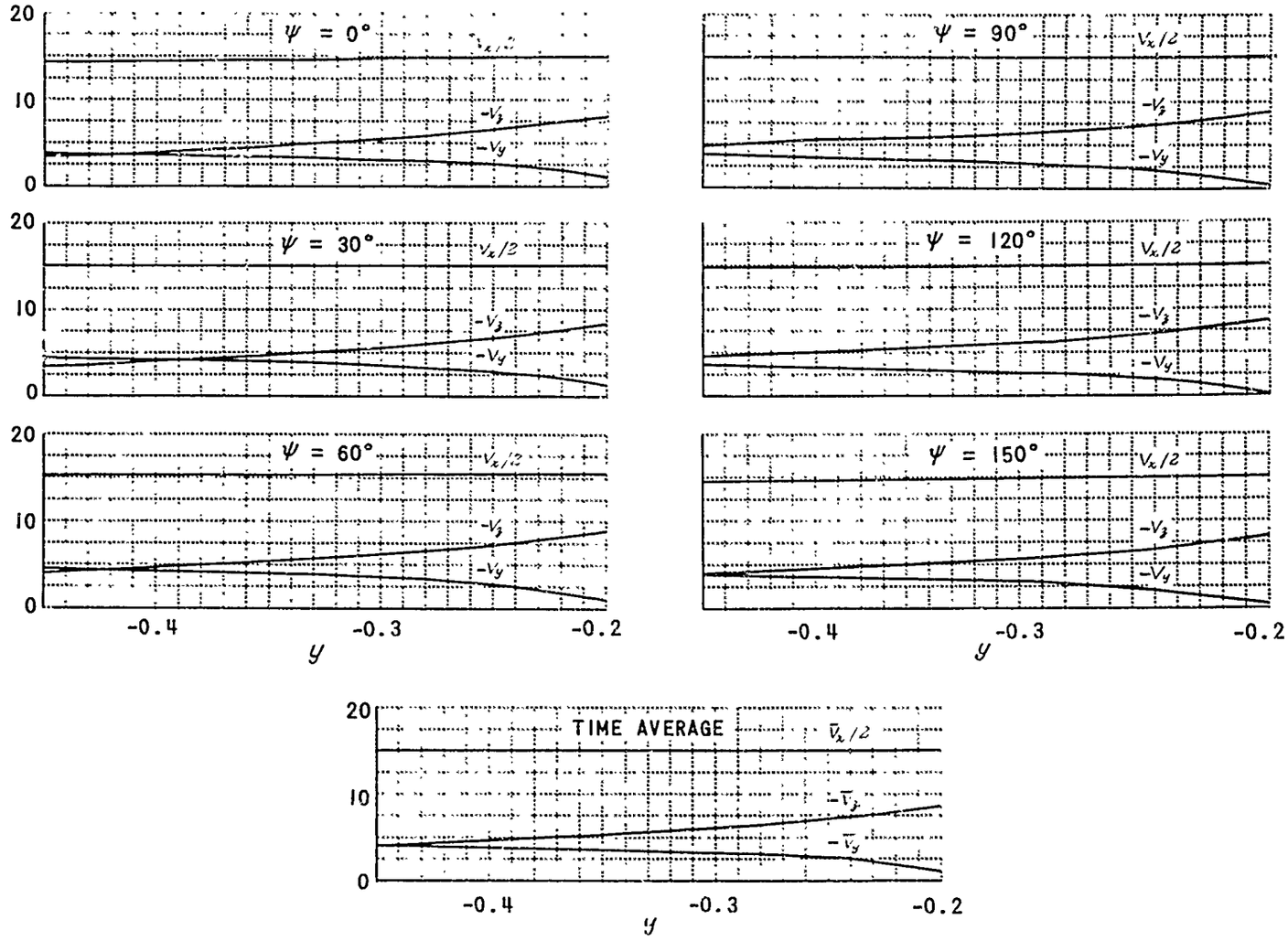

Figure 39 VARIATION OF VELOCITY COMPONENTS WITH y FOR $x = -0.25$, $z = -0.45$, $\mu = 0.0732$ AND $y < 0$

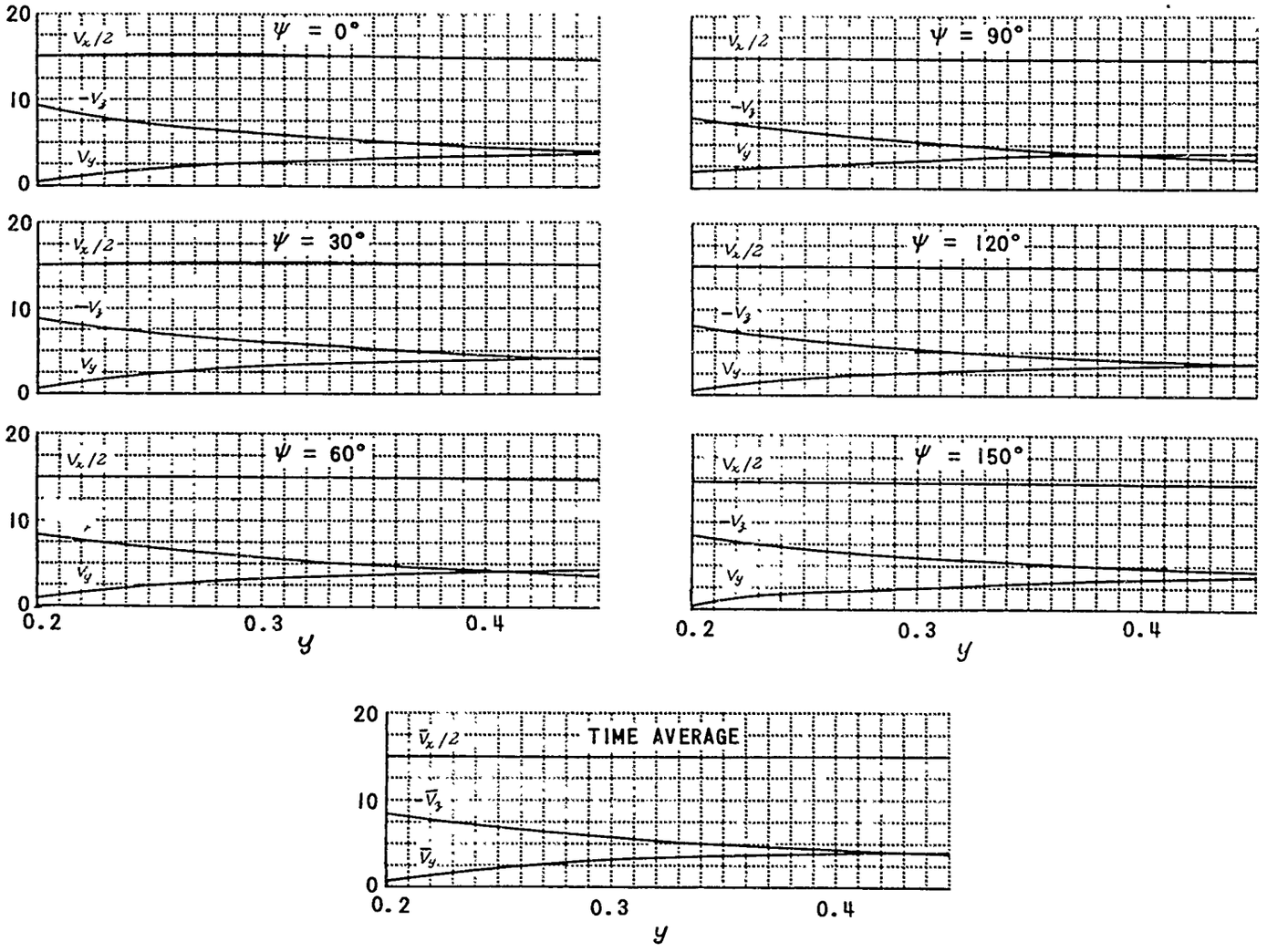

Figure 40 VARIATION OF VELOCITY COMPONENTS WITH y FOR $x = -0.25$, $z = -0.45$, $\mu = 0.0732$ AND $y > 0$

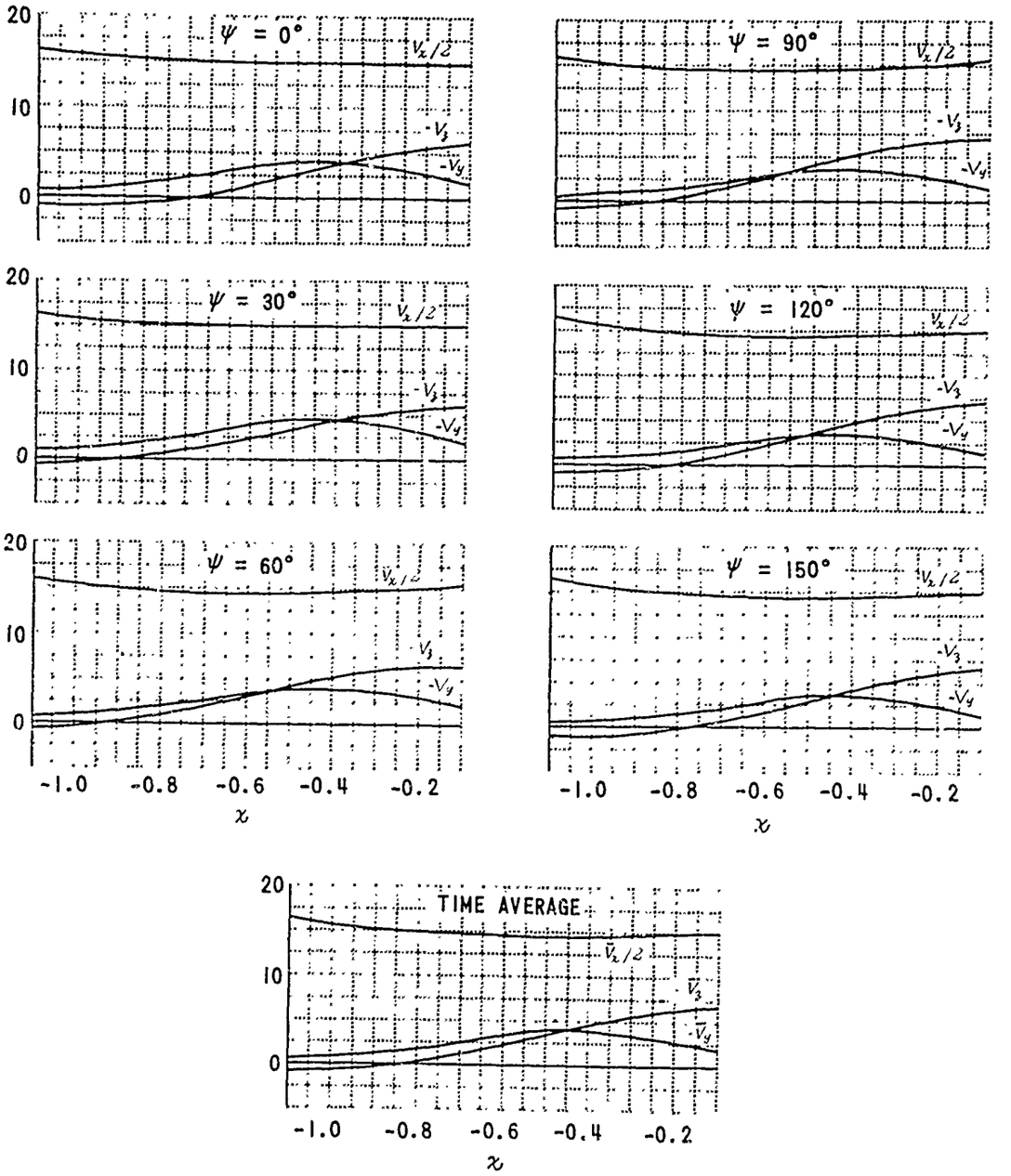

Figure 41 VARIATION OF VELOCITY COMPONENTS WITH x FOR y = -0.3, z = -0.45 AND μ = 0.0732

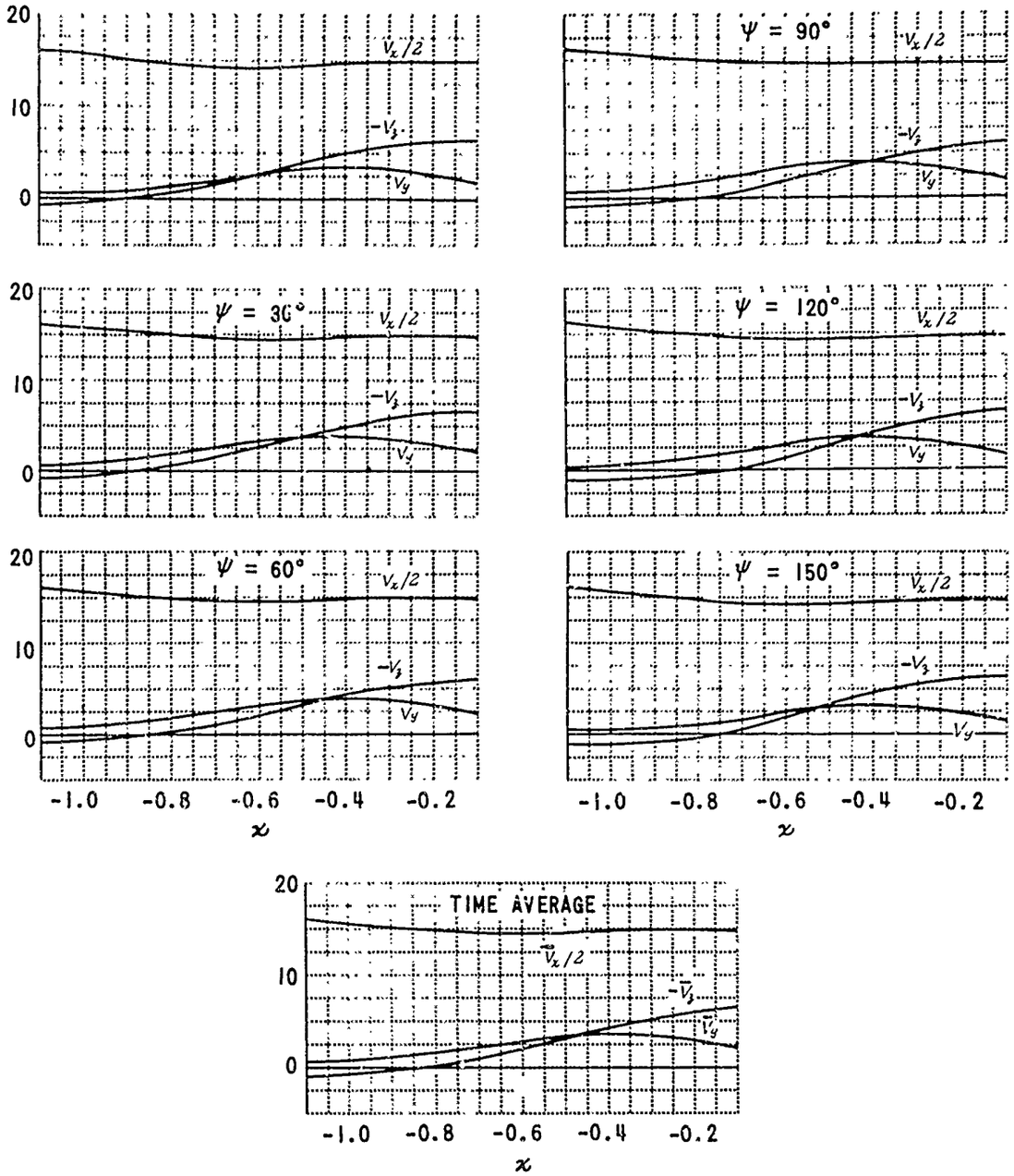

Figure 42 VARIATION OF VELOCITY COMPONENTS WITH x FOR y = 0.3, z = -0.45 AND μ = 0.0732

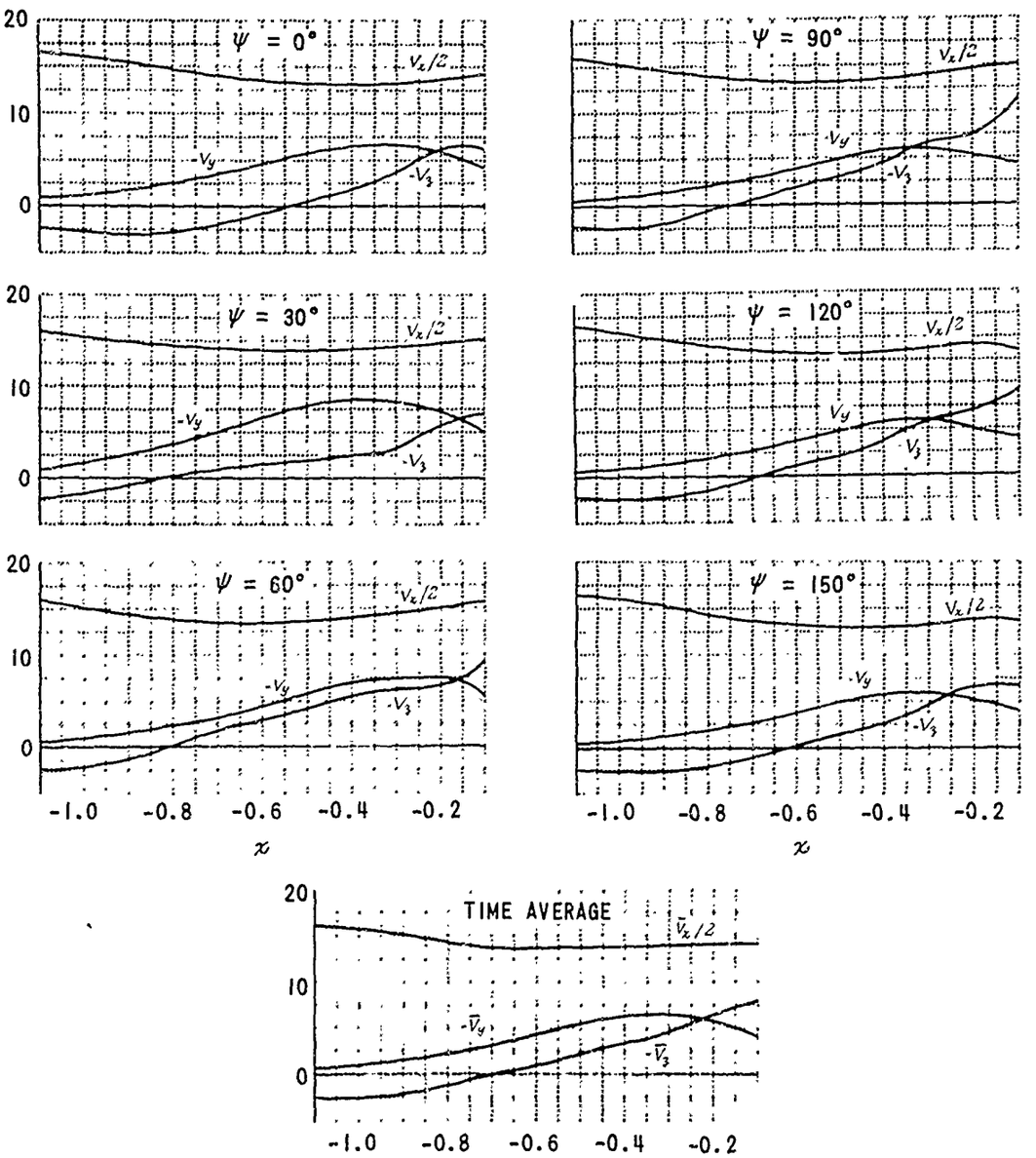

Figure 43 VARIATION OF VELOCITY COMPONENTS WITH x FOR $y = -0.3$, $z = -0.25$ AND $\mu = 0.0732$

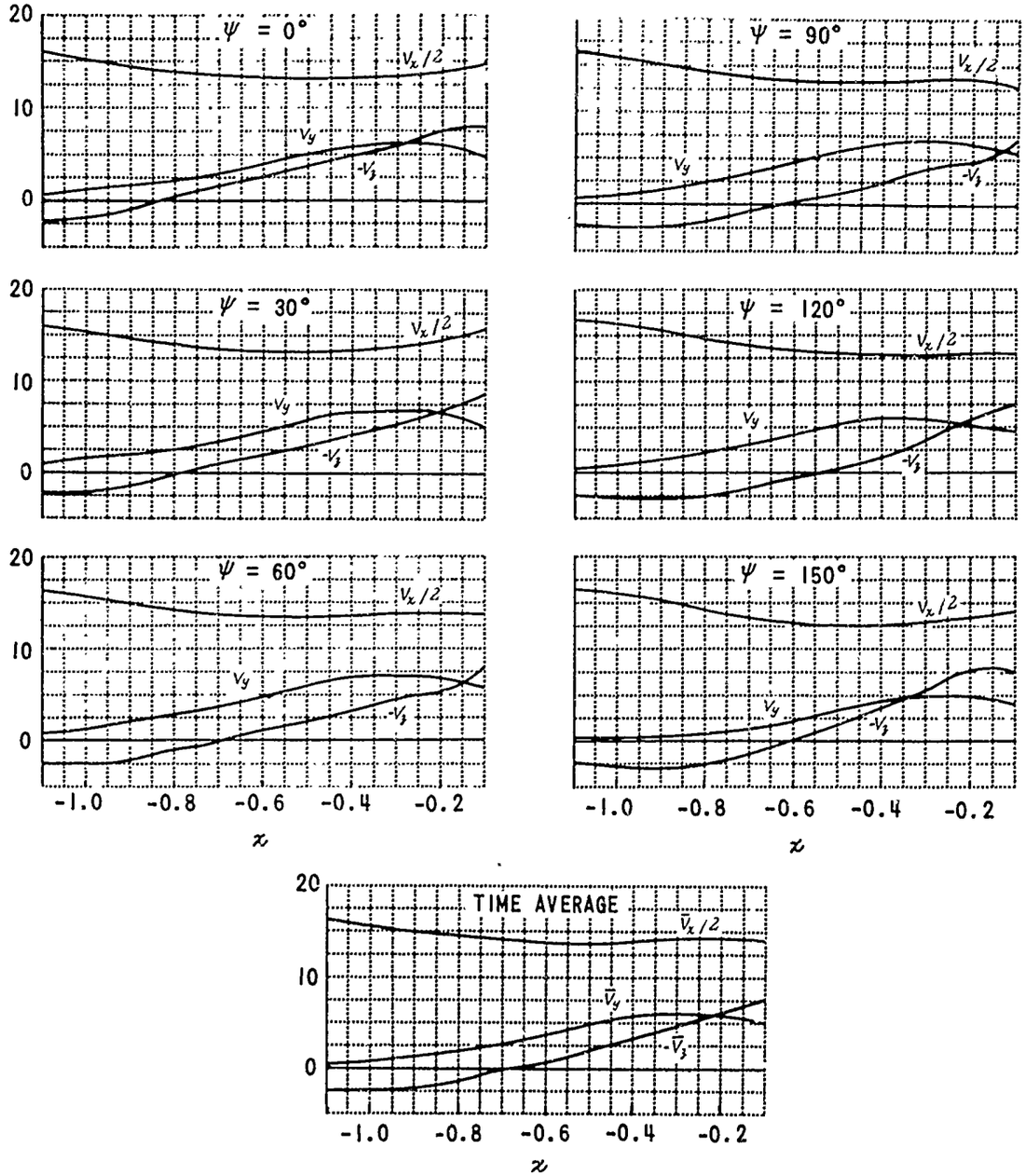

Figure 44 VARIATION OF VELOCITY COMPONENTS WITH x FOR $y = 0.3$, $z = -0.25$ AND $\mu = 0.0732$

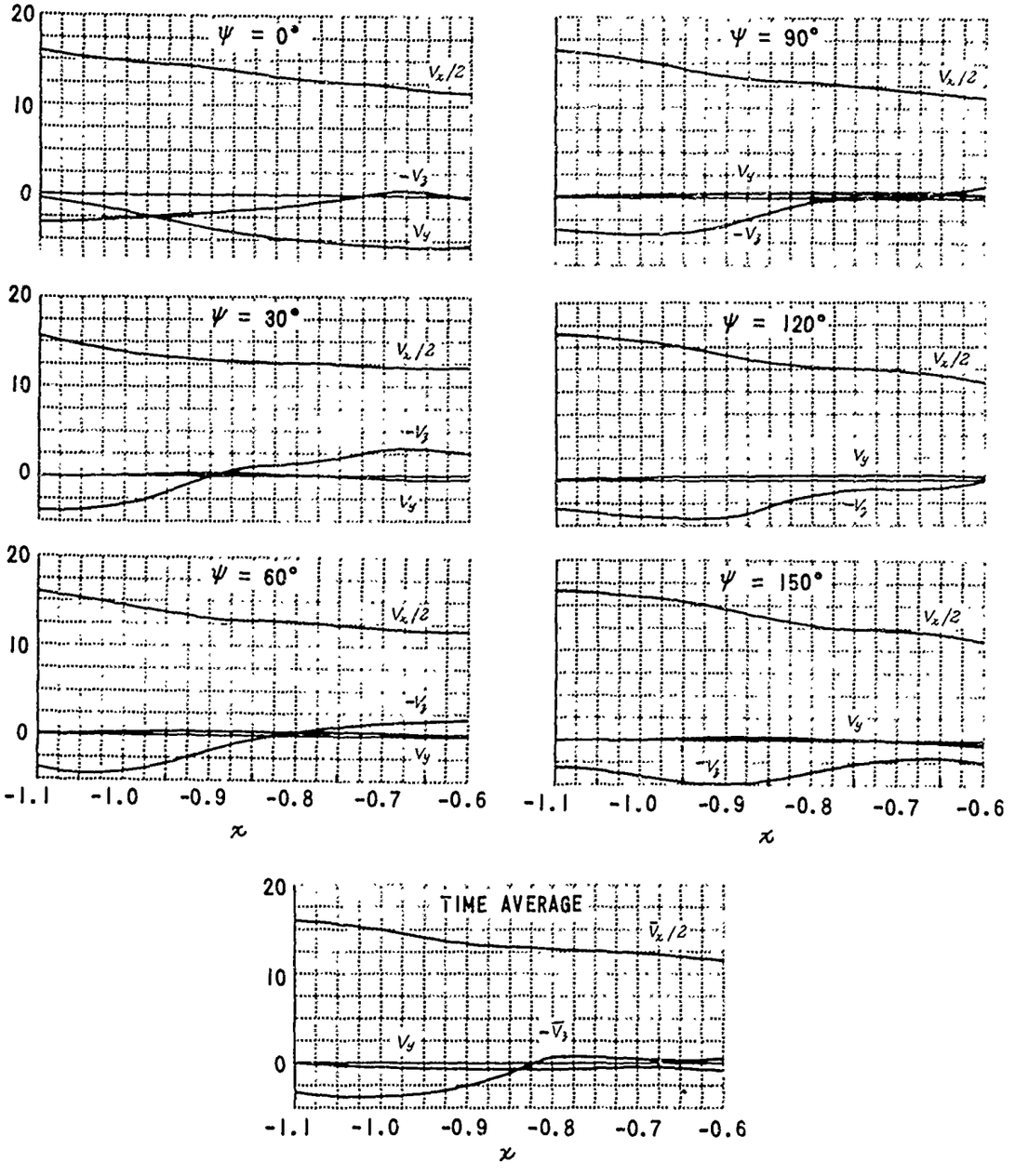

Figure 45 VARIATION OF VELOCITY COMPONENTS WITH x FOR $y = 0$, $z = -0.15$ AND $\mu = 0.0732$

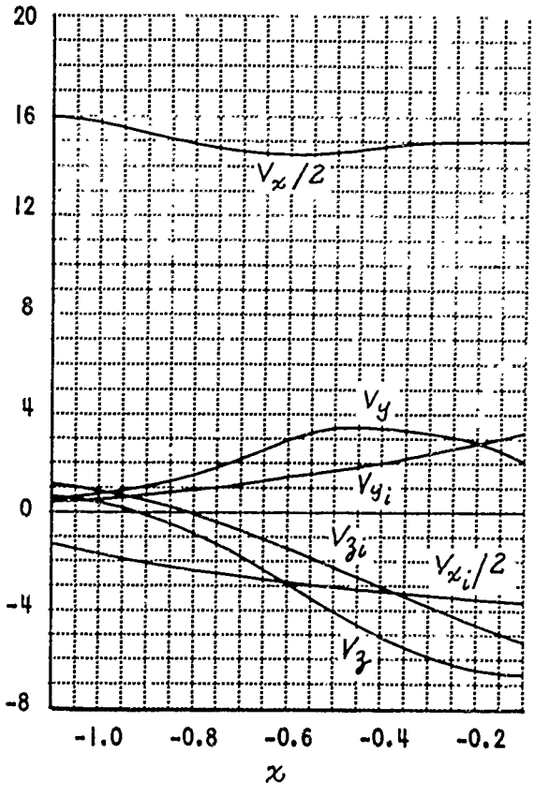

Figure 46 COMPARISON OF TOTAL FLOW WITH WAKE- AND BLADE-INDUCED FLOW FOR y = 0.3, z = -0.45 AND μ = 0.0732

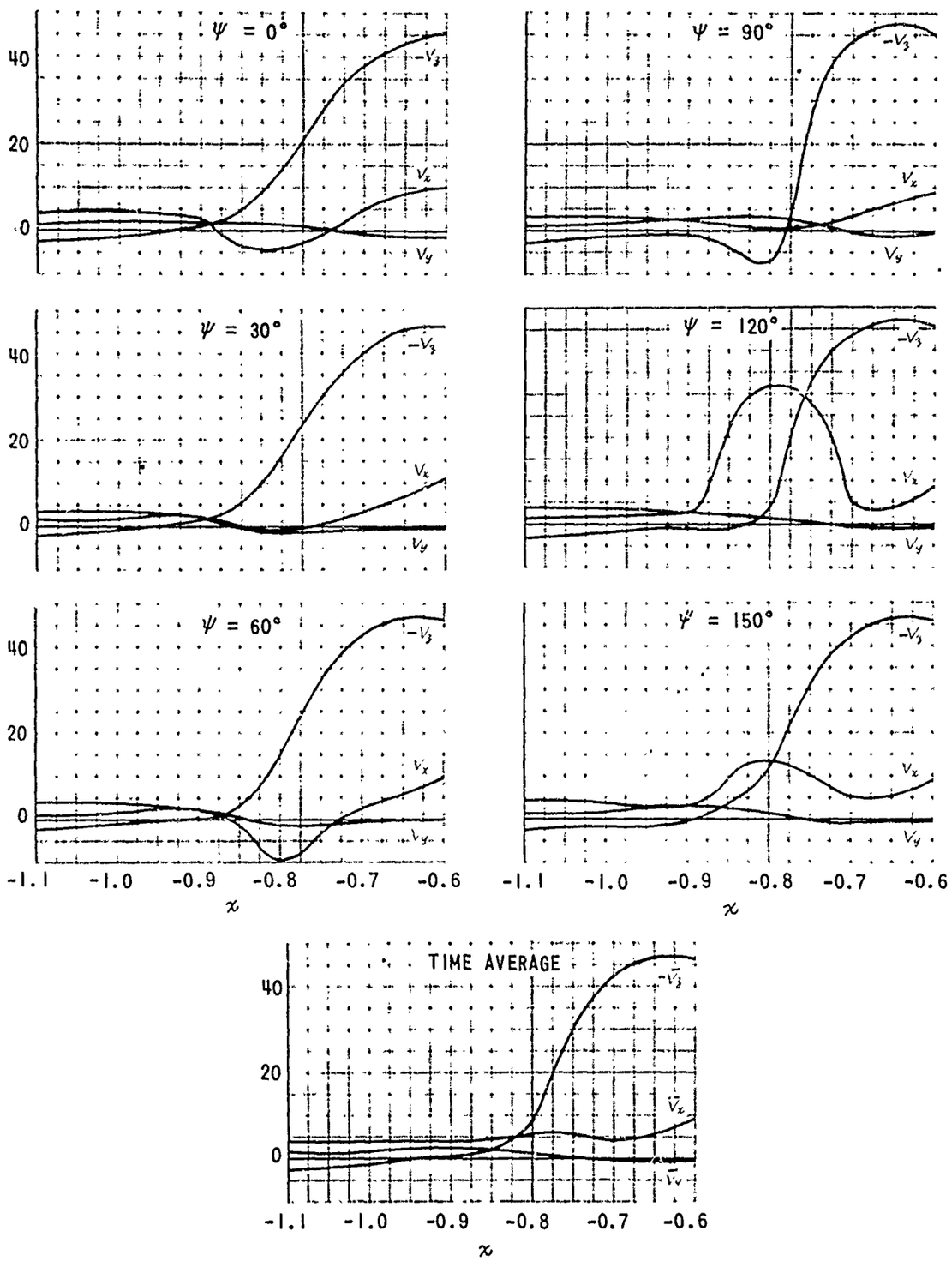

Figure 47 VARIATION OF VELOCITY COMPONENTS WITH x FOR $y = 0$, $z = -0.45$ AND $\mu = 0$

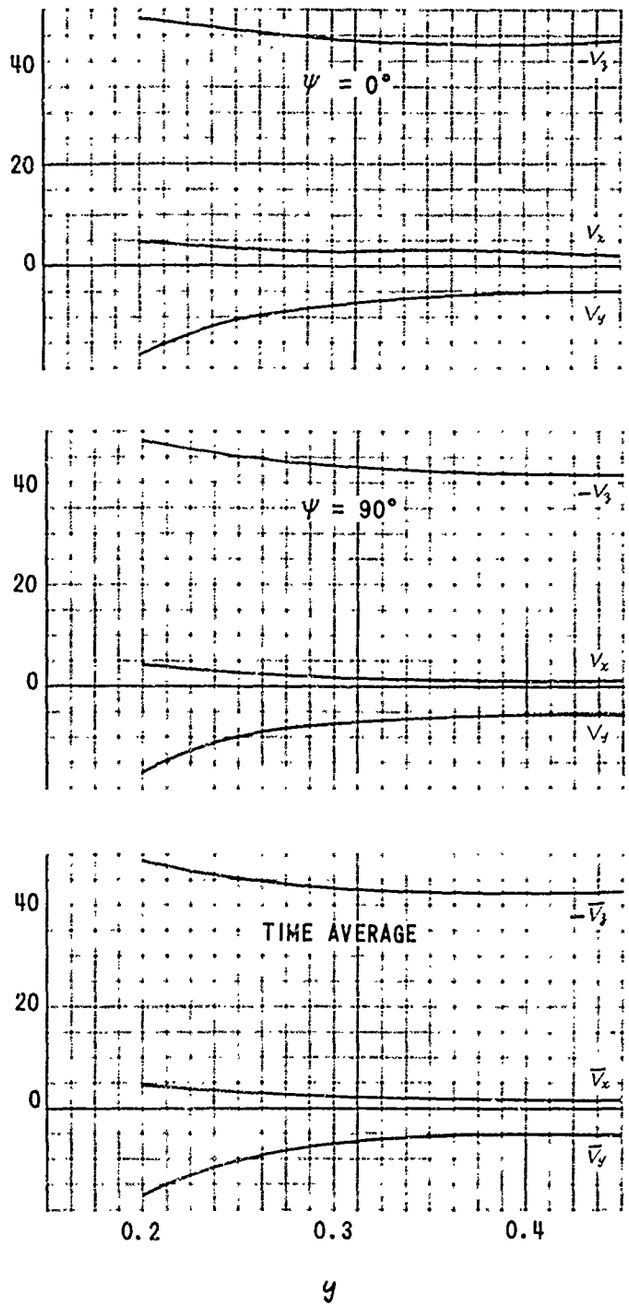

Figure 48 VARIATION OF VELOCITY COMPONENTS WITH y FOR x = -0.25, z = -0.45 AND μ = 0

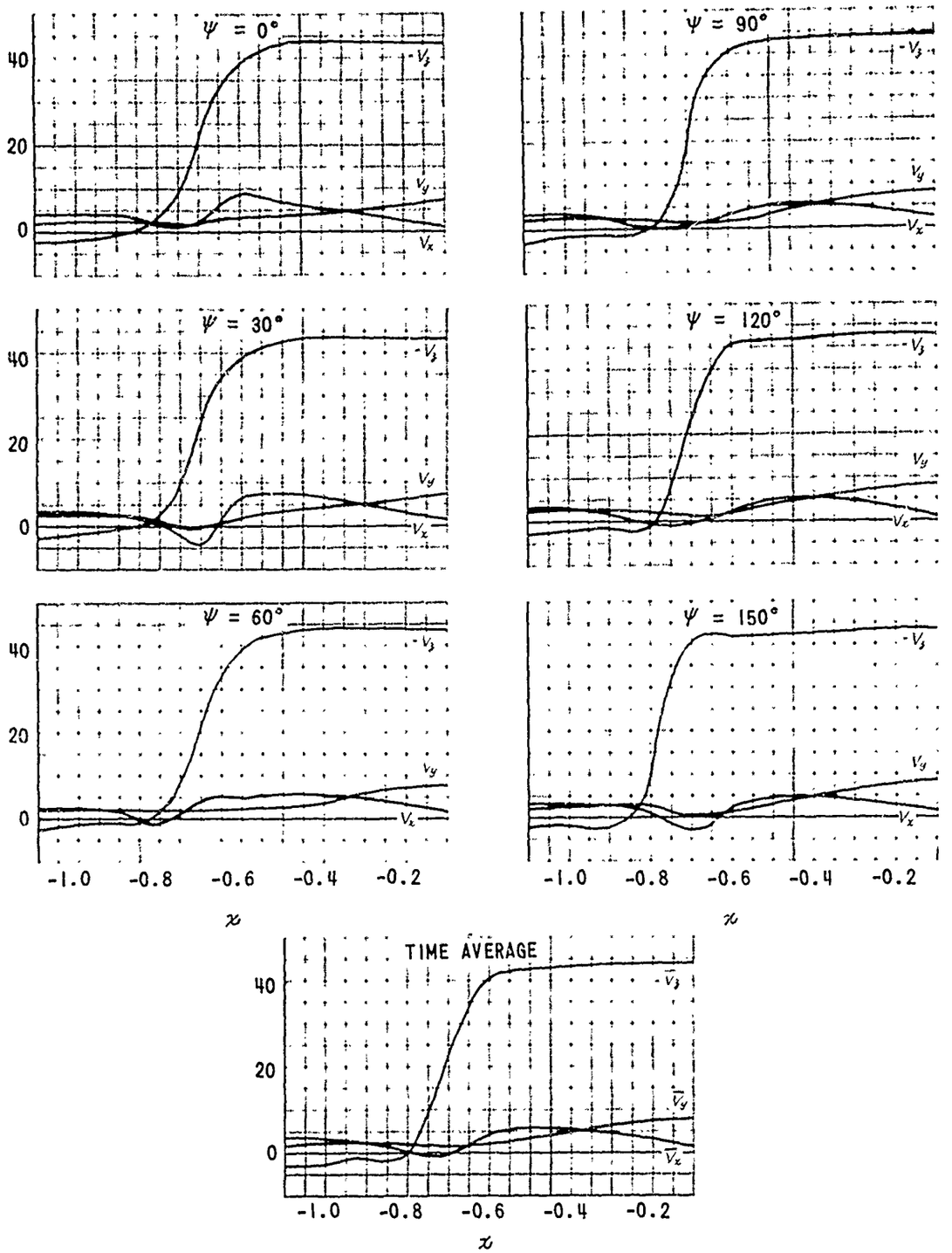

Figure 49 VARIATION OF VELOCITY COMPONENTS WITH x FOR $y = -0.3$, $z = -0.45$ AND $\mu = 0$

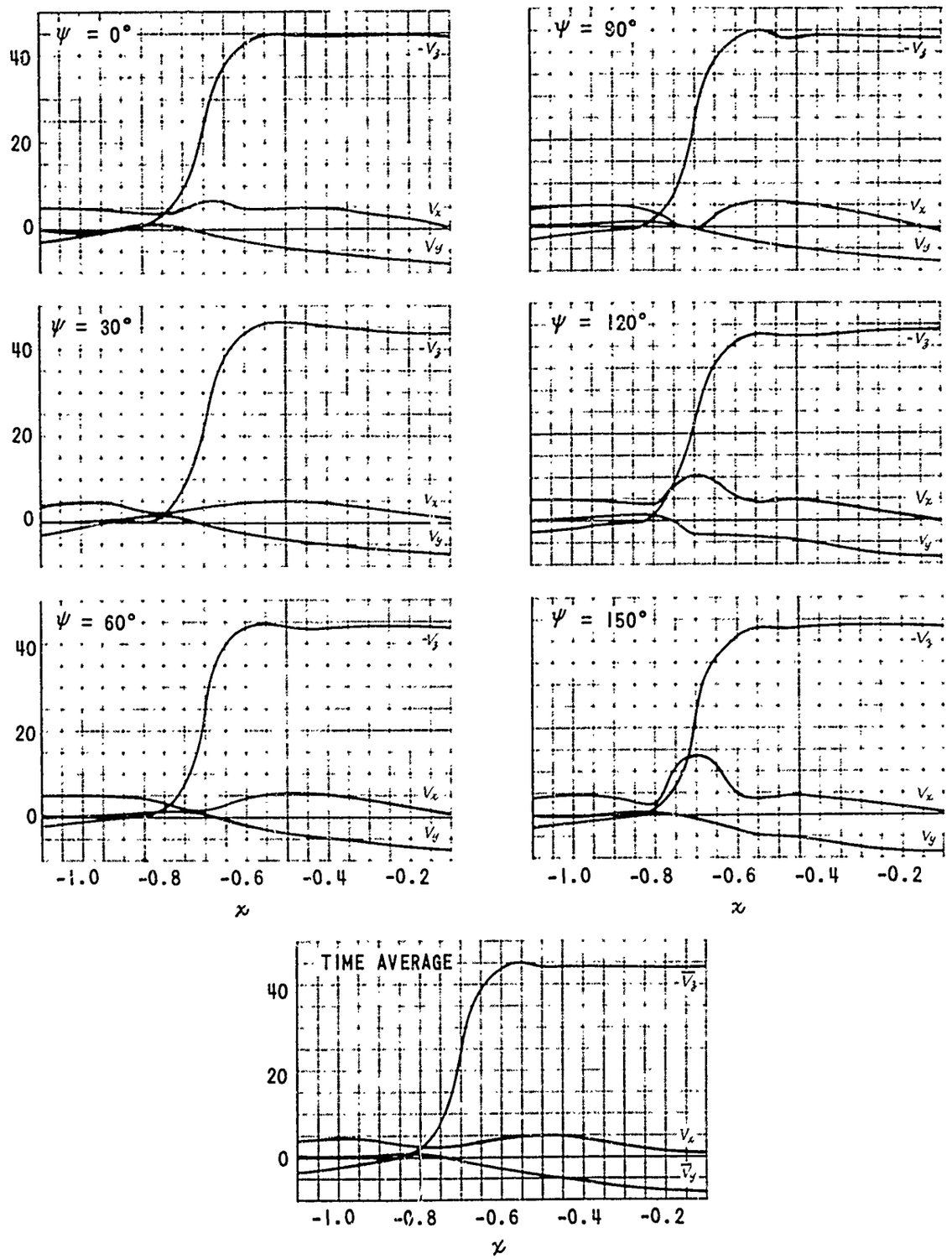

Figure 50 VARIATION OF VELOCITY COMPONENTS WITH x FOR $y = 0.3$, $z = -0.45$ AND $\mu = 0$

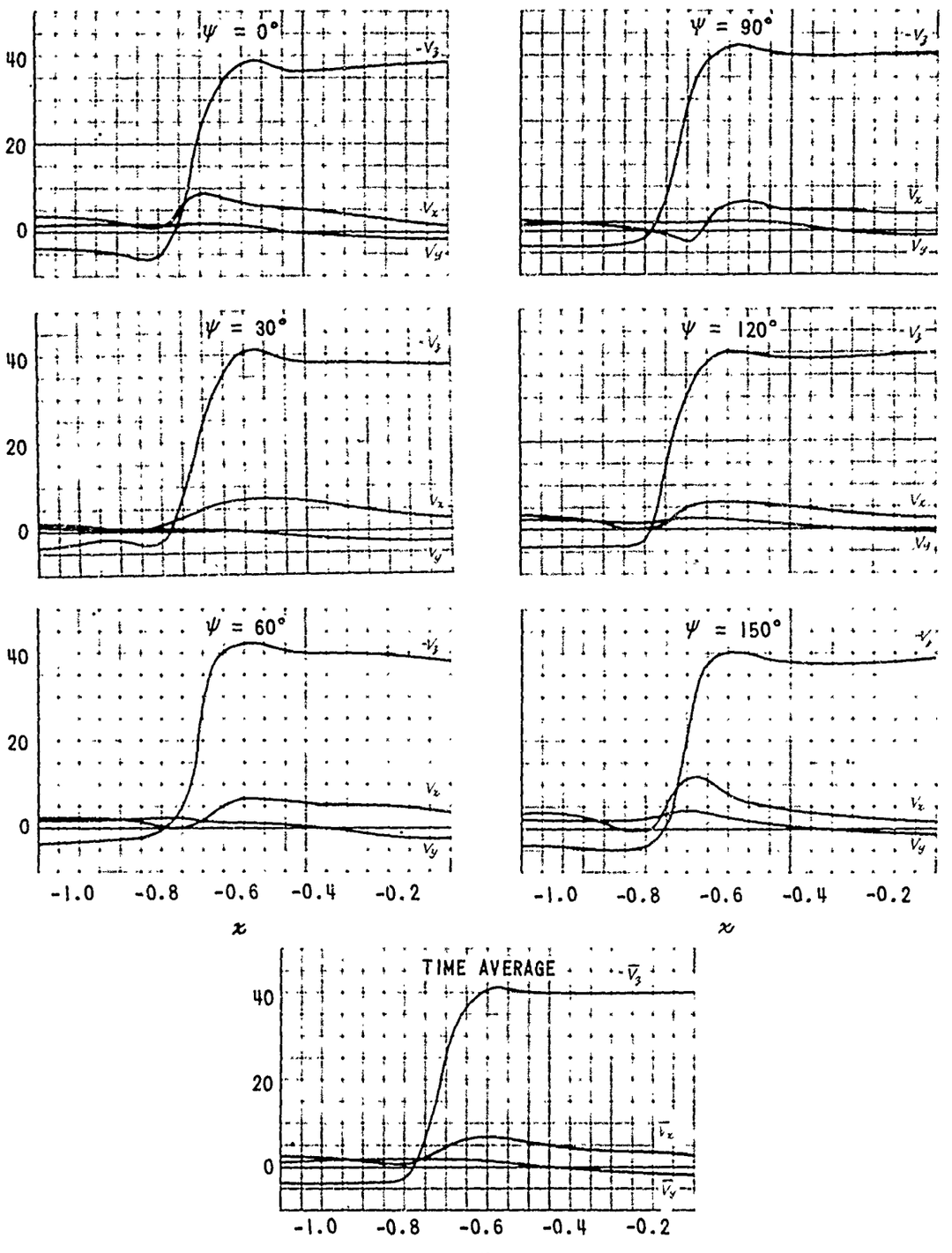

Figure 51 VARIATION OF VELOCITY COMPONENTS WITH x FOR $y = -0.3$, $z = -0.25$ AND $\mu = 0$

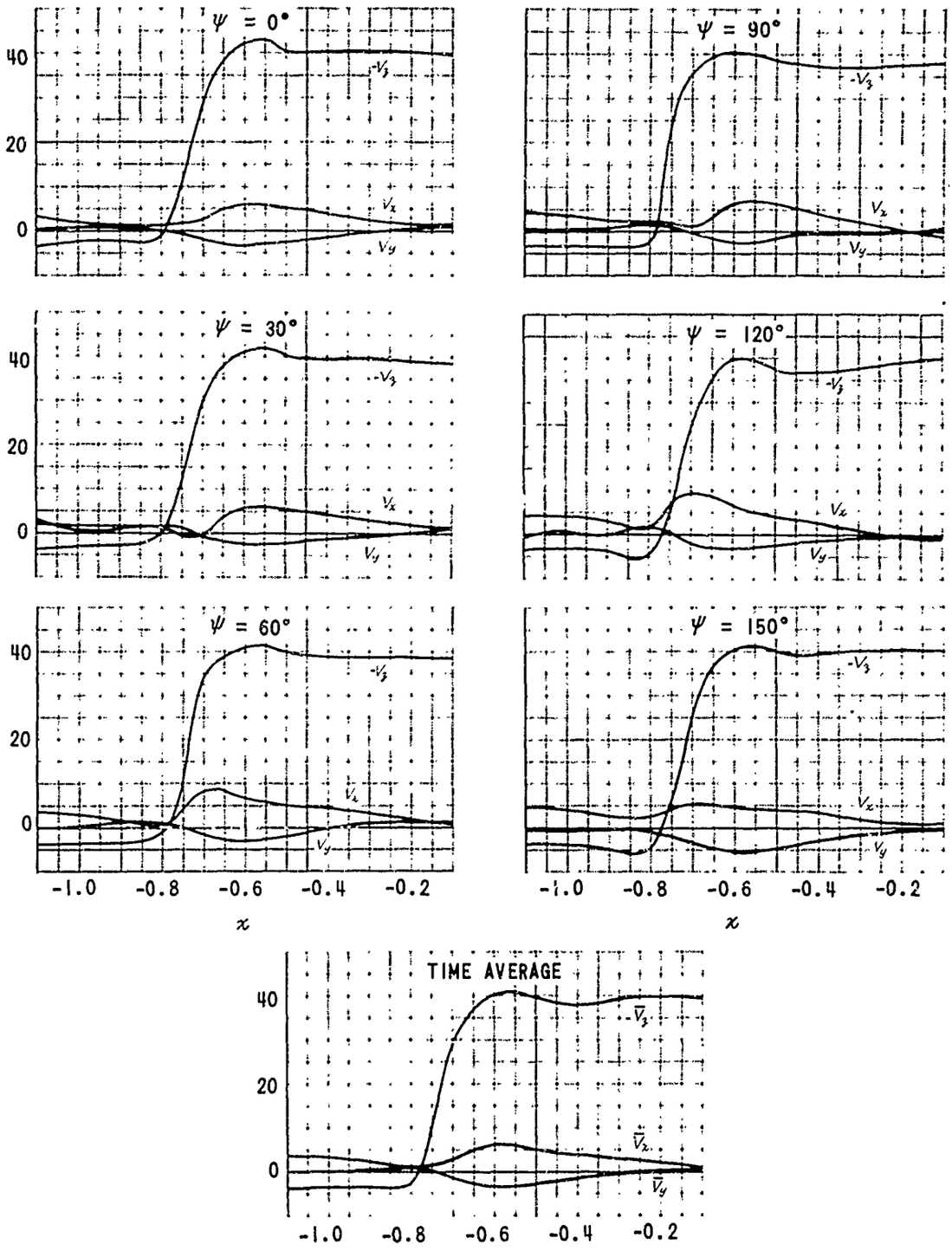

Figure 52 VARIATION OF VELOCITY COMPONENTS WITH x FOR $y = 0.3$, $z = -0.25$ AND $\mu = 0$

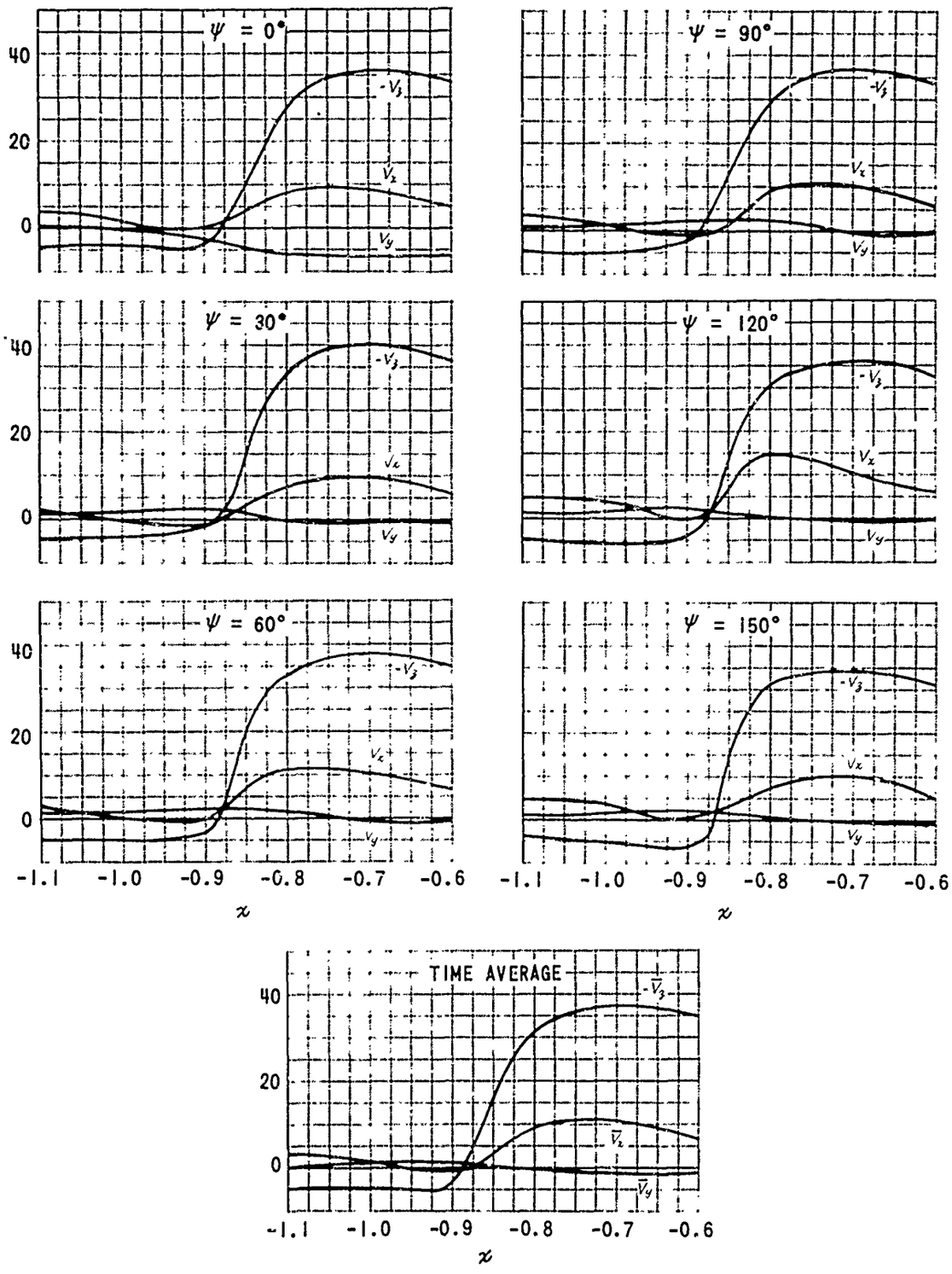

Figure 53 VARIATION OF VELOCITY COMPONENTS WITH x FOR $y = 0$, $z = -0.15$ AND $\mu = 0$

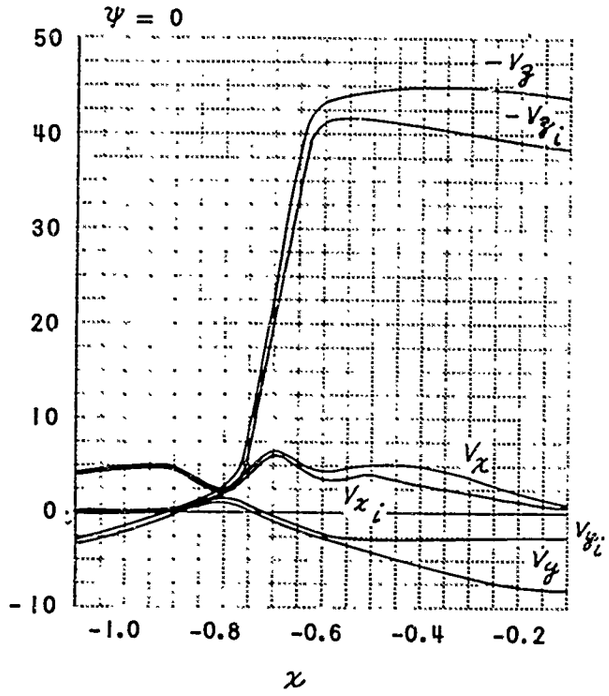

Figure 54 COMPARISON OF TOTAL FLOW WITH WAKE- AND BLADE-INDUCED FLOW FOR $y = 0.3$, $z = -0.45$ AND $\mu = 0$

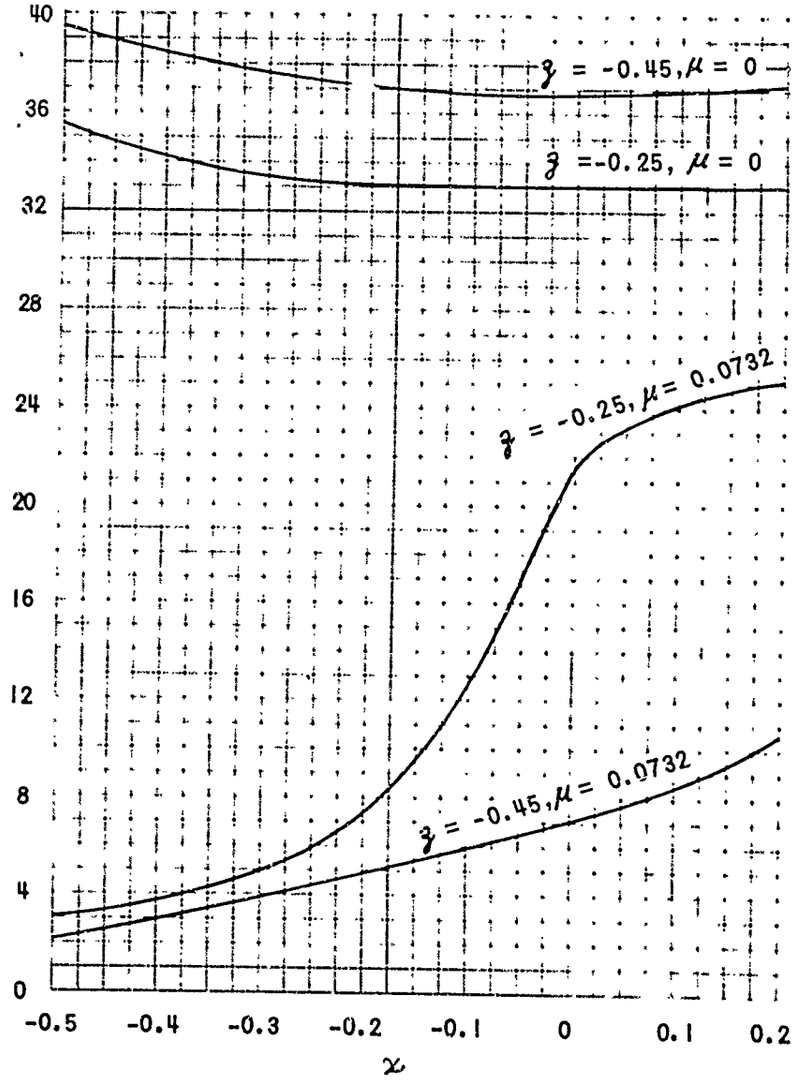

Figure 55 SPACIAL VARIATION OF DOWNWASH IN THE ABSENCE OF A FUSELAGE FOR $y = 0$, $\psi = 0$

6. CONCLUSIONS AND RECOMMENDATIONS

On the basis of the comparisons with experimental data and the analysis of the calculations made for a UH-1B helicopter, it may be concluded that the theory developed provides a valid representation of the time-varying flow in the vicinity of a helicopter. The simplifications employed in formulating the model exclude its application from two specific regions, however. Because the detailed structure of the wake in the vicinity of the blades has been omitted, the flow in the rotor plane itself cannot be accurately reproduced. Similarly, because it was assumed that the fuselage experiences a uniform, constant free stream, the model must be applied with caution in the immediate vicinity of the fuselage. Two areas for refinement of the theory then suggest themselves.

In order to allow for the prediction of the flow in the rotor plane, some approximation to the actual wake within five or ten chord-lengths of the blades could be added. For example, a sheet of vorticity of the proper dimensions and strength distribution might be used. This could then lead to a determination of blade loads, by computing the instantaneous circulation about the blade vortices from the downwash computed at that instant.

The fuselage representation could be improved in two different ways. One possibility is to assume that the free stream to which the fuselage is subjected is constant in time but varies spatially, with the variation determined by computing the time average of the flow obtained in the absence of the fuselage. This could be accomplished with only minor modifications to the existing computer programs, and would measurably improve the flow representation near the fuselage at high advance ratios.

The other possibility for refinement of the fuselage representation, while requiring more extensive reprogramming, would insure that the fuselage is precisely represented regardless of the flow to which it is subjected. This entails the construction of an exact numerical analogue to the flow.

That is, at each azimuth position of the blade vortices, the strengths of the fuselage source elements would be recomputed so that the flow at each fuselage element is tangent to the surface; the fuselage boundary condition would then be satisfied exactly (within the limits of the digital analogue approximation itself) both spacially and in time. Preliminary estimates indicate that this procedure would be operationally feasible, computer running time only being increased by a factor of about two for a representative case.

REFERENCES

1. Piziali, R. A. and DuWaldt, F. A., A Method for Computing Rotary Wing Airload Distribution in Forward Flight, Cornell Aeronautical Laboratory Report BB-1495-S-1, TCREC TR 62-44, November 1962.

2. Castles, W. and DeLeeuw, J., The Normal Component of the Induced Velocity in the Vicinity of a Lifting Rotor and Some Examples of Its Application, NACA TR 1184, 1954.

3. Fradenburgh, E. A., Flow Field Measurements for a Hovering Rotor Near the Ground, Paper presented at AHS 5th Annual Western Forum, Los Angeles, California, September 25-26, 1958.

4. Brady, W. G., and Crimi, P., Representation of Propeller Wakes by Systems of Finite Core Vortices, Cornell Aeronautical Laboratory Report BB-1665-S-2, February 1965.

5. Hess, J., and Smith, A., Calculations of Nonlifting Potential Flow About Arbitrary Three-Dimensional Bodies, J. Ship Research, Vol. 8, No. 2, September 1964.

6. Payne, P. R., Helicopter Dynamics and Aerodynamics, MacMillan, New York, 1959.

7. Burpo, F., and Lynn, R., Measurement of Dynamic Air Loads on a Full-Scale Semirigid Rotor, TCREC TR 62-42, December 1962.

8. McCloud, J., and Biggers, J., Full-Scale Wind-Tunnel Tests of a Medium-Weight Utility Helicopter at Forward Speeds, NASA TN D-1887, May 1963.

9. Lamb, H., Hydrodynamics, Sixth Edition, Dover, New York, 1945.

10. Heyson, H., and Katzoff, S., Induced Velocities Near a Lifting Rotor With Nonuniform Disk Loading, NACA TR 1319, 1957.

Unclassified
Security Classification

DOCUMENT CONTROL DATA - R&D

(Security classification of title, body of abstract and indexing annotation must be entered when the overall report is classified)

1. ORIGINATING ACTIVITY (Corporate author) Cornell Aeronautical Laboratory, Inc Buffalo, New York 14221	2a. REPORT SECURITY CLASSIFICATION Unclassified 2b. GROUP

3 REPORT TITLE
Theoretical Prediction of the Flow in the Wake of a Helicopter Rotor
Part 1 - Development of Theory and Results of Computations

4. DESCRIPTIVE NOTES (Type of report and inclusive dates)
Final Report - Part 1, September 1964 - September 1965

5. AUTHOR(S) (Last name, first name, initial)
Crimi, Peter

6. REPORT DATE	7a. TOTAL NO. OF PAGES	7b. NO. OF REFS
September 1965	79	10

8a. CONTRACT OR GRANT NO. DA 30-069-AMC-645(R) b. PROJECT NO. c d.	9a. ORIGINATOR'S REPORT NUMBER(S) BB-1994-S-1 9b. OTHER REPORT NO(S) (Any other numbers that may be assigned this report)

10. AVAILABILITY/LIMITATION NOTICES

11. SUPPLEMENTARY NOTES Part 2 of this report (BB-1994-S-2) describes two digital computer programs.	12. SPONSORING MILITARY ACTIVITY U. S. Army Ballistic Research Laboratories Aberdeen Proving Ground, Maryland

13 ABSTRACT

An analytical model is formulated to represent the time-varying flow due to the rotor The rotor wake and the fuselage of a helicopter in hovering or forward flight. The wake which is represented by tip vortices emanating from each blade, is allowed to convect under the influence of the blades, the fuselage itself.

A digital computer program was written which implements the model developed. Flow calculations agree well with measurements of the time average of the flow in the wake of a two-bladed rotor.

DD FORM 1 JAN 64 1473

Unclassified
Security Classification

14. KEY WORDS	LINK A		LINK B		LINK C	
	ROLE	WT	ROLE	WT	ROLE	WT
Helicopter Rotor Rotor Flow Field Aerodynamics Fluid Dynamics Digital Computations						

INSTRUCTIONS

1. ORIGINATING ACTIVITY: Enter the name and address of the contractor, subcontractor, grantee, Department of Defense activity or other organization *(corporate author)* issuing the report.

2*a*. REPORT SECURITY CLASSIFICATION: Enter the overall security classification of the report. Indicate whether "Restricted Data" is included. Marking is to be in accordance with appropriate security regulations.

2*b*. GROUP: Automatic downgrading is specified in DoD Directive 5200.10 and Armed Forces Industrial Manual. Enter the group number. Also, when applicable, show that optional markings have been used for Group 3 and Group 4 as authorized.

3. REPORT TITLE: Enter the complete report title in all capital letters. Titles in all cases should be unclassified. If a meaningful title cannot be selected without classification, show title classification in all capitals in parenthesis immediately following the title.

4. DESCRIPTIVE NOTES: If appropriate, enter the type of report, e.g., interim, progress, summary, annual, or final. Give the inclusive dates when a specific reporting period is covered.

5. AUTHOR(S): Enter the name(s) of author(s) as shown on or in the report. Enter last name, first name, middle initial. If military, show rank and branch of service. The name of the principal author is an absolute minimum requirement.

6. REPORT DATE: Enter the date of the report as day, month, year; or month, year. If more than one date appears on the report, use date of publication.

7*a*. TOTAL NUMBER OF PAGES: The total page count should follow normal pagination procedures, i.e., enter the number of pages containing information.

7*b*. NUMBER OF REFERENCES: Enter the total number of references cited in the report.

8*a*. CONTRACT OR GRANT NUMBER. If appropriate, enter the applicable number of the contract or grant under which the report was written.

8*b*, 8*c*, & 8*d*. PROJECT NUMBER: Enter the appropriate military department identification, such as project number, subproject number, system numbers, task number, etc.

9*a*. ORIGINATOR'S REPORT NUMBER(S): Enter the official report number by which the document will be identified and controlled by the originating activity. This number must be unique to this report.

9*b*. OTHER REPORT NUMBER(S): If the report has been assigned any other report numbers *(either by the originator or by the sponsor)*, also enter this number(s).

10. AVAILABILITY/LIMITATION NOTICES: Enter any limitations on further dissemination of the report, other than those imposed by security classification, using standard statements such as:

(1) "Qualified requesters may obtain copies of this report from DDC."

(2) "Foreign announcement and dissemination of this report by DDC is not authorized."

(3) "U. S. Government agencies may obtain copies of this report directly from DDC. Other qualified DDC users shall request through _____."

(4) "U. S. military agencies may obtain copies of this report directly from DDC. Other qualified users shall request through _____."

(5) "All distribution of this report is controlled. Qualified DDC users shall request through _____."

If the report has been furnished to the Office of Technical Services, Department of Commerce, for sale to the public, indicate this fact and enter the price, if known.

11. SUPPLEMENTARY NOTES: Use for additional explanatory notes.

12. SPONSORING MILITARY ACTIVITY: Enter the name of the departmental project office or laboratory sponsoring *(paying for)* the research and development. Include address.

13. ABSTRACT: Enter an abstract giving a brief and factual summary of the document indicative of the report, even though it may also appear elsewhere in the body of the technical report. If additional space is required, a continuation sheet shall be attached.

It is highly desirable that the abstract of classified reports be unclassified. Each paragraph of the abstract shall end with an indication of the military security classification of the information in the paragraph, represented as *(TS), (S), (C), or (U)*.

There is no limitation on the length of the abstract. However, the suggested length is from 150 to 225 words.

14 KEY WORDS: Key words are technically meaningful terms or short phrases that characterize a report and may be used as index entries for cataloging the report. Key words must be selected so that no security classification is required. Identifiers, such as equipment model designation, trade name, military project code name, geographic location, may be used as key words but will be followed by an indication of technical context. The assignment of links, roles, and weights is optional.